Pergamon

PII: S0022-4073(98)00078-8

J. Quant. Spectrosc. Radiat. Transfer Vol. 60, No. 5, pp. 665–710, 1998
Published by Elsevier Science Ltd
Printed in Great Britain
0022–4073/98 $19.00 + 0.00

THE HITRAN MOLECULAR SPECTROSCOPIC DATABASE AND HAWKS (HITRAN ATMOSPHERIC WORKSTATION): 1996 EDITION

L. S. ROTHMAN,*†‡ C. P. RINSLAND,§ A. GOLDMAN,¶ S. T. MASSIE,‖ D. P. EDWARDS,‖ J.-M. FLAUD,** A. PERRIN,** C. CAMY-PEYRET,†† V. DANA,†† J.-Y. MANDIN,†† J. SCHROEDER,‡‡ A. MCCANN,‡‡ R. R. GAMACHE,§§ R. B. WATTSON,¶¶ K. YOSHINO,‡ K. V. CHANCE,‡ K. W. JUCKS,‡ L. R. BROWN,‖‖ V. NEMTCHINOV†§ and P. VARANASI†§

† AF Research Laboratory, VSBM, 29 Randolph Rd, Hanscom AFB MA 01731-3010, U.S.A.; ‡ Harvard-Smithsonian Center for Astrophysics, Cambridge MA 02138, U.S.A.; § Atmospheric Sciences Division, NASA Langley Research Center, Hampton, VA 23681, U.S.A.; ¶ Department of Physics, University of Denver, Denver, CO 80208. U.S.A.; ‖ National Center for Atmospheric Research, Boulder, CO 80307, U.S.A.; ** Laboratoire de Photophysique Moléculaire, CNRS, Bât. 210, Université Paris-Sud, 91405 Orsay, France; †† LPMA, Université Pierre et Marie Curie, Case 76, 4 Place Jussieu, 75252 Paris 05, France; ‡‡ Ontar Corp, 9 Village Way, North Andover MA 01845-2000, U.S.A.; §§ Department of Environmental Earth and Atmospheric Sciences, Univ. of Mass Lowell, Lowell, MA 01854, U.S.A.; ¶¶ Stewart Radiance Laboratory, Utah State University, Bedford, MA 01730, U.S.A.; ‖‖ Jet Propulsion Laboratory, Pasadena, CA 91109, U.S.A. and †§ State University of New York at Stony Brook, Stony Brook, NY 11794, U.S.A.

(Received 13 March 1998)

Abstract—Since its first publication in 1973, the HITRAN molecular spectroscopic database has been recognized as the international standard for providing the necessary fundamental spectroscopic parameters for diverse atmospheric and laboratory transmission and radiance calculations. There have been periodic editions of HITRAN over the past decades as the database has been expanded and improved with respect to the molecular species and spectral range covered, the number of parameters included, and the accuracy of this information. The 1996 edition not only includes the customary line-by-line transition parameters familiar to HITRAN users, but also cross-section data, aerosol indices of refraction, software to filter and manipulate the data, and documentation. This paper describes the data and features that have been added or replaced since the previous edition of HITRAN. We also cite instances of critical data that are forthcoming. Published by Elsevier Science Ltd.

1. INTRODUCTION

A new edition of the HITRAN (**HI**gh-resolution **TRAN**smission) database was released on CD-ROM in 1996. This line-by-line compilation of spectroscopic parameters is a widely recognized international standard. It is used for a vast array of applications such as terrestrial atmospheric remote sensing, transmission simulations, fundamental laboratory spectroscopy studies, industrial process monitoring, pollution regulatory studies, etc. HITRAN is now a component of a larger set of spectroscopic data and software called HAWKS (**H**ITRAN **A**tmospheric **W**or**ks**tation). The goal of HITRAN and HAWKS is to provide a functional and flexible set of software and data in order to accurately model the simulation of transmission and radiance from the microwave through ultraviolet spectral regions. Besides an updated HITRAN high-resolution molecular database of about one million transitions, there are files of aerosol indices of refraction, UV line-by-line and cross-section parameters, supplemental files of gases that have undergone less validation or whose parameters require new definitions, such as ionic species, and extensive IR cross-sections now at different pressures and temperatures. In addition, the compilation contains a moderate-resolution band-model code, MODTRAN3. There is also vastly improved software handling of the data in

* To whom all correspondence should be addressed.

both WINDOWS and UNIX platforms, such as more sophisticated selection filters, plotting capabilities, pointers to significant references, and documentation.

In Sec. 2 of this paper we present a discussion of positions, intensities, widths, temperature-dependence, and pressure-shifts (if nonzero) of all new data since the 1992 (previous) edition of the HITRAN database.[1] (All earlier work and related subjects are cited therein.) Reported in Sec. 2 are updates to the contents, their accuracy, and limitations of the data. The sub-sections are given sequentially according to the molecular species in HITRAN and have been organized by region (increasing frequency) if there is more than one band that has been updated or added. We also mention each species even if no changes have been made since the last edition, and, since the progress in spectroscopy has been proceeding at a rapid rate, we occasionally mention significant improvements or enhancements expected in the near future. This section is the prime focus of this paper.

Section 3 presents a discussion of the infrared cross-section files that are new to this edition of the compilation. As with the discussion of some of the line-by-line data in Sec. 2, separate articles alleviate us of providing all of the details. In Sec. 4, the ultraviolet data on the compilation are presented. The UV data comprise a line-by-line section (the Schumann–Runge bands) and UV cross-sections. These data are a new extension to HITRAN and are formatted in the equivalent way as the standard HITRAN line-by-line and cross-sections portions. Sec. 5 describes the files of indices of refraction that are placed on the compilation for the first time. In Sec. 6 is a discussion of spectroscopic features such as line-coupling that have special significance in atmospheric remote sensing, but have not been part of the HITRAN database suite; formalisms are proposed that lend themselves to parametrization in order to assist the modeling codes. Finally in the last section, we report on some of the software and features that are now available on this compilation. The software includes useful data and computational aids that are companions and addendums to the HITRAN database, such as partition sum generation, temperature conversion of parameters, molecular degeneracy factors, and the standard isotopic abundances and weights used on the compilation.

The HITRAN database has now evolved for over three decades. In its first incarnation it was made available to the public on large magnetic tape (drawers and drawers of cards to the contributors). The spectral range, number of molecular species and their isotopomers, and comprehensiveness of the parameters have steadily increased. The 1986 edition[2] saw the format for the line-by-line (HITRAN) portion expanded to 100 characters per transition. In 1992, the medium used to distribute the database became CD-ROM. The current edition is also on CD-ROM and has ancillary data types and files; updates and corrections are now available on the world wide web (http://www.HITRAN.com). The general file structure of the compilation is given in Table 1. The data files are in ASCII and can be accessed by a variety of operating systems, although most of the

Table 1. Primary file structure of the HAWKS compilation

DIRECTORY	SUB-DIRECTORIES	MEGABYTES
SOFTWARE	Generic Programs and Tables	0.7
SOFTWARE	MS WINDOWS	1.8
SOFTWARE	UNIX	4.3
HITRAN		101.9
HITRAN	BY_MOLEC	101.9
Supplemental LBL		19.4
IR Cross-Sections		18
UV	Line-by-Line	1.1
UV	Cross-Sections	2.5
Indices of Refraction		0.2
Documentation		21.3
Models	MODTRAN	22.8
	Total =	295.9

value-added software has been made for the Microsoft WINDOWS and UNIX operating systems on the HAWKS CD-ROM.

There has been some misunderstanding prevalent in the community concerning the units and definitions employed in the HITRAN database. We include in this paper an appendix that summarizes the definitions and usage associated with the compilation.

2. DISCRETE MOLECULAR TRANSITIONS: THE HITRAN DATABASE

The line-by-line portion of the compilation, HITRAN, now contains transitions for 37 molecular species. Table 2 presents a summary of the species that are contained on the compilation. The numbering of the species is simply by chronological entry into the HITRAN database, the last six entries being new species added since the last edition. Furthermore, the final two species, NO^+ and HOBr, reside in the supplemental directory, not in the main HITRAN database. It should also be noted that one of the new species is in fact an atom (oxygen). The table lists the number of isotopic variants (isotopomers) per molecule represented in HITRAN, as well as the number of vibration–rotation or ro-vibronic bands. One also notices that certain "heavy" molecules, such as ozone and nitric acid, have a very large number of transitions; this occurs as new bands or more extensive coverage of bands are achieved on new editions. On the other hand, species like water vapor and carbon dioxide remain rather constant in terms of the number of transitions, even though there may be considerable improvement in the quality of the individual parameters.

Table 2. Summary of species represented in HITRAN

Mol. no.	Molecule	Number of isotopomers	Number of bands	Number of lines	Spectral coverage (cm^{-1})
1	H_2O	4	137	49 444	0–22 657
2	CO_2	8	589	60 802	442–9649
3	O_3	5	106	275 133	0–4033
4	N_2O	5	164	26 174	0–5132
5	CO	6	47	4 477	3–6418
6	CH_4	3	51	48 032	0–6185
7	O_2	3	19	6 292	0–15 928
8	NO	3	50	15 331	0–3967
9	SO_2	2	9	38 853	0–4093
10	NO_2	1	12	100 680	0–2939
11	NH_3	2	40	11 152	0–5295
12	HNO_3	1	13	165 426	0–1770
13	OH	3	103	8 676	0–9997
14	HF	1	6	107	41–11 536
15	HCl	2	17	533	20–13 458
16	HBr	2	16	576	16–9759
17	HI	1	9	237	12–8488
18	ClO	2	12	7 230	0–1208
19	OCS	4	7	858	0–2089
20	H_2CO	3	10	2 702	0–2999
21	HOCl	2	6	15 565	0–3800
22	N_2	1	1	120	1922–2626
23	HCN	3	8	772	2–3422
24	CH_3Cl	2	8	9 355	679–3173
25	H_2O_2	1	2	5 444	0–1500
26	C_2H_2	2	11	1 668	604–3375
27	C_2H_6	1	2	4 749	720–3001
28	PH_3	1	2	2 886	708–1411
29	COF_2	1	7	54 866	725–1982
30	SF_6	1	1	11 520	940–953
31	H_2S	3	15	7 151	2–2892
32	HCOOH	1	1	3 388	1060–1162
33	HO_2	1	4	26 963	0–3676
34	O	1	1	2	68–159
35	$ClONO_2$	2	3	32 199	763–798
36	NO^+	1	6	1 206	1634–2531
37	HOBr	2	2	4 358	0–316

The enhancements to the new compilation have been particularly focused on improving the capabilities for atmospheric remote sensing. Parameters for molecular transitions that will be needed for remote observations from space-borne missions such as the Earth Observing System[3] (EOS) of NASA and ground-based measurements as exemplified by the Atmospheric Radiation Measurement (ARM) program[4] of the DOE have been a high priority of the recent development of the compilation.

Before entering into the discussion of the improvements, changes, and enhancements of each molecular species, it is prudent to repeat some caveats: (1) The HITRAN database was originally designed for simulations and analysis of observations in the terrestrial atmosphere. Consequently transitions and bands which are significant at higher temperatures may be missing or poorly simulated because of extrapolations outside the range of conditions used in the original laboratory experiments. For some applications and conditions (e.g. biomass fires, plumes from industrial chimneys, cool stars, combustion, etc) it may be preferable to use the HITEMP[5] database which is dedicated to such special problems. (2) Since the intensities have been standardized to room temperature (296 K), there exist very small exponents for some intensities (e.g. OH and NO high-vibrational sequence bands). Codes using HITRAN as input should take this into account. (3) There is a duplication of cross-sections and some line-by-line bands (for example for SF_6 and $ClONO_2$). Again, the user has to exercise discretion. (4) There is an overlap of ozone parameters and data in the ozone contained in the supplemental directory (non-LTE ozone calculations). The ozone parameters in the supplemental directory have not been validated. (5) As mentioned in previous articles on HITRAN editions, for some lines (for water vapor and methane) where there were incomplete quantum identification of states involved in the transition, a lower state energy was not determined. We have used negative unity (-1.0) in the lower state energy field to flag these lines, which nonetheless can be useful for many applications. (6) The parameter for the weighted transition-moment squared has in a few cases not been calculated, and is in error for the $^2\Pi$ molecules (NO, OH, ClO).

As a guide to the discussion, we present a "slice" of HITRAN in Table 3 to illustrate the definition of the fields for the parameters. A more complete discussion is given in the Appendix. Table 4 displays the scheme employed to characterize the "local" quanta (primarily the unique labeling of rotational levels of the upper and lower states of the transition in HITRAN).

2.1. H_2O (molecule 1)

The rotational transitions for HDO have been updated since the 1992 release, which only covered the region from 0 to 100 cm^{-1}. The current positions and intensities are derived from the JPL submillimeter wave catalogue[6] and extend to 764 cm^{-1}. Considerable uncertainty exists in the positions and strengths for the rotational transitions of the $H_2{}^{16}O$, $H_2{}^{18}O$, and $H_2{}^{17}O$ (AFGL abbreviated code 161, 181, and 171) isotopomers of H_2O, especially at higher values of J and K. Examples of the magnitude of the uncertainties for these transitions are contained in Rinsland et al[7] where strengths and positions of many pure rotational transitions near 1000 cm^{-1} are measured to have significantly different positions than those currently contained in HITRAN, and the strengths differ by as much as 30%. More recent laboratory measurements of high J and K rotational transitions are now included in HITRAN (described below). The positions for the rotational transitions can also be recalculated using the energy levels calculated by Toth[8,9] which have been shown to agree satisfactorily with the positions observed in atmospheric emission spectra.[10] More measurements of the absolute strengths, along with calculations such as those of Coudert[11] are needed to reduce the uncertainties for these atmospherically important transitions.

Line positions were updated for 549 H_2O lines in the 720–1400 cm^{-1} region. This update was based on experimental observations[12] made with the Michelson interferometer (0.009 cm^{-1} resolution) at the AF Geophysics Directorate of a 20 torr sample of H_2O heated to 1000 K in a high temperature absorption cell. Line positions were measured with an accuracy of approximately 0.0004 cm^{-1}. The wavenumber scale of the spectrometer was calibrated using residual H_2O lines present in the spectrum of the evacuated absorption cell. A direct numerical diagonalization (DND) calculation[13] was used to calculate a starting line list to help in identifying the observed spectral lines. The DND calculation used a 47-parameter potential surface with up to sextic powers in

Table 3. Example of HITRAN line-transition format.

Mol/Iso	$\nu_{\eta\eta'}$	$S_{\eta\eta'}$	$\Re_{\eta\eta'}$	γ_{air}	γ_{self}	E″	n	δ	iv'	iv''	q'	q''	ierr	iref
21	800.451076	3.197E–26	6.579E–05	0.0676	0.0818	2481.5624	0.78	0.000000	14	6		P 37	465	2 2 1
291	800.454690	9.724E–22	1.896E–02	0.0845	0.1750	369.6303	0.94	0.000000	9	1	341619	331519	000	4 4 1
291	800.454690	3.242E–22	2.107E–03	0.0845	0.1750	369.6303	0.94	0.000000	9	1	341519	331419	000	4 4 1
121	800.455380	1.037E–22	1.657E–03	0.1100	0.0000	530.3300	0.75	0.000000	32	14	46 640	45 540	000	4 4 1
121	800.455380	1.037E–22	1.657E–03	0.1100	0.0000	530.3300	0.75	0.000000	32	14	46 740	45 640	000	4 4 1
101	800.456743	1.680E–23	1.659E–04	0.0670	0.0000	851.0494	0.50	0.000000	2	1	45 244 0–	44 143 0–	301	6 6 1
101	800.457045	1.710E–23	1.689E–04	0.0670	0.0000	851.0469	0.50	0.000000	2	1	45 244 1–	44 143 1–	301	6 6 1
101	800.457310	1.740E–23	1.718E–04	0.0670	0.0000	851.0442	0.50	0.000000	2	1	45 244 2–	44 143 2–	301	6 6 1
121	800.457760	4.726E–23	4.614E–03	0.1100	0.0000	920.0900	0.75	0.000000	32	14	502922	492822	000	4 4 1
121	800.457760	4.726E–23	4.614E–03	0.1100	0.0000	920.0900	0.75	0.000000	32	14	502822	492722	000	4 4 1
24	800.465942	9.792E–27	6.063E–04	0.0754	0.1043	1341.2052	0.69	0.000000	8	3		R 13	425	2 2 1
121	800.466160	1.061E–22	2.720E–03	0.1100	0.0000	632.1200	0.75	0.000000	32	14	471236	461136	000	4 4 1
121	800.466160	1.061E–22	2.720E–03	0.1100	0.0000	632.1200	0.75	0.000000	32	14	471136	461036	000	4 4 1
35	800.472900	3.878E–26	6.919E–04	0.0686	0.0871	629.0354	0.76	0.000000	2	1	1814 4	1713 5	455	5 5 1
101	800.473083	1.270E–23	1.254E–04	0.0670	0.0000	851.0095	0.50	0.000000	2	1	45 244 0 +	44 143 0 +	301	6 6 1
101	800.474860	1.210E–23	1.195E–04	0.0670	0.0000	851.0064	0.50	0.000000	2	1	45 244–1 +	44 143–1 +	301	6 6 1
31	800.475500	1.680E–24	3.617E–05	0.0653	0.0890	1092.4340	0.76	0.000000	2	1	51 547	50 248	002	1 1 2
291	800.476220	9.597E–22	6.010E–03	0.0845	0.1750	361.9747	0.94	0.000000	9	1	341420	331320	000	4 4 1
291	800.476220	3.199E–22	6.010E–03	0.0845	0.1750	361.9747	0.94	0.000000	9	1	341520	331420	000	4 4 1
101	800.476937	1.160E–23	1.145E–04	0.0670	0.0000	851.0037	0.50	0.000000	2	1	45 244–2 +	44 143–2 +	301	6 6 1
101	800.484334	1.740E–23	2.153E–05	0.0670	0.0000	106.0760	0.50	0.000000	2	1	8 4 4–1 +	9 3 7–1 +	301	6 6 1

Note: FORTRAN Format (I2,I1,F12.6,1P2E10.3,0P2F5.4,F10.4,F4.2,F8.6,2I3,2A9,3I1,3I2) corresponding to the following:

Mol	I2	molecule number
Iso	I1	isotope number (1 = most abundant, 2 = second most abundant, etc.)
$\nu_{\eta\eta'}$	F12.6	frequency in cm^{-1}
$S_{\eta\eta'}$	E10.3	intensity in $\text{cm}^{-1}/(\text{molecule}\cdot\text{cm}^{-2})$ @ 296 K
$\Re_{\eta\eta'}$	E10.3	weighted transition moment-squared in Debye^2
γ_{air}	F5.4	air-broadened halfwidth (HWHM) in $\text{cm}^{-1}/\text{atm}$ @ 296 K
γ_{self}	F5.4	self-broadened halfwidth (HWHM) in $\text{cm}^{-1}/\text{atm}$ @ 296 K
E''	F10.4	lower state energy in cm^{-1}
n	F4.2	coefficient of temperature dependence of air-broadened halfwidth
δ	F8.6	airbroadened pressure shift of line transition in $\text{cm}^{-1}/\text{atm}$ @ 296 K
iv',iv''	2I3	upper state global quanta index, lower state global quanta index
q',q''	2A9	upper state local quanta, lower state local quanta
ierr	3I1	accuracy indices for frequency, intensity, and air-broadened halfwidth
iref	3I2	indices for table of references corresponding to frequency, intensity, and halfwidth

Table 4. Formats (in FORTRAN) for the six classes of local quanta identification.

Group 1: Asymmetric rotors H_2O, O_3, SO_2, NO_2,† HNO_3, H_2CO, HOCl, H_2O_2, COF_2, H_2S, HO_2, HCOOH, $ClONO_2$, HOBr	
J', K'_a, K'_c, F', Sym′ I2, I2, I2, I2, A1	J'', K''_a, K''_c, F'', Sym″ I2, I2, I2, I2, A1
Group 2: Diatomic and linear molecules with integer J CO_2, N_2O, CO, HF, HCl, HBr, HI, OCS, N_2, HCN, C_2H_2, NO^+	
——, Br, F'', — 5X, A1, I2, 1X	——, Br, J'', Sym″ 4X, A1, I3, A1
Group 3: Spherical rotors CH_4 (not CH_3D)	
J', R', C', N', Sym′ I2, I2, A2, I2, A1	J'', R'', C'', N'', Sym″ I2, I2, A2, I2, A1
Group 4: Symmetric rotors CH_3D, NH_3, CH_3Cl, C_2H_6, PH_3, SF_6	
J', K', C', ——, Sym′ I2, I2, A2, 2X, A1	J'', K'', C'', ——, Sym″ I2, I2, A2, 2X, A1
Group 5: Triplet ground electronic states O_2	
——, Br, F'', —3 X, A1, F4.1, 1X	Br, N'', Br, J'', —, Sym″ A1, I2, A1, I2, 2X, A1
Group 6: Doublet ground electronic states (half-integer J) NO††, OH, ClO	
——, Br, F'', —5 X, A1, I2, 1X	——, Br, J'', Sym″ 3X, A1, F4.1, A1

Notes: Prime and double primes refer to upper and lower states, respectively; Br is the O-, P-, Q-, R-, or S-branch symbol; J is the rotational quantum number; Sym is e or f for l-type doubling, + or − for required symmetry symbols.
†For NO_2, F—J was used instead of F.
††For NO, F is half-integer and both F′ and F″ have been given for some rovibration bands.

internal coordinates. The observed line positions were not used directly to update the HITRAN H_2O line positions. Instead, they were first combined with observed transitions from other studies to form a self-consistent set of line positions. These additional lines were microwave spectral transitions measured by Pearson et al[14] and lines calculated from energy levels reported by Toth.[8]

When the updated H_2O line positions were compared with the line positions on the HITRAN92 database,[1] discrepancies of up to 0.8 cm^{-1} were found for some transitions. These large discrepancies presumably arose from the inclusion of data from misidentified H_2O lines on the HITRAN92 database. There were 8 lines where the difference between the observed line position and the HITRAN92 value was greater than 0.1 cm^{-1} and 49 lines where the difference was greater than 0.01 cm^{-1}.

The data for the air-broadened, γ_{air}, and self-broadened, γ_{self}, halfwidths and the temperature dependence, n, of the air-broadened halfwidth on HITRAN are a mixture of experimental and theoretical values. No longer present on the database are air-broadened halfwidths determined from the empirical algorithm[2] used previously. The new algorithm adds halfwidths to water vapor lines following several criteria and was developed as follows. First, a small database of experimentally determined halfwidths[15,16] was compiled. This list consists of 276 air-broadened halfwidths and 261 self-broadened halfwidths. The vibrational dependence of the data was ignored (this dependence is presumed to be a small correction[17]); hence the data are functions of the rotational transition quantum numbers only. Where duplicate values occur, the experimental data are averaged. This data set corresponds to only a small number of transitions that occur for H_2O and thus the set has been augmented by theoretical calculations. The data are that of Gamache and Davies[18] and Gamache and Rothman[19] for γ_{air} and n, and that of Gamache and Davies (unpublished data, 1983) for γ_{self}. In addition, an average of the calculated air- and self-broadened halfwidths as a function of

J'' was determined by scaling to match the average of the measured values. The average scaled values are used to determine halfwidths for transitions for which no measurements are made.

The algorithm to add the halfwidths to the database operates as follows: for a given spectral line, the algorithm first attempts to add measured halfwidths, γ_{air} and γ_{self}, to the line. If no measurements are available, the algorithm defaults to the theoretical value for the halfwidths. If no theoretical value is available for the particular transition, the algorithm takes the scaled average halfwidth and adds that to the HITRAN line. A similar procedure is followed for the temperature dependence of the halfwidth.

Average values are determined for $J'' \leq 20$. For $J'' > 20$, default values of $\gamma_{air} = 0.018\ cm^{-1}/atm$ and $\gamma_{self} = 0.12\ cm^{-1}/atm$ are used. For the temperature exponent when the measured or calculated exponent does not exist, the default value of $n = 0.68$ is used.[19]

There are numerous deficiencies that remain with respect to the water vapor parameters. Because of the extreme importance of these parameters in many of the applications of HITRAN, we highlight some of the progress that will soon be forthcoming in improving the parameters. A very serious issue relates to flux anomalies when calculating the earth's radiation budget in the near infrared.[20] W.J. Phillips (Arnold AFB, private communication, 1997) has taken high-resolution spectra of self-broadened water vapor in the 1.5- and 1.9-μm regions. These spectra are being analyzed, and will represent the first update of many of the line positions and intensities in these regions since the first edition of HITRAN (line positions, intensities, and halfwidths prior to the 1986 database[2] are designated with the reference index zero).

The quantum mechanical study of the H_2O bands in the 0.4–0.6 μm region, originated by Camy-Peyret et al,[21] is still incomplete and a number of partial assignments appear in the HITRAN line list. Recent work by Harder and Brault[22] provides high-resolution cross-sections for the 22 230–22 700 cm^{-1} region, dominated by the $4\nu_1 + 3\nu_3$ and $5\nu_1 + 2\nu_3$ bands, in which individual lines are resolved, and low-resolution cross-sections derived from the high-resolution data are determined.

Finally, R. A. Toth (Jet Propulsion Laboratory, private communication, 1998) has completed an analysis of laboratory spectra of water vapor, isotopes, and hot bands for the 500–2580 cm^{-1} regions. Updates are in preparation for positions, intensities, air-broadening coefficients, self-broadening coefficients, and pressure-induced shifts. It has also been noticed that the current compilation does not include the improved HDO positions and intensities reported in the literature.[23]

2.2. CO_2 (molecule 2)

For each edition of the HITRAN database, there has been a new global least-squares fit of the energy levels of carbon dioxide, giving rise to enhanced accuracy of line positions. The method has been described by Rothman et al.[24] However, for this edition the only new data for CO_2 line positions since HITRAN92 were the results of M.P. Esplin (Utah State Univ., private communication, 1994) from measured line positions in high-resolution spectra of carbon dioxide, at elevated temperature, in the region from 500 to 1100 cm^{-1}. Some 43 bands of the $^{12}C^{16}O_2$ principal isotopomer, 42 bands of the $^{13}C^{16}O_2$ isotopomer, and 6 bands of the $^{16}O^{13}C^{18}O$ isotopomer were identified. These new positions were added to previously available data for the respective isotopomers, and spectroscopic constants re-determined by the global least-squares fitting procedure. The new data have allowed all the fitted levels to be connected to the ground state by observations; there are no longer any "floating" levels for the $^{13}C^{16}O_2$ and the $^{16}O^{13}C^{18}O$ species, as was the case in HITRAN92.

The updates of the line intensity parameters for CO_2 on the HITRAN96 spectroscopic database as compared to the HITRAN92 database have resulted from the work of L.P. Giver of the NASA Ames Research Center and represent the only changes in intensities since the previous database. These updates in the 1.2- to 2.5-μm region have a major impact on the interpretation of the Venus dark-side IR emission.[25] The particular bands are described in the next few paragraphs and the experimental conditions are summarized in Table 5. The observations at Kitt Peak were made with the 6-m White cell and Solar Fourier transform spectrometer (FTS) utilizing a resolution of 0.011 cm^{-1}, while the spectra obtained with the NASA Ames 25-m White cell and a Bomem

Table 5. Experimental conditions for CO_2 intensity measurements

v_0 (cm^{-1})	Band	Spectrometer	Pressure (Torr)	Path length (m)	Number of spectra
4006†	00021–01101	Kitt Peak	59.7	193	1
5315†	01121–00001	Kitt Peak	59.7	73,193	2
6503	30011–00001	Kitt Peak	30–80	25–400	7
6538†	11122–00001	Bomem	139–305	400–1300	5
6680†	11121–00001	Bomem	139–305	400–1300	5
7460†	40014–00001	Bomem	10–360	400–1700	22
		Kitt Peak	59.7	193	1
7593	40013–00001	Bomem	10–100	400–1600	6
		Kitt Peak	59.7	193	1
7734	40012–00001	Bomem	10–100	400–1600	6
		Kitt Peak	59.7	193	1
7921†	40011-00001	Bomem	10–360	400–1700	22

† Bands observed for the first time in high resolution.
Note: In column 3, Kitt Peak and Bomem refer to the spectrometer systems cited in the text.

DA3.002 FTS utilized resolutions ranging from 0.024 to 0.045 cm^{-1}. The longer total path lengths achievable at NASA Ames were necessary for the measurement of the very weak CO_2 bands, whereas the higher resolution spectra at Kitt Peak were most useful for measuring lines at low pressures in crowded spectral regions.

Preliminary intensity measurements were made on isolated P- and R-branch lines of the 00021–01101 band at 4006 cm^{-1}. These preliminary line-intensity measurements were found to be closer to calculated intensities on the 1986 HITRAN listing than the 1992 HITRAN listing, so the band intensity and a_1 (first order) Herman-Wallis parameter from the 1986 HITRAN were adopted for the 1996 HITRAN compilation. The definitions used for the intensity and Herman–Wallis parameters are given in Eqs. (7) and (14) of Ref. 24. Preliminary intensity measurements were also made on isolated P- and R-branch lines of the 01121–00001 band at 5315 cm^{-1}. The band intensity and a_1 Herman–Wallis parameter were determined[26] from these line intensities.

Intensities were measured[27] on lines of the 30011–00001 band at 6503 cm^{-1}. The band intensity and Herman-Wallis parameters were then determined from the averaged line intensity measurements. The new value for the a_2 Herman–Wallis parameter is negative, in agreement with theoretical expectations. Prior measurements incorporated into the 1992 HITRAN tabulation had determined positive a_2 values for all the bands of the 3001r–00001 tetrad, which conflicted with theoretical calculations. The new a_2 parameter for this band is also in qualitative agreement with the earlier measurements of Toth et al.[28]

Line intensities were measured[29] on the 11112–00001 and 11122–00001 perpendicular bands at 6680 and 6538 cm^{-1}. The 11121–00001 band is much cleaner than the 11122–00001 band, which lies in the R branch of the much stronger 30011–00001 band at 6503 cm^{-1}. Therefore, it was possible to determine the a_1, a_2, and b_2 Herman–Wallis parameters for the 11121–00001 band, while only a_1 could be determined for the 11122–00001 band.

Intensities were measured[30] on lines of the 40011–00001 and 40014–00001 bands at 7921 and 7460 cm^{-1}. The averaged individual line intensity measurements were reduced to band intensities and Herman–Wallis a_1 and a_2 parameters. In addition, using these spectra a few intensities were measured on lines of the 40012–00001 and 40013–00001 bands at 7734 and 7593 cm^{-1}. Lines of these bands had been previously measured[31,32], and our new measurements agreed with the prior published values. We then reduced the published line intensities to band intensities and Herman–Wallis parameters with the identical procedures we used for the 40011–00001 and 40014–00001 bands. This resulted in an intensity for the 40012–00001 band that is 5% larger than the 1992 HITRAN value; this intensity correction is in agreement with the reanalysis[33] by Valero and Boese of their own data.31 The new intensity value of the 40013–00001 band is only 2% higher than the 1992 HITRAN value. Herman–Wallis a_1 and a_2 parameters were also determined for this band, which replace the values of zero assigned in the 1992 HITRAN table. However, the values for this band are small and the uncertainties are of the same order as the parameters.

The data for the air-broadened halfwidth, γ_{air}, the self-broadened halfwidth, γ_{self}, and the temperature dependence of the air-broadened halfwidth, n, for CO_2 transitions on HITRAN are discussed in depth in Ref. 24. For γ_{air}, a table of halfwidths has been derived by third-order polynomial fits to measured data and to scaled theoretical data over particular ranges of m, where m is the running index ($m = -J$ for the P-branch, $m = J$ for the Q-branch, and $m = J + 1$ for the R-branch). The resulting data cover the range of $m = 0$ to 120 and the default value of $0.055\ cm^{-1}$/atm is taken above $m = 121$.

For the self-broadening halfwidths, a table was compiled by a third-order polynomial fit of data that extrapolated to $m = 120$. For $m = 1$ to 4, averaged experimental data were used due to deficiencies in the polynomial. Beyond $m = 121$, a constant value of $\gamma_{self} = 0.051\ cm^{-1}$/atm has been adopted. Note, however, that these high-m default values will only be utilized in high-temperature applications[5] since the HITRAN intensity cutoff for CO_2 does not produce a value of m greater than 108.

The exponents describing the temperature dependence of the air-broadened halfwidths are from R.R. Gamache and L. Rosenmann (unpublished results, 1991) and the line shifts for the ν_3 transitions are the data of Devi et al.[34]

2.3. O_3 (molecule 3)

The updates and new entries for ozone are based on laboratory measurements recorded with the Fourier transform spectrometers at Kitt Peak, Arizona, U.S.A., and at the University of Reims, France. The measurements were obtained in the infrared at spectral resolutions of 0.0025–0.01 cm^{-1}. The changes to the compilation are summarized in Table 6, where the new or modified band systems are listed in ascending wavenumber order. A more detailed description of the changes, accuracies, and limitations of the ozone parameters in HITRAN96 is given in the accompanying paper by Rinsland et al.[35] A summary of the changes is provided below.

At 14 μm, the ν_2 bands of the rarer isotopes $^{16}O^{16}O^{17}O$ and $^{16}O^{17}O^{16}O$ have been added. In this work,[36] the rotational constants of the ground state were redetermined by combining published microwave measurements with combination differences measured from the infrared spectra. Based on these results, complete linelists for the pure rotation bands of both isotopes were generated and also added to HITRAN.

At shorter wavelengths, a consistent set of spectroscopic parameters has been used to generate several new bands and several revised bands of $^{16}O_3$. The first assignment of the weak, previously unobserved $3\nu_1$ band at 3.3 μm resulted in an improved calculation[37] of the energy levels of the four interacting states (0 0 3), (3 0 0), (1 0 2), and (2 0 1). These improved energy levels were used to generate parameters for the bands at 3.3 μm and add several hot bands at 4.8 and 10 μm. The previously unobserved $\nu_1 + 3\nu_3 - \nu_2$ hot band at 3.0 μm was also added. The intensity of this band is about one-third that of the weak $3\nu_1$ cold band.[37]

Table 6. Summary of the differences in the parameters for ozone between the 1992 and 1996 HITRAN databases

Isotopomer	Region (μm)	Upper vibrational state	Lower vibrational state	New	Update
667	MW	000	000	×	
676	MW	000	000	×	
667	14	010	000	×	
676	14	010	000	×	
666	10	{003,102,201,300}	{200,101,002}	×	
666	4.8	{003,102,201,300}	{100,001}		×
666	3.3	{003,102,201,300}	000		×
666	3.3	{004,103,310}	{100,001}	×	
666	3.3	{013,112}	010	×	
666	3.0	{004,103,310}	010	×	
666	2.7	{013,112}	000	×	
666	2.5	{004,103,310}	000	×	

MW = microwave, 667 = $^{16}O^{16}O^{17}O$, 676 = $^{16}O^{17}O^{16}O$, 666 = $^{16}O_3$. Updates are defined as changes relative to HITRAN 1992 (Ref. 1).

At 3.0 and 3.3 μm, a total of 8 hot bands of $^{16}O_3$ were added. The calculated transitions involve the {(1 0 3), (0 0 4),(3 1 0)} ← {(1 0 0), (0 0 1)} and {(0 1 3), (1 1 2)} ← (0 1 0) band systems. A description of the calculations and sample comparisons of measured laboratory spectra with simulations were reported by Flaud et al.[38] The improved upper vibrational state energy levels derived from this work were also used to generate line lists for the $^{16}O_3$ cold bands in the 2.5- and 2.7-μm regions.

2.4. N_2O (molecule 4)

Several updates for nitrous oxide were accomplished for this edition: the pure rotational bands, the ν_2 and associated hot band region from 523 to 728 cm^{-1}, and the region from 3046 to 3625 cm^{-1}.

The update of pure rotational bands involves the first four isotopomers and comprises almost 2600 lines from 10 to 727 cm^{-1}. These data have been assimilated from the Smithsonian Astrophysical Observatory Database.[39]

There has been a continuing program to update the nitrous oxide rovibrational bands carried on by R.A. Toth of the Jet Propulsion Laboratory. Similar to our work on carbon dioxide, this effort aims at achieving a self-consistent set of parameters for all bands. For this edition of HITRAN, the bands in the two aforementioned regions, 14 and 3 μm, have been replaced. The update in the latter region is extensive. On the other hand, parameters now exist for the ν_2 band (580–670 cm^{-1}) and associated hot bands[40,41] based on new laboratory measurements; these parameters will be included in a future HITRAN release. This analysis contains Herman-Wallis factors which are not included in the current HITRAN study, where strengths are in error by up to 25% at higher J.

An anomaly in the HITRAN96 release is that the R3 line of the ν_2 fundamental of the principal isotope, $^{14}N_2{}^{16}O$, was inadvertently omitted (it *was* present in previous editions of HITRAN).

2.5. CO (molecule 5)

The carbon monoxide line parameters remain unchanged in the pure rotation region except for minor updates to the positions of R2 and higher J lines based on the positions of Varberg and Evenson.[42] The positions, intensities, and lower state energies for the fundamental, first, and second overtone bands have been replaced by a new calculation that adds data for a sixth isotope ($^{13}C^{17}O$) to data for the five principal isotopes ($^{12}C^{16}O$, $^{13}C^{16}O$, $^{12}C^{18}O$, $^{12}C^{17}O$, and $^{13}C^{18}O$). The transition frequencies calculated using mass-independent Dunham parameters,[43] and the intensities calculated using the dipole moment of Chackerian and Tipping[44] have not substantially altered HITRAN. The current linelist is adapted from the tables by Goorvitch,[45] which were based on Refs. 43 and 44. Parameters for the lines of the (4–0) band of $^{12}C^{16}O$, the only third overtone band, have not been changed since the 1992 edition.

The air-broadening coefficient at 296 K, the self-broadening coefficient at 296 K, and the coefficient of the temperature dependence of the air-broadening coefficient are the same as on the 1992 edition. Note that the temperature-dependence coefficient is set to 0.69 for all lines and the default value of zero remains for the pressure-shift coefficient of all lines.

2.6. CH_4 (molecule 6)

The only change made for the 1996 edition regarding methane was the replacement of the prediction of the three lowest fundamentals of CH_3D with one that utilized all the dipole moments and Herman-Wallis like terms reported by Tarrago et al.[46] However, the upper- and lower-state quantum numbers on these transitions between the 900- and 1700-cm^{-1} region were mistakenly reversed. Users should refer to Ref. 46 for the correct notation.

A comprehensive revision of methane parameters is in progress at the University of Bourgogne in Dijon, France. In the region of the lowest fundamentals of CH_4 (900–2000 cm^{-1}), improved parameters are now available from the modeling of some 1700 observed line intensities for 9 hot bands by Ouardi et al[47] combined with the analysis of upper state levels near 3000 cm^{-1} (Hilico et al[48]) to determine the hot-band positions. New (but still preliminary) predictions of the 2000 to 3300 cm^{-1} and 3500 to 4700 cm^{-1} regions have been made (J.C. Hilico, Université de Bourgogne, France, private communication, 1997). For $^{12}CH_3D$, new studies that are in progress are expected to provide complete predictions up to 3300 cm^{-1}. A new analysis of the triad (ν_6, ν_3, and ν_5) between

900 and 1700 cm^{-1} by Nikitin et al[49] has produced a new prediction with line positions improved by almost an order of magnitude. While these studies were completed after the 1996 HITRAN database was formed, new results[47,49] for the lowest regions were included in the 1996/1997 GEISA databank.[50]

2.7. O_2 (molecule 7)

The spectral parameters for the oxygen molecule were calculated for the electronic-vibrational bands listed in Table 7. Complete details of the calculations can be found in Gamache et al.[51] All lines passing a wavenumber-dependent intensity cutoff procedure (see Eq. (17) of Ref. 51) are retained for the 1996 HITRAN database, with several noted exceptions. These data represent an improvement to the data contained on the 1992 version of the HITRAN molecular absorption database,[1] which are from calculations made in 1982.[52] The calculations consider the lower state energy, the wavenumber of the transition, the line intensity, and transition probability squared of the spectral lines. The calculation of the energies and positions benefitted from newer, more accurate Hamiltonian formalisms and constants.[53,54] In addition, halfwidths as a function of transition quantum number were determined from the available experimental measurements.

Line intensities were calculated using several different formulations depending on the particular electronic-vibrational-rotational transition in question. The method used for each band is discussed in Ref. 51. Some of the significant changes are highlighted here. For electric quadrupole transitions in the $X^3\Sigma_g^-(v=0) \rightarrow X^3\Sigma_g^-$ $(v=0)$ band, a newer value of the quadrupole moment derived from far-IR pressure-induced absorption spectra[54] was adopted. The resulting line intensities and transition probabilities squared are a factor of 5.8 weaker than previous calculations.[55] For this band, no electric quadrupole lines survived the cutoff for the 1996 data set.

For the $X^3\Sigma_g^-$ $(v=1) \rightarrow X^3\Sigma_g^-$ $(v=0)$ band of the principal species, the line intensities were not filtered through the cutoff procedure. Thus, many of the lines have very small intensities. (In fact, one zero intensity magnetic dipole and one electric quadrupole transition have been retained in the data for theoretical considerations; it helps to see the effects of assumed parameters on these lines.)

For the $a^1\Delta_g$ $(v=0) \rightarrow$ $X^3\Sigma_g^-$ $(v=0)$ band there are available three measurements[56–58] of the Einstein-A coefficient which differ by roughly factors of 2 from each other. In addition, the relationship between the line intensity and Einstein-A coefficients in Refs. 57 and 58 leads to additional confusion. Reference 51 gives the correct degeneracy factors for relating the Einstein-A coefficient, the integrated band intensity, and the line intensities. Using these relations and unpublished data for this band (J.W. Brault and M.M. Brown, Kitt Peak National Solar Observatory) yields a band intensity of $S_{00} = 3.69 \times 10^{-24}$ $cm^{-1}/(molecule \cdot cm^{-2})$ which is close to the Badger et al[56] value. The calculation of the line intensities for the 1996 database used the Einstein-A coefficient

Table 7. Electronic-vibrational bands of O_2 in the 1996 HITRAN database

Electronic band	$^{16}O_2$		$^{16}O^{18}O$		$^{16}O^{17}O$	
	$v' \leftarrow v''$	Spectral range (cm^{-1})	$v' \leftarrow v''$	Spectral range (cm^{-1})	$v' \leftarrow v''$	Spectral range (cm^{-1})
$X^3\Sigma_g^- \leftarrow X^3\Sigma_g^-$	0 ← 0	0–276	0 ← 0	1–214	0 ← 0	0–252
	1 ← 1	1–207				
	1 ← 0	1366–1718				
	0 ← 1	6256–6432				
$a^1\Delta_g \leftarrow X^3\Sigma_g^-$	0 ← 0	7664–8065	0 ← 0	7779–7998		
	1 ← 0	9250–9477				
$b^1\Sigma_g^+ \leftarrow X^3\Sigma_g^-$	0 ← 1	11 483–11 617				
	1 ← 1	12 847–13 011				
	0 ← 0	12 899–13 166	0 ← 0	12 975–13 165		
	1 ← 0	14 301–14 558	1 ← 0	14 367–14 520	1 ← 0	14 453–14 537
	2 ← 0	15 719–15 928	2 ← 0	15 789–15 852		
$B^3\Sigma_u^- \leftarrow X^3\Sigma_g^-$	†	44 606–57 027				

† $v' = 0$–19, $v'' = 0$–2 (see Section 4 on ultraviolet datasets).

$A = 2.59 \times 10^{-4}\ s^{-1}$ with statistical degeneracy factors of $d_l = 3$ and $d_u = 2$. The resulting line intensities are larger than in HITRAN92 by roughly a factor of 2 due to incorrect conversion of the A of Ref. 56 to S used in previous versions of HITRAN. Suspicion of such missing factors of 2, and concerns about the interpretation of upper atmosphere emissions, such as inferring ozone from SME (Solar Mesosphere Explorer via the $a^1\Delta_g$ 1.27-μm airglow) were expressed by Mlynczak and Nesbitt[59] (who conjectured a significant change in A from one of the reported S values in Table 5 of Hsu et al[58]) and by Pendelton et al.[60] Recent observations in the mesosphere[61] confirm the Badger et al[56] value of the Einstein-A coefficient. Moreover, new line intensity measurements made at National Institute for Standards and Technology[62] and at the Rutherford Appleton Laboratory[63] are roughly 15% larger than the HITRAN96 values. Preliminary comparisons indicate agreement between these two new independent high-resolution studies.

For the $X^3\Sigma_g^-$ ($v = 0$) $\rightarrow$ $X^3\Sigma$ ($v = 0$) band of the $^{16}O^{17}O$ species, the isotopic abundance factor was inadvertently omitted from these line intensities in the 1996 HITRAN database. Thus, the ratio of the line intensity (S92/S96) is 0.000750 on average. In order to properly use the intensities for these data, they should be multiplied by $I_a = 0.000742235$. Other changes in the line intensities are documented in Ref. 51.

Measured halfwidths[64–67] for several bands of the O_2 molecule were collected and compared to derive a consistent set of values.[51] The resulting procedure for addition of the halfwidths to the 1996 HITRAN database is as follows. The $X^3\Sigma_g^-$ pure rotation band uses the data reported by Krupenie[64] for the 60 GHz lines. The electric quadrupole transitions and the transitions involving the $a^1\Delta_g$ state use the A-band values.[65] For the A- and γ-bands, the halfwidths of Ritter and Wilkerson[65] are averaged as a function of N'' for the ^PP and ^PQ lines grouped together and for the ^RR and ^RQ lines grouped together. The halfwidths for both the R and P lines are extrapolated to an asymptotic limit of $\gamma = 0.032\ cm^{-1}$/atm for $N'' = 40$ after which the constant asymptotic limit value is used. The values of the halfwidths of O_2 used in HITRAN96 are given in Ref. 51. New measurements of halfwidths and shifts for the bands beyond $10000\ cm^{-1}$ are in progress (L.R. Brown, private communication, 1998).

The error code (see HITRAN96 manual) for the halfwidths is set to 4. The error code for the line positions of $X^3\Sigma_g^- \rightarrow X^3\Sigma_g^-$ electronic band is set to 4 and all other error codes are not utilized for oxygen (i.e., set to 0). The electric-quadrupole and magnetic-dipole transitions are labeled by the lower case letters q and d, respectively, in the sym field of the rotational quantum number character string, i.e. Br, F'',_,; Br, N'', Br, J'', __, Sym (Group 5 in Table 4).

2.8. *NO (molecule 8)*

For the $^{14}N^{16}O$ isotopic species of nitric oxide (99.39% in natural abundance), a synthetic spectrum was calculated in the fundamental region. This calculation was made possible through more accurate measurements[68,69] of line positions and intensities in the allowed and forbidden sub-bands of the fundamental band 1–0, as well as in the allowed sub-bands of the hot-band 2–1. The accuracy of the lambda-doublings and of the absolute line intensities was noticeably improved, and the hyperfine structure was taken into account in the measurement procedure when it was necessary.

In the involved spectral region, i.e. between 1487 and 2189 cm^{-1}, positions and intensities of 9196 transitions were included in the updated HITRAN database version (for these lines, data related to pressure broadening and shifts were not changed). The computation was performed for J'' up to 45.5 for the $1 \leftarrow 0$ sub-bands, and up to 30.5 for the $2 \leftarrow 1$ sub-bands. No cutoff was fixed for the line intensities. The quantum numbers F'' and F' of the transitions, associated with the total angular momentum of the lower and upper rovibrational levels respectively, were indicated in the local quanta dedicated columns of the HITRAN format. Note that the reported value of E'', the energy of the lower level of the transition, is purely rovibrational, i.e., it does not take into account the hyperfine structure; the origin of energy for E'' is zero for the lowest level. In the concerned spectral region, the uncertainty in the absolute line positions is between 0.0001 and 0.001 cm^{-1}, and the uncertainty in the absolute line intensities is 7% or better.

A critical evaluation of the HITRAN NO line parameters is presented in a separate paper in this issue by Goldman et al.[70] In particular, it emphasizes the improvements in the database, but also specifies some setbacks, such as the loss of the individual halfwidths of the (1–0) band and some of

the lines of the (2–1) band. This paper also includes a detailed account of ongoing NO studies beyond HITRAN, which will be incorporated in future editions of the database.

2.9. SO_2 (molecule 9)

Because of its presence in interstellar clouds and in the atmosphere of Venus, sulfur dioxide is well known to be both of astrophysical and planetary importance. In the terrestrial atmosphere, SO_2 is produced by both anthropogenic and natural sources, and is responsible for the production of acid rain. Strong volcanic eruptions, such as the Mount Pinatubo eruption in the Philippines in June 1991, can deposit a large amount of SO_2 in the atmosphere. Once in the stratosphere, sulfur dioxide is converted into sulfate aerosols which affect both stratospheric chemistry and climate.[71–73]

The HITRAN database provides SO_2 parameters for two isotopic species, namely $^{32}S^{16}O_2$ and $^{34}S^{16}O_2$, in seven different spectral regions, which correspond to transitions within the ground vibrational state, and the 19.3-, 8.6-, 7.3-, 4-, 3.7- and 2.5-μm spectral regions (respectively the bands ν_2, ν_1, ν_3, $\nu_1 + \nu_3$ and $\nu_1 + \nu_2 + \nu_3 - \nu_2$, $2\nu_3$, and $3\nu_3$). The corresponding line lists are extensively described in the accompanying article by Perrin et al;[74] we give here only comments concerning the spectral range recently updated. A more global overview, with recommendations for future improvements, is also given in the same article.[74]

2.9.1. The 8.6- and 7.3-μm regions. The 8.6- and 7.3-μm regions correspond to the ν_1 and ν_3 bands of SO_2. The ν_3 band is actually the strongest infrared band of SO_2. This ν_3 band unfortunately presents the disadvantage of being overlapped with the strong ν_2 band of water vapor, preventing measurements of SO_2 in this infrared region from the ground. However, this infrared band may be used from space-borne instruments for stratospheric measurements of SO_2.[73] On the other hand, the ν_1 band, although about nine times weaker than ν_3, corresponds to a rather clear atmospheric window.[71] In 1992, the SO_2 ν_1 and ν_3 line parameters were included in HITRAN92,[1] but we still believe that these parameters need refinements: first because the line positions which were generated for the ν_1 and ν_3 bands did not take into account the rovibrational resonances, thus preventing a correct calculation of the positions of lines involving high-rotational quantum numbers, and second, because the line intensities were generated using various low resolution total band intensity measurements. Actually, a recent study of these bands was performed: the resonances involving the ν_1, ν_3 and $2\nu_2$ interacting bands were taken into account explicitly leading to more accurate line positions.[75] The line intensity study of the ν_1 and ν_3 bands is in progress, using both medium- and high-resolution line intensity measurements.[76]

2.9.2. The 4-μm spectral region. This spectral range corresponds to the $\nu_1 + \nu_3$ band and the $\nu_1 + \nu_2 + \nu_3 - \nu_2$ first associated hot band. Although this band is not the strongest infrared band of this molecule, it corresponds to a very clear atmospheric window, and is thereby of atmospheric importance. Lines from these two bands were recently updated for the $^{32}S^{16}O_2$ isotopic species using the line list which was generated in Lafferty et al.[77] As compared to the previous line lists, the line positions are more accurate because they were generated using new experimental data recorded by a difference-frequency laser spectrometer and because the rovibrational resonances were explicitly taken into account. On the other hand, the line intensities were derived using both high- and medium-resolution experimental data, leading to values of the total band intensity $S_v(\nu_1 + \nu_3) = 0.539 \times 10^{-18}$ cm^{-1}/(molecule·cm^{-2}) and $S_v(\nu_1 + \nu_2 + \nu_3 - \nu_2) = 0.425 \times 10^{-19}$ cm^{-1}/(molecule·cm^{-2}). These values differ significantly from the previous ones quoted in HITRAN92 (0.395×10^{-18} and 0.211×10^{-19} cm^{-1}/(molecule·cm^{-2})). It is worth noticing that the $\nu_1 + \nu_3$ band of the $^{34}S^{16}O_2$ isotopic variant needs improvement: indeed according to the total band intensity presently quoted in HITRAN for $^{34}S^{16}O_2$ (i.e. 0.6027×10^{-20} cm^{-1}/(molecule·cm^{-2})) the ratio of $^{34}S^{16}O_2$ and $^{32}S^{16}O_2$ band intensity for the $\nu_1 + \nu_3$ band differs significantly from the isotopic ratio of these two isotopomers.

2.9.3. The 3.7-μm spectral region. The line parameters corresponding to this spectral range have been introduced for the first time in HITRAN using the $2\nu_3$ line positions and line intensities recently obtained by Lafferty et al.[78]

2.9.4. The 2.5-μm spectral region. The SO_2 line parameters in the 2.5-μm spectral region, which corresponds to the $3\nu_3$ bands, were included in the HITRAN database for the first time because this rather weak band corresponds to an infrared window for the Venus atmosphere. More explicitly, the

SO_2 signature in the $3\nu_3$ Q branch could be identified at 4050 cm^{-1} in the Venus infrared spectrum.[79] These $3\nu_3$ line parameters were generated from the extensive line-position and line-intensity study[80,81] which was performed using various techniques (Fourier transform spectra and difference-frequency laser measurements) and taking into account all the relevant rovibrational resonances.

2.9.5. Line-broadening parameters. In HITRAN 1996, different broadening parameters ($\gamma_{air} = 0.110$–$0.152\ cm^{-1}/atm$, $n = 0.5$–0.75 and $\gamma_{self} = 0.39$–$0.40\ cm^{-1}/atm$ or no value) are reported for the various SO_2 microwave or infrared bands. At first approximation, no rotational dependence is included for these broadening parameters. These values are based on theoretical calculations of averages of measurements of Tejwani[82] and Yang et al[83] which are in rather reasonable agreement with the diode laser measurements performed in the microwave region or in the ν_3 and ν_1 bands except for lines involving rather high rotational quantum numbers.[84,85] The pressure-shift coefficients are set to the default value of zero for all lines.

2.10. NO_2 (molecule 10)

Because of the importance of nitrogen dioxide in the photochemistry of the atmosphere, this molecule has been the subject of numerous studies. In the HITRAN database,[1,86] four spectral domains involve $^{14}N^{16}O_2$ namely, the pure rotation region, and the 13.3-, 6.2-, and 3.4-μm regions. Tables 1 and 2 of Perrin et al[74] give a summary of the existing linelists, the number of lines, the frequency range, the intensity range, and the band intensity together with the year of their most recent update.

$^{14}N^{16}O_2$ is an asymmetric rotor with a doublet structure due to the electron spin-rotation interaction and a hyperfine structure due to interactions involving the ^{14}N nuclear spin ($I = 1$). Also starting from the first triad of interacting states, one has to consider rovibrational interactions. Depending on the spectral range of interest, it is necessary to take explicitly into account some of these interactions to accurately calculate the line positions and intensities. The rotational quantum numbers which need to be defined are N, K_a, K_c, $J = N \pm 1/2$, and, when the hyperfine structure has to be considered, $F = J, J \pm 1$. The coding of the J and F quantum numbers, which differ from one spectral region to the other, is given in Table 2 of Ref. 74. We will describe here only the spectral ranges which were recently updated or for which specific recommendations for the future are given.

2.10.1 The 13.3-μm region. In the 13.3-μm region, a new analysis of the ν_2 band[87] has shown that the hyperfine interaction should be taken into account together with the spin-rotation interaction because the hyperfine structure is easily observable in some parts of the ν_2 band. Consequently, a new line list was generated for the ν_2 band and included in HITRAN96. Subsequently, the first hot band $2\nu_2$–ν_2 (i.e. the $020 \leftarrow 010$ vibrational transition), which was not present in the previous versions of the database, was included in this linelist: for this hot band the hyperfine structure was not modeled. For these two linelists generated in the 13 μm region, new experimental line positions obtained from Fourier transform spectra[87] and ν_2 experimental lines intensities measured by Devi et al[88] were used.

2.10.2. The 6.2-μm region. The 6.2-μm region corresponds to the strongest infrared band of this molecule and is largely used for measurements of atmospheric nitrogen dioxide from high-altitude experiments (balloon or satellite). Because of the importance of the 6.2-μm region, the spectral linelist corresponding to the ν_3 band (which is the main cold band in this region), and to the ν_1 and $2\nu_2$ interacting cold bands were updated in HITRAN96. This line list was generated using the new measurements on line positions[89] and line intensities[90,91] performed for the ν_1, $2\nu_2$ and ν_3 interacting cold bands. For the line position calculations, the theoretical model takes explicitly into account the (1 0 0)↔(0 0 1) and the (0 2 0)↔(001) first- and second-order Coriolis interactions affecting the rovibrational levels. Furthermore, the contribution to the energy levels due to the spin-rotation interaction was taken into account explicitly in this new line list. Let us recall that this interaction was only taken into account through a perturbation method in the previous HITRAN version.[1] Finally, the first hot band, namely $\nu_2 + \nu_3 - \nu_2$, was not updated: it is anticipated that this first hot band in the 6.2-μm region will be improved in the future using the results of the recent and more accurate analysis performed for this band in Perrin et al.[92]

According to the results of the spectra recorded by the NASA Limb Infrared Monitor of the Stratosphere instrument performed in the 6.2-μm region where an excess of stratospheric NO_2 radiance was observed, Kerridge and Remsberg[93] suggested the existence of a Non-Local Thermodymical Equilibrium (NLTE) situation for NO_2 in the stratosphere involving highly excited v_3 vibrational states. Because of the higher spectral resolution provided by future emission sensing instruments such as MIPAS (Michelson Interferometer for Passive Atmospheric Sounding),[94] we can expect to see this effect much better. For this reason it may be necessary to include in a future version of HITRAN the line lists corresponding to the $(n+1)v_3 - nv_3$ hot bands of NO_2. The first member of this sequence is the $2v_3 - v_3$ hot band, for which very accurate line parameters are now available.[95]

2.10.3. The 3.4-μm region. The 3.4-μm region corresponds to the $v_1 + v_3$ cold band and to its associated first hot band $v_1 + v_2 + v_3 - v_2$. The 3.4-μm band, which is about 20 times weaker than the 6.2-μm band, is also of atmospheric interest because it falls in a relatively clear atmospheric window and is then usable for atmospheric measurements from the ground. The linelists included in HITRAN for the $v_1 + v_3$ and $v_1 + v_2 + v_3 - v_2$ bands were generated in 1982.[96] The line positions and intensities used as input for the 1982 calculations were obtained, depending on the bands, from grating and Fourier transform spectra (see Refs. 74 and 96 and references therein). When dealing with the line positions, the rovibrational resonances involving the $\langle v_1, v_2, v_3\rangle \Leftrightarrow \langle v_1, v_2 \pm 2, v_3 \mp 1\rangle$ resonating states were explicitly taken into account, but on the other hand, the spin-rotation interaction was only taken into account through a second-order perturbation treatment. Accordingly, the accuracy of the line positions is of the order of $1\text{–}5 \times 10^{-3}$ cm^{-1} for most of the lines appearing at 3.4 μm in the HITRAN96 line list, this accuracy deteriorating for lines affected by a spin-rotation resonance or involving high rotational quantum numbers. A new analysis of the $v_1 + v_3$ band has been performed recently using Fourier transform spectra[97] and an improved theoretical model described in Ref. 74. Also in the work of Mandin et al,[97] line-intensity measurements were performed: as compared to those presently quoted in HITRAN, these experimental intensities are in good agreement for the $v_1 + v_3$ band, but are about 1/1.48 lower for the $v_1 + v_2 + v_3 - v_2$ hot band. For all these reasons, a future update of NO_2 in the 3.4-μm region is recommended.

2.10.4. Line-broadening parameters. As compared to HITRAN92, there is no update of the broadening parameters, i.e. the same value of the air-broadening coefficient (namely $\gamma_{air} = 0.067$ cm^{-1}/atm) is quoted for all lines of all bands, with the value $n = 0.5$ for its temperature dependence. Also no value is quoted in HITRAN for the self-broadening parameter and for the air-broadened pressure shift.

2.11. NH_3 (molecule 11)

Bands of ammonia are now included for the first time between 2100 and 5300 cm^{-1}, increasing the spectral region covered by the ammonia parameters by nearly 150%. Below 2100 cm^{-1}, the positions and intensities of the transitions remained essentially unchanged from the values on the 1986 HITRAN database;[2] the only major change was to decrease the intensity of v_2–v_2 by a factor of two. Throughout the NH_3 compilation, the prior default constant line widths were replaced by estimates provided by a polynomial fit of measurements for transitions of $J'' < 13$. The temperature dependence of the widths was set to a constant, however, and no pressure shifts were provided.

The additional regions were available from completed studies of four different band systems at 4-, 3-, 2.3- and 2-μm.[98–101] At 4 μm, the positions and intensities of the $3v_2$ and $v_2 + v_4$ bands were measured using the Kitt Peak FTS and modeled by Kleiner et al[98] to provide a prediction of nearly 1100 transitions of the main isotope. Some 270 unassigned lines based on measured positions and intensities were also included; the lower state energies of these features were set to 300 cm^{-1} (thereby being inconsistent with the customary HITRAN flag of − 1). At 3 μm, a prediction of nearly 900 transitions of the v_1 and v_3 bands of the main isotope was made using the energy-level analysis of Guelachvili et al.[99] At 2.3 μm, a similar energy-level study of the $v_1 + v_2$ and $v_2 + v_3$ bands by Urban et al[100] provided the fitted constants for a prediction of the two strongest bands in the region. Finally, at 2 μm, the empirical study of Brown and Margolis[101] resulted in a comprehensive linelist of measured positions and intensities. Lower state energies were determined either from some 900

quantum assignments to the $\nu_1 + \nu_4$ and $\nu_3 + \nu_4$ of both isotopes or from the measurement of intensities at different sample temperatures. Over 1100 unassigned features were included.

The intensities of the 4- and 2-μm bands are based on recent measurements using the Fourier transform spectrometer at Kitt Peak (Refs. 98 and 101, respectively). The intensities in the 3- and 2.3-μm bands were set using unpublished results of Š. Urban and P. Pracna (Czech Academy of Science, 1993), but these values are somewhat different from those in the literature. For example, for ν_1 and ν_3, the database has band intensities of 20.5 and 21.4 cm^{-2}/atm compared to 22.3 and 13.1 cm^{-2}/atm reported by Pine and Dang-Nhu,[102] while for $\nu_1 + \nu_2$ and $\nu_2 + \nu_3$, the database has band strengths of 2.8 and 16.1 cm^{-2}/atm compared to 2.71 and 19.0 cm^{-2}/atm reported by Margolis and Kwan.[103]

All prior editions of the ammonia linelists contained a constant default value of 0.075 cm^{-1}/atm for most of the air-broadened line widths and zero for the self-broadened widths. However, measurements of self- and foreign-broadened widths of ammonia in the ν_1 Q branch were made by Pine et al[104] and Markov et al[105] for 58 transitions. Later, Brown and Peterson[106] determined that the N_2 and O_2 data could be reproduced to within $\pm 4\%$ using a simple polynomial expression involving J'' and K''. These expressions and constants for Q-branch lines were applied to all the ammonia transitions for $J'' < 13$. At higher quanta, default values of 0.06 and 0.40 were used for air- and self-broadening respectively. It is seen that the P-, Q-, and R-branch transitions at the same J'' and K'' had widths that differed by 5–10% even at low quanta and so applying Q-branch widths to R- and P-branch transitions are not as reliable as individual measurements. Thus, using Q-branch line widths for the P and R branches will introduce small systematic errors.

For the 1996 HITRAN database, an attempt was made to standardize the information in the rotational fields. Because past updates were done in different decades, the parameters in the rotational, ν_2, and ν_4 regions had different notations to indicate the inversion symmetries. Early editions had used the symbols + and − in the rotational fields to show identification of the levels, while later providers made line lists with the inversion symmetry indicated only by the vibrational code or only in the rotational fields. In the 1996 HITRAN, the new entries, and many of the old below 2000 cm^{-1}, are written with a scheme in which "a" and "s" appear in both the rotational and vibrational fields. Unfortunately, some errors were made. The rotational lines of the $^{15}NH_3$ isotopomer are still written + and − rather than a and s. In the main isotope, the far-infrared rotational a → s lines have been incorrectly written as s → a throughout. In the 2-μm region, the lower-state vibrational indices for the "s" states are listed as "a", although the inversion symmetries are correct in upper state vibrational field and both the rotational fields. For these regions, users should review the original references to understand if the database identifications are correct for specific transitions. With new work in progress for the 3- and 6-μm regions (I. Kleiner, Université Paris-Sud, France, private communication, 1998), some of these inconsistencies can be corrected in future editions.

One should note that the vibrational indices were selected to maintain backward compatibility with the prior version of the database. The first four codes indicate the vibrational states without the inversion symmetry; code 1 to 4 are respectively, 0000, 0100, 0200, and 0001. Codes 5–8 involve the same states with for the "a" levels (0000a, 0100a, 0200a, 0001a), while codes 9–12 are the same states for the "s" levels. Code 13 is used to indicate unassigned lines that appear in the 4- and 2-μm regions. The higher codes are used for the new bands above 2100 cm^{-1}. The correspondence of the HITRAN codes used for these "global" quanta to standard spectroscopic notation are given in several places in the HAWKS compilation.

2.12. HNO_3 (molecule 12)

An extensive HNO_3 line-parameter update was incorporated into the 1992 HITRAN as summarized in Rothman et al,[1] with more details given by Goldman and Rinsland.[107] Subsequently, a number of studies have been completed which provide significant improvements in the quantitative spectral parameters of HNO_3. These include the works of Perrin et al,[108–111] Sirota et al,[112] Coudert and Perrin,[113] Goyette et al,[114] Paulse et al,[115] and Wang et al.[116] The only changes from the 1992 HITRAN to 1996 HITRAN databases are in the (ν_5, $2\nu_9$) lines. These changes, and the more recent studies are reviewed in a separate paper in this issue by Goldman et al,[117] which also includes

recommendations for the next version of the database. A few of the findings detailed in that paper will be highlighted in the discussion below, which will proceed by the wavelength regions.

In the 25-μm region, both 1992 HITRAN and 1996 HITRAN have only the same ν_9 (458.2 cm^{-1}) lines, taken from the work of Goldman et al.[118] Hot bands and combination bands associated with the ν_9 band between 380 and 450 cm^{-1} are currently not contained in HITRAN96. These transitions are easily observable in atmospheric remote sensing measurements[10] and should be included in future releases. New ν_9 line-intensity measurements by Sirota et al[112] provide a new band intensity of 0.842×10^{-17} $cm^{-1}/(molecule \cdot cm^{-2})$ at 296 K, i.e. a value 0.78 times that in HITRAN. Of the several hot bands that are observable in the ν_9 region, preliminary line parameters have been generated for $3\nu_9 - 2\nu_9$ (392.4 cm^{-1}) and $3\nu_9 - \nu_5$ (409.8 cm^{-1}) by Perrin et al.[111] The generation of line parameters for the stronger hot bands $\nu_5 - \nu_9$ (420.88 cm^{-1}) and $2\nu_9 - \nu_9$ (438.22 cm^{-1}), which overlap significantly with the ν_9 lines, is still to be done. The positions for these bands can be calculated from the spectroscopic constants contained in Refs. 108, 109, and 118.

In the 11-μm region, the line parameters of the HNO_3 (ν_5, $2\nu_9$) lines in the 1996 HITRAN have been taken from the work of Perrin et al,[109] normalized to the band intensity of Giver et al.[119] It should be noted that approximate parameters of the two 11-μm hot bands from the 1992 HITRAN have not been updated for the 1996 HITRAN. These are listed as $\nu_5 + \nu_9 - \nu_9$ at 877.0 cm^{-1} and $3\nu_9 - \nu_9$ at 885.0 cm^{-1}. It is recommended that both be removed from the database. The recent studies show that the first one should be eliminated, as there is no hot band there, and the second should be replaced by the strong Q branch at 885.42 cm^{-1} which has been analyzed as the $\nu_5 + \nu_9 - \nu_9$ hot band. Preliminary line parameters have been generated (see Goldman et al[117]), and used, together with the new ν_5, $2\nu_9$ lines, for a number of atmospheric studies, but have not yet been included in HITRAN. Other new findings have been recently reported in the 11-μm region. The weak band observed in spectra near 830 cm^{-1} has been analyzed as the $3\nu_9 - \nu_9$ Q branch by Perrin et al.[111] Preliminary line parameters have been generated for the main absorption region of 828–832 cm^{-1}. The studies with the new parameters show significantly improved modeling of atmospheric absorption and emission spectra in the 11-μm region.

A number of recent studies have been dedicated to the effects of torsional splitting of HNO_3 energy levels on the millimeter/submillimeter and infrared spectra, as reported by Goyette et al,[114] Coudert and Perrin,[113] and by Paulse et al.[115] Except for $\nu_9 = 3$, these effects are too small for infrared transitions of interest in atmospheric spectra. None is included at this time in the HITRAN database.

Several recent and ongoing lab efforts have been dedicated to more accurate and consistent determination of the absolute band intensities in the ν_2, ν_3, ν_4 and (ν_5, $2\nu_9$) regions. Several aspects of these comparisons are summarized in Goldman et al.[117] The comparisons show significant inconsistencies in the laboratory measurements and improper hot-band correction for the 11-μm (ν_5,$2\nu_9$) and 7.6-μm (ν_3,ν_4) bands, but good consistency for the 5.8-μm (ν_2) bands. The work is not complete, and the recommendation adopted for the 1996 HITRAN, was to normalize to Giver et al,[119] with the proper hot band correction, using $Q_V = 1.304$ at 296 K. Thus, the ν_5, $2\nu_9$ lines of Perrin et al[109] are normalized to Giver et al,[119] without the hot bands, while the 11-μm obsolete hot bands are still in the database.

The ν_3 and ν_4 band line parameters in the 1992 HITRAN were taken from Perrin et al,[120] and normalized approximately to the intensity measurements of May and Webster.[121] The subsequent work of Perrin et al[108] discusses some of the standing theoretical difficulties in the analysis of these bands and provide a new normalization of the same line parameters, with a different intensity ratio of ν_3 to ν_4 bands that has not been implemented for the 1996 database.

Improvements in the HNO_3 line parameters are needed in other spectral regions. Spectral fitting to high-resolution laboratory and field spectra in the $\nu_8 + \nu_9$ band (1205.7 cm^{-1}) show disagreements between the observed and calculated spectra. Recently, Wang et al[116] re-analyzed the $\nu_8 + \nu_9$ region and provided new spectroscopic constants. Spectral fitting using line parameters generated with these constants show improved agreement, but additional work on both positions and intensities is needed for this region.

Laboratory spectra indicate several other bands of importance to atmospheric spectra that have not been analyzed yet. In particular, the ν_1 band (3551.7 cm^{-1}) is clearly visible in the ATMOS

(Atmospheric Trace Molecule Spectroscopy experiment[122,123]) spectra below ~30 km tangent height. The laboratory spectra also show a number of other weak bands of some importance in the atmosphere in the 700–1200 cm^{-1} region.

The air-broadened halfwidths and the temperature-dependent coefficient were retained from the 1992 HITRAN (Goldman and Rinsland[107]). Air-broadened widths of 0.11 cm^{-1}/atm at $T = 296$ K and the temperature-dependence coefficient of $n = 0.75$ have been taken from May and Webster.[121] No self-broadened halfwidth value is included; however, it was listed as 0.73 cm^{-1}/atm at $T = 296$ K by Goldman and Rinsland.[107]

2.13. OH (molecule 13)

The OH $X^2\Pi$–$X^2\Pi$ line parameters in the HITRAN databases have remained essentially unchanged since HITRAN82.[1,2,124] These databases contain the sequences $\Delta v = 0,1,2,3$ with $v' = 0, \ldots, 9$, and $J_{max} = 15.5$. The pure rotation portion of both the 1992 and 1996 editions contain only the 0–0 band (for the 3 leading isotopes), and come from (respectively) the 1985 and 1996 versions of the JPL catalog.[125,6] In these editions, the pure-rotation lines include hyperfine structure. The vibration–rotation line parameters are based on the work of Goldman[126] and include main and satellite Λ-doubling transitions (no hyperfine) of ^{16}OH. The HITRAN editions do not include accuracy information about the OH line parameters, and assume the classical value of 0.5 for the temperature dependent broadening coefficient. In the 1992 edition, a single value for the air-broadened halfwidth had been assumed for all OH lines. In the 1996 edition the air-broadened widths for the pure-rotation lines have been revised.

The transition probabilities for all the lines have been altered slightly in the 1996 version due to an updated version of the partition function (from the TIPS program[127]) used to calculate the transition probability from the intensity. In addition, the line parameters for most of the pure rotation lines from the JPL catalog have revised values for (all except the Q-branch lines between 0 and 7.4 cm^{-1}) the transition frequency, the intensity, and the lower state energy.

A significant update of the OH $X^2\Pi$–$X^2\Pi$ line parameters beyond HITRAN96, has been recently completed.[128] The new set is composed of the $\Delta v = 0, \ldots, 6$ dipole-allowed transitions between $v = 0$ and $v = 10$, with J up to a maximum value of 49.5, with low intensity cutoffs applicable to both atmospheric and high temperature studies. In all, line parameters for 56 separate bands were calculated: 11 pure rotation bands and 45 vibration–rotation bands with both main and satellite branches. The transition frequencies were determined from three different sets[129–131] of calculated term values in order to have the most accurate set of line positions over a wide range of both vibration and rotation quantum numbers. An improved method for calculating vibrational wavefunctions for the $X^2\Pi$ states of OH has been adopted,[132] and as used in conjunction with the latest OH dipole-moment function,[133] yields improved transition-moment integrals, leading to more accurate line intensities. In addition to updating the line parameters themselves, estimates have been included for the uncertainties associated with the line parameters using the HITRAN accuracy indices.

The single value (0.083 cm^{-1}/atm) for the air-broadened halfwidth assigned to all OH lines in the 1992 HITRAN database, and all vibration–rotation lines in the 1996 edition, dates back to Bastard et al.[134] This corresponds to the measured halfwidths of the transitions around 13.4 GHz between the four levels with $v = 0$ and $J = 7/2$. A number of recent papers (Chance et al,[135] Schiffman and Nesbitt[136] (who also presented evidence for collisional narrowing), and Park et al[137]) extend the range of J values whose halfwidths are measured, and also cast doubts about the accuracy of the results of Bastard et al.[134] The measured halfwidths show a linearly decreasing dependence on N that is consistent with theory. Averaging these experimental values yielded $T = 296$ K halfwidths for $N = 1$ to 4 (0.095, 0.086, 0.0065, and 0.053 cm^{-1}/atm, respectively). Extending linearly to $N = 5$ leads to the halfwidth of 0.040 cm^{-1}/atm, which has been assigned to all transitions with lower levels $N'' > 4$.

The temperature dependence of the halfwidths remains much less studied. A theoretical study by Buffa et al[138] has calculated the broadening coefficient for four different strong pure rotation OH lines using the impact approximation. The values vary between 0.59 and 0.72, from which the average value of 0.66 was adopted for all lines.

Complete details on the procedures used for the new data set are given in Ref. 128. Due to a lack of available experimental data, no values were assigned for the air-broadened pressure shift, nor for the self-broadened halfwidth. Re-measurement of the 118 cm^{-1} air-broadening coefficient is in progress (K. Chance, private communication, 1997).

It is also of interest that line parameters for the $A^2\Sigma$–$X^2\Pi(0, 0)$ OH band in the 3085 Å region have been available[139] but not yet incorporated into the HITRAN database. Some of these calculations have been updated recently by Cageao et al.[140]

2.14. HF (molecule 14)

The only modifications to hydrogen fluoride have been in the pure rotational region. The positions for the rotational transitions up to R4 have been updated to those measured by Nolt et al.[141] The strengths of the rotational transitions are taken from the compilation of Chance et al[39] which have been calculated based on the constants of Ref. 141. The pressure broadening widths for the rotational transitions are taken from the measurements of Pine and Looney[142] where they exist. The parameters for the rotational hot bands are unchanged from the HITRAN92 release.

2.15. HCl (molecule 15)

Similar changes to the rotational band have been made to HCl that have been made to HF. The positions are updated to those measured by Nolt et al,[141] the strengths are calculated based on Nolt measurements and accurate dipole-moment measurements,[39] and the pressure-broadening parameters are taken from Pine and Looney.[142] For rotational transitions where no updated positions or pressure broadening were measured, the HITRAN92 values were retained.

Accurate line positions and molecular constants of the (1–0) band of $H^{35}Cl$ and $H^{37}Cl$ have been derived recently from high-resolution laboratory measurements by Rinsland et al.[143] These values are significantly different from the current HITRAN values for $J > 10$, and will be incorporated in future editions.

2.16. HBr (molecule 16)

The positions and strengths for the rotational band of HBr are taken from the compilation of Chance et al.[39] The positions up to 200 cm^{-1} are those from the measurements of DiLonardo et al[144] and the strengths are based on these measurements and accurate dipole-moment measurements. The parameters for lines above 200 cm^{-1} are taken directly from HITRAN92. All pressure-broadening terms are taken directly from HITRAN92.

New parameters have recently become available for the fundamental, which include hyperfine structure, as described in an accompanying article in this issue by Coffey et al.[145] The hyperfine structure is required for modeling both pure-rotation and vibration–rotation low-J lines at high resolution. These data will be incorporated in a future release of HITRAN.

2.17. HI (molecule 17)

There have been no updates of this species for the 1996 database. However, it has been found that the HITRAN line-position calculations are not consistent with the Dunham coefficients quoted in Ref. 1 as the source for the calculations. For example, differences of ± 0.004 cm^{-1} are observed for the (0–1) band. Also, the (1–0) intensities are not consistent with the quoted laboratory measurements.

It should also be noted that the hyperfine splitting in HI is the largest of the hydrogen halide molecules, and is required for low-J lines. The hfs line parameters and molecular constants for both the pure-rotation (0–0) and the fundamental band (1–0) have recently been generated.[146] These data will be made available for the next edition of HITRAN.

2.18. ClO (molecule 18)

The HITRAN96 line parameters for the $X^2\Pi$–$X^2\Pi$ (1–0) bands of ^{35}ClO and ^{37}ClO were calculated as described by Goldman et al.[147] The improvements were made possible on the basis of the work of Burkholder et al[148,149] and yielded more accurate line positions and intensities than previously available for HITRAN92.

The absolute wavenumber accuracy of these lines is estimated as $\pm 0.0003\ cm^{-1}$. The integrated band intensity has been normalized to the laboratory value of $S = 9.68 \pm 1.45(2\sigma)\ cm^{-2}/atm$ at 296 K, following Burkholder et al.[149] This corresponds to $3.904 \times 10^{-19}\ cm^{-1}/(molecule\,cm^{-2})$ at 296 K, compared to $4.884 \times 10^{-19}\ cm^{-1}/(molecule\,cm^{-2})$ adopted for HITRAN92. The air-broadened halfwidth for all lines was taken to be the same as that for the measured N_2 broadening,[147] i.e. $\gamma = 0.093 \pm 0.018\ (2\sigma)\ cm^{-1}/atm$ at 296 K, and for the temperature dependence $n = 0.75$ was adopted.[150]

The linear and quadratic Herman–Wallis coefficients of Burkholder et al[148] were $\alpha_{10} = 0.00563(47)$ and $\beta_{10} = 0.23(50) \times 10^{-4}$, respectively. Because of the large uncertainty in β_{10}, it was not used for the line-parameter calculations.

The search for ClO (1–0) features in the atmospheric absorption solar spectrum conducted by Rinsland and Goldman[150] showed that optimal detection could be achieved with a few lines near $833\ cm^{-1}$. A tentative identification of these lines from solar spectra in the Arctic atmosphere has been published by Notholt et al.[151] Quantitative measurements of these lines from high signal to noise spectra have been reported by Bell et al.[152]

New experimental line intensities have been recently provided by Birk and Wagner.[153] The newly measured line strengths were used to determine a vibrational transition dipole moment $-0.03224 \pm 0.00047D$, as well as the linear and quadratic Herman–Wallis coefficients, $+0.00684 \pm 0.00080$ and $+(1.56 \pm 0.64) \times 10^{-4}$ respectively, where quoted errors are 1σ. The corresponding measured band intensity is $9.01 \pm 0.27\ cm^{-2}/atm$ at 296 K, and thus smaller by $\sim 7\%$ from the HITRAN value. Individual lines, however, are smaller by up to $\sim 10\%$ in intensity. These have not been yet incorporated into the HITRAN database.

The pure rotation ClO lines have not been updated from 1992 to 1996. They remain from the JPL catalogs of 1985, as adopted in HITRAN86. The latest JPL catalog,[6] however, contains both $v = 0$ and $v = 1$ lines, while the HITRAN database contains only $v = 0$ lines. The updated parameters of the ClO lines used for Microwave Limb and Sounder (MLS) on the Upper Atmosphere Research Satellite (UARS), as described by Waters et al[154] and by Oh and Cohen[155] have not been yet incorporated into the HITRAN database.

It should be also noted that the transition probabilities listed in the HITRAN96 database for ClO Λ-doubling transitions are too large by a factor of 4. This is due to the extra factor of the nuclear spin degeneracy $\Pi(2I + 1)$ (where $I(^{35}Cl) = I(^{37}Cl) = 3/2$, $I(^{16}O) = 0$) in the conversion from S to $|R|^2$. The transition probabilities for the hyperfine transitions need the same correction.

A recent paper by Donovan et al[156] clearly shows several IR ClO absorption features in ground-based solar spectra recorded from the high Arctic.

2.19. OCS (molecule 19)

There have been no updates of carbonyl sulfide for the 1996 database on the CD-ROM. However, an extensive self-consistent IR linelist is now available from Fayt et al.[157] These parameters have been amalgamated with the pure rotation bands already existing in HITRAN to form a complete set that is available on the HITRAN web-site and represents a total replacement for OCS. It should be remarked that an additional isotopomer is now included in this list for the first time, namely $^{16}O^{12}C^{33}S$ (623 in AFGL code). In keeping with the HITRAN system of numbering isotopes sequentially based on terrestrial abundances, the isotope $^{18}O^{12}C^{32}S$ (822) which has been labeled 4 including the current edition of HITRAN, becomes number 5 hereafter.

2.20. H_2CO (molecule 20)

There have been no updates of this species for the 1996 database. It should be remarked that in the current database, lines sharing quantum identifications (blends) have intensities corresponding to the total intensity of the particular feature.

2.21. HOCl (molecule 21)

No changes have been made to the HOCl compilation since the 1992 release. Improved positions for the rotational band of HOCl exist[158] that should be included in future releases of HITRAN.

2.22. N_2 (molecule 22)

There have been no changes to the $^{14}N_2$ (1–0) vibration–rotation quadrupole band parameters on HITRAN 1996 relative to those on the HITRAN 1992 compilation,[1] except for minor updates to the calculated transition-probability squared parameter. See Rinsland et al[159] for a description of the parameters in HITRAN 1992 and 1996.

2.23. HCN (molecule 23)

There have been no updates of this species for the 1996 database.

2.24. CH_3Cl (molecule 24)

There have been no updates of this species for the 1996 database.

2.25. H_2O_2 (molecule 25)

There have been no updates of this species for the 1996 edition. A new and complete compilation of the rotational transitions have been assembled from recent laboratory data.[160] This updated compilation can now be obtained from the HITRAN web site and will be in future editions of HITRAN.

The strengths of the v_6 band of hydrogen peroxide are currently based on laboratory measurements where the concentration of H_2O_2 was determined by ultraviolet absorption at 254 nm.[161] More recent experiments obtained absolute strengths which are roughly one half as strong as those currently used.[162] This discrepancy needs to be resolved as it has a significant effect on the interpretation of atmospheric retrievals of H_2O_2.[163]

2.26. C_2H_2 (molecule 26)

The positions and intensities of the acetylene bands in the 3- and 13-μm regions have been updated. At 13 μm, the line positions and intensities for the v_5 fundamental, 4 hot bands of $^{12}C_2H_2$ (lower states v_4 or v_5), and the v_5 fundamental of $^{12}C^{13}CH_2$ were replaced with the values reported by Hillman et al[164] and Weber,[165] respectively. The error code for positions corresponds to the overall standard deviations of the fits. Error estimates for the intensities were more conservatively estimated.

The positions and intensities of the 3-μm $^{12}C_2H_2$ bands v_3 and $v_2 + v_4 + v_5$, which are strongly coupled by a Fermi-type interaction, were updated based on the work of Vander Auwera et al.[166] The parameters for the v_3 band of $^{12}C^{13}CH_2$ were not updated for HITRAN 1996.

Air-broadening coefficients for the updated bands are based on the tunable diode laser measurements of $(v_4 + v_5)^0$ band of $^{12}C_2H_2$ reported by Devi et al.[167] Values are assumed to vary as a function of the absolute value of the running index, $|m|$. Self-broadening coefficients for the updated bands were calculated on the basis of the expression reported by Varanasi et al.[168]

Recently, Babay et al[169] reported measurements of pressure-broadening and pressure-shift coefficients for R- and Q-branch lines in the v_5 band broadened by several gases. The shifts in N_2 are small but show a steady increase in magnitude with increasing J in the R branch (from -0.74×10^{-3} at R3 to -2.34×10^{-3}, in cm^{-1}/atm). It is anticipated that the measured values will be added to the next HITRAN update.

2.27. C_2H_6 (molecule 27)

There have been no changes to the ethane parameters on HITRAN 1996 relative to those on the HITRAN 1992 compilation.[1] Concerns noted previously[1,170] regarding the normalization of the intensities of the v_9 band at 822 cm^{-1} remain unresolved.

The compilation still contains a calculation of the Q sub-branches of the v_7 band near 3000 cm^{-1} based on the study by Dang Nhu and Goldman.[171] Improved predictions for the $^pQ_3$ and $^rQ_0$ sub-branches have been used in several recent atmospheric studies.[172] It is anticipated that the parameters for one or both of these sub-branches will be incorporated in the next HITRAN update on the basis of the results from these atmospheric studies or the recent laboratory measurements by Pine and Stone.[173] The analysis of these latter observations includes modeling of tunneling and A1–A2 splittings on the basis of sub-Doppler measurements.

The C–H stretch region of ethane (2870–3050 cm^{-1}) produces numerous strong absorptions[174] not yet incorporated in HITRAN. Missing lines of C_2H_6 are observable in solar occultation spectra, for example, in the region of the Q branches of CH_3Cl (G.C. Toon, Jet Propulsion Laboratory, private communication, 1997).

2.28. PH_3 (molecule 28)

There have been no updates of this species for the 1996 database.

2.29. COF_2 (molecule 29)

The ν_4 band at 8 μm has been totally updated for this edition. This band is the strongest of the IR bands on the compilation. The $2\nu_5$ band in the same region has been added (J.-F. Flaud, private communication, 1994).

The lower-state rotational assignments of ν_1 and $2\nu_2$ have been discovered to be incorrectly transcribed in the current edition of HITRAN, i.e., J'', K_a'', K_c'' have been inadvertently set to J', K_a', K_c' for these bands.

2.30. SF_6 (molecule 30)

There have been no changes to the SF_6 parameters on HITRAN 1996 relative to those on the HITRAN 1992 compilation,[1] except for the inclusion of nonzero values for the calculated transition probability squared parameter. See Rinsland et al[159] for a description of the parameters in HITRAN 1992 and 1996. Note that these parameters include only the strong ν_3 band of $^{32}SF_6$ at 948.1 cm^{-1}. Because of the absence of parameters for the associated hot bands, which contribute about half of the total absorption under stratospheric conditions,[175] it is strongly recommended that users adopt the SF_6 absorption cross-sections in HITRAN rather than the parameters contained in the line-by-line portion of the compilation.

2.31. H_2S (molecule 31)

The line parameters for the ν_1 and ν_3 fundamentals and the $2\nu_2$ overtone of $H_2{}^{32}S$, $H_2{}^{34}S$ and $H_2{}^{33}S$ at 4 μm have been included for the first time. The prediction for these parameters were generated as part of an extensive study of hydrogen sulfide[176] from 1 to 5 μm. The constants for the line positions and intensities for the HITRAN list are a combination of the earlier results of Lechuga-Fossat et al[177] and preliminary results from new work that have since been completed.[178] Air- and self-broadened widths were set respectively to constant values of 0.08 and 0.175 cm^{-1}/atm with the temperature-dependence coefficient of 0.75. However, completed results of Brown et al[178] have produced a prediction of both the 4- and 2.7-μm region that includes 24 bands (from the ground state and several of the strongest hot bands for three isotopes); these appear on the GEISA databank.[50]

2.32. HCOOH (molecule 32)

The formic acid (HCOOH) line parameters for ν_6 included in HITRAN96 originate from the 1984 work of Goldman and Gillis.[179] For that work, a listing of Hamiltonian constants and assigned lines for the ν_6 band of HCCOH was provided (E. Weinberger, private communication, 1983). The Hamiltonian used is the Watson S-form for P^2 and P^4 terms and the Watson A-form for P^6 terms. The ν_6 band is predominantly type A but also includes type B and C transitions as well as electric-dipole forbidden Q-branch transitions. The contributions from each transition type was estimated to be proportional to the number of lines assigned to that type.

Because our calculation did not handle forbidden transitions, the intensity of the forbidden transitions was given to the type A transitions. Line parameters were generated from 1000 to 1200 cm^{-1}, $T = 296$ K, $S = 225$ cm^{-2}/atm. A-, B-, and C-type transitions were assigned relative strengths of 79%, 6%, and 15%, respectively. This intensity gives the 28 cm^{-2}/atm intensity in the Q-branch region used by Goldman et al.[180]

Comparisons of a University of Denver laboratory spectrum (1.6 torr in a 10-cm cell at room temperature, 0.05 cm^{-1} resolution) and a calculated spectrum were made.[175] For the calculated

spectrum an arbitrary self-broadening Lorentz halfwidth of 0.4 cm^{-1}/atm was chosen and the intensities of all lines were multiplied by 2.0. This gave good agreement in the Q-branch region. Agreement throughout the rest of the band is somewhat poorer for three reasons: (1) perturbations of ν_6 line positions (some exceeding 0.1 cm^{-1}) are ignored because they have not been analyzed; (2) no effort has been made to account for a significant part of the intensity (perhaps 10 or 20%); and (3) the value of the Lorentz halfwidth is unknown. Because of these shortcomings, it is not surprising that the observed and calculated spectra agree in some regions and disagree in others.

Based on the good match between the observed and calculated Q-branch intensities using the scale factor of 2.0 and 0.4 cm^{-1}/atm halfwidth, HCOOH ν_6 line parameters were regenerated in HITRAN format. These line parameters include all lines stronger than 1% of the strongest line. The intensities of all lines on the file sum to 1.757×10^{-17} cm^{-1}/(molecule cm^{-2}) at 296 K. It should be noted that the calculated Q-branch intensity is approximately twice as large as that used by Goldman et al.[180] The air-broadened halfwidth on the HITRAN database is 0.1 cm^{-1}/atm at 296 K, with temperature dependence of $n = 0.75$, for all lines. The self-broadened halfwidth is not given.

These HCOOH line parameters have been used successfully in a number of atmospheric studies, such as the measurement of HCOOH in surface-level air based on Kitt Peak black-body spectra by Rinsland and Goldman[181] and the analysis of biomass fire spectra by Yokelson et al.[182]

More recent spectroscopic constants and line positions (but not intensities), for both ν_6 and ν_8, have been published by Bumgarner et al.[183] These data have not been applied yet for updating the HCOOH line parameters. Line positions and intensities for the pure rotation spectrum of formic acid are available from the work of Vander Auwera.[184]

2.33. HO_2 (molecule 33)

The HO_2 radical is a new addition to HITRAN. The positions for the pure rotational transitions are calculated based on the measurements of Chance et al.[185] The strengths are calculated using the dipole-moment measurements of Saito and Matsumura.[186] All of the pressure broadening parameters for these transitions, which cover the spectral range up to 334 cm^{-1}, are set to the value measured for the 83.32 cm^{-1} transitions.[187]

The three fundamentals, ν_3 at 1098 cm^{-1}, ν_2 at 1392 cm^{-1}, and ν_1 at 3436 cm^{-1}, have been added to HITRAN. The positions and energy levels for these bands come respectively from Nelson and Zahniser,[188] Nagai et al,[189] and Yamada et al.[190] The intensities for all three fundamentals have been calculated by Zahniser et al,[191] while a default value of 0.108 cm^{-1}/atm for the air-broadened halfwidths based on the work of Nelson and Zahniser[192] has been adopted.

2.34. O (specie 34)

Atomic oxygen is a new addition to HITRAN. Only 2 transitions in the far-infrared (68.716508 and 158.268741 cm^{-1}) have been compiled. Both of these transitions have significant optical depths in the mesosphere and thermosphere and have been observed in remote sensing atmospheric spectra.[10] The positions have been accurately measured by Zink et al.[193] The strengths for these two lines were obtained from the JPL catalogue[6] and the pressure broadening values were arbitrarily set to 0.05 cm^{-1}/atm. As this entry in HITRAN is not a molecule, the quantum fields (iv′, iv″, q′, and q″ of Table 3) for these two transitions do not have any definition.

2.35. $ClONO_2$ (molecule 35)

Chlorine nitrate lines for the ν_4 band from 763 to 798 cm^{-1} have been placed on the line-by-line HITRAN database. The compilation contains over 32 000 lines for this "heavy" molecular species and the positions come from an analysis of the data of Bell et al.[194] The intensities and halfwidths were the result of a study by Goldman et al.[195]

The above line parameters are provided in addition to the cross-sections (see Sec. 3). It must be reiterated that, analogous to the situation for SF_6, the use of these discrete line parameters must be made with caution: they lack significant hot bands and also do not provide the modeler with pressure effects such as line coupling. For scenarios where these effects are likely to be important, we recommend using the $ClONO_2$ cross-sections instead which are provided on the compilation. A detailed review of the $ClONO_2$ line parameters and cross-sections on 1996 HITRAN is given in

a separate paper by Goldman et al.[196] This paper also discusses recent results and ongoing studies not yet included in the database, as well as needs for further improvements.

2.36. NO^+ (molecule 36)

NO^+ represents the first ionic species to be placed on the HITRAN database. It is of particular interest in upper atmosphere emission problems; production of NO^+ is created in vibrationally excited states by molecule-ion collisions, especially during aurora (see, for example, Chapter 12 of Jursa[197]). For this objective, the $\Delta v = 1$ series, with $v'' = 0$ to 5, has been calculated and placed in the supplemental directory of HAWKS. The ion is in the $^1\Sigma^+$ ground electronic state and thus the format for the rotational quanta is represented under *group 2* of Table 4.

The line positions were calculated using the spectroscopic constants of Billingsley[198] and Huber and Herzberg.[199] Higher-order terms have been introduced based on the analysis by D.R. Smith of the AF Geophysics Directorate of band heads seen in interferometer data taken aboard the space shuttle.[200] The intensities have been calculated based on the dipole-matrix elements of Werner and Rosmus.[201] A default value of 0.06 cm^{-1}/atm was chosen for the air-broadened halfwidth, although most applications are not expected to require operation in the Lorentzian regime.

2.37. HOBr (molecule 37)

Line parameters are given in the supplemental directory for the pure rotation (000–000) transitions of hypobromous acid for both isotopes of bromine. The molecular parameters are from high-resolution IR spectra of Cohen et al,[202] and the calculation uses pure rotational data and the dipole moment from Koga et al.[203] The spectral coverage is from 0 to 316 cm^{-1}, but the user is cautioned that the maximum value of K_a observed in the infrared study is 5 and that predictions of higher K_a transitions are extrapolations which may be less accurate than their calculated uncertainties indicate. A constant value of 0.06 cm^{-1}/atm has been assumed for the air-broadened halfwidth with a temperature-dependence coefficient $n = 0.67$.

3. IR CROSS-SECTIONS

When it became evident that data on individual spectral lines belonging to certain heavy molecular species such as chlorofluorocarbons (CFCs), hydrochlorofluorocarbons (HCFCs), SF_6, and oxides of nitrogen (for example, N_2O_5) could not be reasonably characterized and tabulated in the traditional HITRAN format, the approach to report spectral absorption cross-sections measured at atmospheric conditions was adopted.[204] The previous two editions of the HITRAN compilation[1,2] introduced temperature-dependent cross-sections but neglected the effect of pressure-broadening,[205] The increasing use of the cross-sections in atmospheric modeling, especially for remote sensing, has engendered numerous laboratory programs for acquiring these data sets.[206]

The absorption cross-section, k_v (cm^2 $molecule^{-1}$), is defined as

$$k_v = (-\ln \tau_v)/\eta L \tag{1}$$

in terms of the spectral transmittance τ_v at the wavenumber v, temperature T and pressure P, of column density η (in molecule/cm^3) along an optical path of length L (cm). It is presented at several (T, P) combinations representing atmospheric layers given in commonly tabulated atmospheric models as well as conditions encountered in the polar regions.

Table 8 shows the datasets that have been added since the last edition of HITRAN. The cross-sections of CFC-11, CFC-12, HCFC-22, and SF_6 were provided by Varanasi et al.[207,175] These cross-sections, as well as other cross-section data in HITRAN, were measured using high-resolution Fourier-transform spectrometers. For the four species above, a spectral resolution of 0.03 cm^{-1} was adequate for most of the broadening pressures used in the experiments, while at 40 torr and lower, 0.01 cm^{-1} was used. The data were obtained at temperatures between 200 and 296 K and are free from instrumental distortion, since the spectra were recorded at a spectral resolution that was sufficiently high at each broadening pressure used. The bands of CFC-12 were measured in the 810–965 cm^{-1} and 1040–1200 cm^{-1} regions at temperatures ranging from 216 to 296 K and pressures from 170 to 760 torr. The bands of CFC-11 in the 810–880 cm^{-1} and 1050–1120 cm^{-1} regions were measured at temperatures in the range from 201 to 296 K and pressures between 40 and

Table 8. IR cross-section data added to 1996 edition

Molecule	Wavenumber range (cm^{-1})	Temperature range (K)	Pressure range (torr)	Number of P,T sets
CCl_4	770–810	170–310	—	12†
CFC–11	810–880	201–296	40–760	33
(CCl_3F)	1050–1120	201–296	40–760	33
CFC–12	810–965	216–296	170–760	15
(CCl_2F_2)	1040–1200	216–296	170–760	15
HCFC–22 ($CHClF_2$)	760–860	216–294	40–760	7
SF_6	925–955	216–295	25–760	7
$ClONO_2$	1265–1325	201–222	–	3†

† Only temperature sets.

760 torr. Measurements of HCFC-22 and SF_6 were made for bands in the 760–860 cm^{-1} and 925–955 cm^{-1} regions, respectively at temperatures in the range from 216 to 296 K and pressures from 40 to 760 torr.

The cross-sections for the $ClONO_2$ in the 1265–1325 cm^{-1} region at 201, 211, and 222 K were provided by Orphal et al.[208] They are made available along with those at 216 and 296 K retained from the earlier editions of the database. The cross-sections of CCl_4 listed at room temperature in the previous editions of the database have been augmented in this edition with data at 170, 223, 248, 273, 298, and 310 K reported by Orlando et al.[209]

The data are presented as separate files for each individual molecule. Each portion of the file corresponding to a particular temperature–pressure pair begins with a header (see Table 9) that contains information on the wavenumber (cm^{-1}) range, number of cross-section data in this set, temperature (K), and pressure (torr). The maximum value of the absorption cross-section (cm^2/molecule) and additional information containing the reference to that observation are also presented in each header. The wavenumber spacing $\Delta\nu$ of the cross-section listings is uniform for each of the pressure-temperature sets, and is determined by taking the difference between the maximum and minimum wavenumber and dividing by the number of points N (cross-section data in this set), i.e. $\Delta\nu = (\nu_{max} - \nu_{min})/(N-1)$.

The increased use of hydrofluorocarbons (HFCs), which are expected to replace CFCs and HCFCs in many applications in order to reduce the deleterious effects of released chlorine on the atmospheric ozone layer, will add another absorber in the IR "window" region, 8–12 μm. Smith et al[210] have recently determined the cross-sections of HFC-134 (CHF_2CHF_2) and HFC-143a (CF_3CH_3), and these data will be available on a future edition of HITRAN.

4. ULTRAVIOLET DATASETS

4.1. Line-by-line parameters

The file, 07_schum.par located in the subdirectory \UV\LBL, contains 11 020 lines of the O_2 Schumann–Runge system in HITRAN format. This system represents transitions between the $B^3\Sigma_u^-$ electronic state and the $X^3\Sigma_g^-$ ground electronic state. Nearly all of the line parameters are based on high-resolution absorption measurements from two groups: one from the Australian National University,[211] and the other from the Harvard-Smithsonian Center for Astrophysics.[212] A description of this line compilation is given in Minschwaner et al,[213] which also contains relevant citations for measured quantities. The file lists all principal branch triplets over the range $v' = 0$–19, $v'' = 0$–2, $N'' = 1$–51. Satellite branches are included for $v' = 0$–19, $v'' = 0$, $N'' = 1$–15. Principal branches for the $^{16}O^{18}O$ isotopomer are listed for $v' = 2$–16, $v'' = 0$, $N'' = 0$–24.

There are two caveats for the user associated with these data: (1) Line positions of high N'' are not reliable. Maximum N'' values are limited by values of the cross-sections of those lines at the highest temperature. (2) There is an error in the indexing of the lower "global" quantum state, in that the $B^3\Sigma_u^-$ electronic state was referred to rather than the $X^3\Sigma_g^-$ state.

Table 9. File structure and format (in FORTRAN) for cross-section files

Molecule	v_{init} (1) (cm^{-1})	v_{final} (1) (cm^{-1})	Number of points	T (1) (K)	P (1) (torr)	σ_{max}	Reference + Additional Info.
A10	F10.4	F10.4	I10	F10.4	F10.4	E10.3	3A10
			Cross-sections (10 per line) [cm^2/molecule @ T(1),P(1)] (10E10.3)				
Molecule	v_{init} (1) (cm^{-1})	v_{final} (1) (cm^{-1})	Number of points	T (2) (K)	P (2) (torr)	σ_{max}	Reference + Additional Info.
A10	F10.4	F10.4	I10	F10.4	F10.4	E10.3	3A10
			Cross-sections (10 per line) [cm^2/molecule @ T(2),P(2)] (10E10.3)				
			ϟϟϟ				
Molecule	v_{init} (2) (cm^{-1})	v_{final} (2) (cm^{-1})	Number of points	T (1) (K)	P (1) (torr)	σ_{max}	Reference + Additional Info.
A10	F10.4	F10.4	I10	F10.4	F10.4	E10.3	3A10
			Cross-sections (10 per line) [cm^2/molecule @ T(1),P(1)] (10E10.3)				
Molecule	v_{init} (2) (cm^{-1})	v_{final} (2) (cm^{-1})	Number of points	T (2) (K)	P (2) (torr)	σ_{max}	Reference + Additional Info.
A10	F10.4	F10.4	I10	F10.4	F10.4	E10.3	3A10
			Cross-sections (10 per line) [cm^2/molecule @ T(2),P(2)] (10E10.3)				

Note: Data sets surviving from earlier editions are only given for different temperatures, not pressure-temperature pairs.

Line positions are calculated from energy level differences based on measured molecular constants. Line intensities are obtained from measured band oscillator strengths normalized according to Hönl–London factors, assuming a Boltzmann distribution of energies at 296 K. The tabulated widths are measured predissociation widths at zero pressure. Pressure-broadened widths are not listed because this effect is comparable to predissociation broadening only for pressures larger than 1 atm. (The self-broadening coefficient is on the order of 0.20 cm^{-1}/atm.[214]) Use of a Voigt line shape, composed of a thermal-broadened Doppler profile and a predissociation-broadened Lorentz profile, is adequate for most atmospheric applications. Line intensities at temperatures other than 296 K can be obtained using the energy of the lower quantum state in conjunction with the temperature dependence of the total internal partition sum. The latter can be obtained using the program TIPS.FOR discussed below in Sec. 7.2.

4.2. UV cross-sections

Cross-sections for two species, nitrous oxide and sulfur dioxide, have been placed in the subdirectory UV/XSECT. These cross-sections have been cast into the same format as the IR cross-section data described above (see Table 9); transforming the UV data into the equal-interval wavenumber scale required interpolation from measured wavelength scales employed in the UV.

High-resolution cross-section measurements of N_2O at 295–299 K have been performed in the wavelength region 170–222 nm with a 6.65 m scanning spectrometer of sufficient resolution to yield

cross-sections that are independent of the instrumental function.[215] The measured cross-sections are available throughout the region 44 925–58 955 cm^{-1} at intervals of 0.1–0.2 cm^{-1}. Previously unresolved details of the banded structure which is superimposed on the continuous absorption in the region 174–190 nm are observed.

Laboratory measurements at high resolution of the absorption cross-section of SO_2 at the temperature 213 K have been performed in the wavelength region 172–240 nm with a 6.65 m scanning spectrometer operated at an instrumental width of 0.002 nm.[216] The measured cross-sections are available throughout the region 172–240 nm at wavenumber intervals of 0.4–0.1 cm^{-1}. The measured cross-sections, which are relevant to the photochemistry of planetary atmospheres. possess significantly more spectroscopic structure, and are more accurate than previous measurments made at lower resolution. However, values at peak cross-sections could be effected by the instrumental widths even at 0.002 nm, which is larger than the Doppler widths.

5. INDICES OF REFRACTION

Aerosol particles also contribute to the infrared opacity in planetary atmospheres, especially for a several-year period following major volcanic eruptions. Within the last two decades, two major volcanic eruptions (El Chichon in 1982 and Mt. Pinatubo in 1991) injected substantial amounts of sulfur dioxide into the Earth's stratosphere. The 1996 HITRAN compilation therefore contains as auxiliary tables the indices of refraction of various atmospheric particles. Indices of refraction of water and ice (the composition of cloud particles), aqueous sulfuric acid (the composition of volcanic aerosol), nitric acid trihydrate and aqueous HNO_3/H_2O (two, of several, compositions of the Polar Stratospheric Clouds), and other indices (discussed below), are included in the compilation. Table 10 specifies the indices included in the 1996 compilation. The indices of refraction are in ASCII tables which have individual wavenumber ranges, increments, and data formats.

Aerosol opacity has a wavelength dependence, though generally the wavelength dependence has structure which varies gradually over several wavenumbers (while molecular spectra have finer structure). Aerosol opacity, however, complicates the interpretation of remote sensing observations of gaseous species. In the presence of substantial volcanic aerosol loading, occultation spectra will have nonuniform background envelopes which deviate from unity. Emission experiments will also display enhanced radiances, which can be misinterpreted as enhanced mixing ratios of gaseous species. A further complication is that aerosol particles both scatter and absorb radiation, and thus

Table 10. Indices of refraction on the HITRAN compilation.

Substance	Comments
Water (liquid)	0.65–1000 μm
Water (ice)	$0.04–8 \times 10^6$ μm
Liquid H_2SO_4/H_2O	Room temperature, 0.35–25 μm; 25, 38, 50, 75, 84.5, 95.6% H_2SO_4 by weight
Liquid H_2SO_4/H_2O	Room temperature, 6.4–13 μm; 75, 90% H_2SO_4 by weight
Liquid HNO_3/H_2O	Room temperature, 2–32 μm; 3, 6, 12, 22, 40, 70% HNO_3 by weight
β NAT	1.4–20 μm, nitric acid trihydrate solid film at 196 K
α NAT	1.4–20 μm, nitric acid trihydrate solid film at 181 K
NAD	1.4–20 μm, nitric acid dihydrate solid film at 184 K
NAM	1.4–20 μm, nitric acid monohydrate solid film at 179 K
Water (ice)	Water ice film at 163 K
aNAT	Amorphous NAT solid solution film at 153 K
aNAD	Amorphous NAD solid solution film at 153 K
aNAM	Amorphous NAM solid solution film at 153 K
NaCl	Room temperature, 0.2 to 30 000 μm
Sea salt	Room temperature, 0.2 to 30 000 μm
Ammonia sulfate	Room temperature, 0.2 to 40 μm
Carbonaceous material	Room temperature, 0.2 to 40 μm
Volcanic dust	Room temperature, 0.2 to 40 μm
Meteoric dust	Room temperature, 0.2 to 40 μm
Quartz	Room temperature, 0.2 to 300 μm
Iron oxide	Room temperature, 0.2 to 300 μm
Sand	Room temperature, 0.2 to 300 μm

equations which describe the radiation field, and the levels of sophistication which are needed to interpret observations in retrieval programs, become more complex.

In the analysis of spectra which contain aerosol features, the indices of refraction enter the analysis through radiative transfer calculations. For spherical particles, Mie theory can be used to calculate the scattering, absorption, and extinction coefficients (see Liou[217]). The extinction coefficient, for example, is calculated from the expression

$$k_{\text{ext}} = 1.0 \times 10^{-3} \int Q_{\text{ext}}(x, m(\lambda)) \pi r^2 \, \mathrm{d}N/\mathrm{d}r \, \mathrm{d}r \tag{2}$$

where Q_{ext} = Mie efficiency factor for extinction (dimensionless), r = particle radius (μm), $\mathrm{d}N/\mathrm{d}r$ = particle size distribution (particles $\text{cm}^{-3}\,\mu\text{m}^{-1}$). The factor 1.0×10^{-3} is used to convert k_{ext} to the km^{-1} unit. Q_{ext} is a function of the complex index of refraction $m = m_{\text{real}} + \text{i}m_{\text{imag}}$, and $x = 2\pi r/\lambda$ = particle size parameter (dimensionless), where λ is the wavelength (μm). Both the real (m_{real}) and the imaginary (m_{imag}) parts of the complex index of refraction are tabulated in the HITRAN compilation. For non-spherical particles, T-matrix (Barber and Hill[218]) and discrete-dipole techniques (Draine and Flatau[219]) can be used to calculate scattering and absorption of light particles, given a particle shape and index of refraction.

Massie[220] reviewed the indices of refraction which form the basis of the 1996 compilation. In the 1996 compilation, indices of ice and water are primarily those of Warren.[221] Warren tabulated the real and imaginary indices of ice between 4.4×10^{-2} and 164 μm, for a temperature of $-7\,^{\circ}\text{C}$, and for the wavelength range between 167 and 8.6 μm at temperatures of -1, -5, -20, and $-60\,^{\circ}\text{C}$. Imaginary indices of Kou et al[222] between 0.65 and 2.5 μm, and the water indices of Downing and Williams[223] at 27 °C, are also included in the compilation.

Real and imaginary H_2SO_4/H_2O indices of refraction at 25, 38, 50, 75, 84.5 and 95.6% H_2SO_4 (by weight), for the wavenumber range between 400 and 27 800 cm^{-1}, for 300 K, are from the compilation of Palmer and Williams.[224] The indices of Remsberg[225] (75% H_2SO_4, between 747 and 1571 cm^{-1}), are also included. The real indices agree to the 2% level for the two data sets, while the Remsberg imaginary indices are 15% larger than the Palmer and Williams indices between 1000 and 1571 cm^{-1}, and 20–35% larger between 747 and 1000 cm^{-1}. Ongoing laboratory work will soon resolve these differences, and also provide indices at the cold temperatures (near 220 K) of the stratosphere.

As sulfuric acid droplets are cooled in the polar stratospheric regions, they take up HNO_3 and from ternary solution droplets. The indices of these droplets, comprised of a mixture of $H_2O/HNO_3/H_2SO_4$ (see the model of Tabazadeh et al[226]), can be approximated using the HNO_3/H_2O indices measured by Querry and Tyler.[227] At temperatures below 200 K, the H_2SO_4 weight percentage of a ternary droplet becomes small. Aqueous HNO_3/H_2O indices, for 3, 6, 11, 22, 40, and 70% HNO_3, for the 250–5000 cm^{-1} range, are compiled.

Polar Stratospheric Cloud particles can also be solid. Indices of refraction for nitric acid trihydrate (α and β NAT), nitric acid dihydrate (NAD), nitric acid monohydrate (NAM), and solid amorphous nitric acid solutions (amorphous NAT, NAD, and NAM) are included (Toon et al[228]). These indices were derived from measurements of transmission of infrared light through thin films of varying thickness at temperatures below 200 K, between 500 and 7000 cm^{-1}.

Indices compiled by Shettle (see Chapter 18 of Jursa[197]), and used to generate the aerosol models in the LOWTRAN, MODTRAN, and FASCODE computer codes, are also included. These tables contain the indices for many diverse composition types (water, ice, sodium chloride, sea salt, ammonium sulfate, carbonaceous particles, volcanic dust, sulfuric acid, meteoric dust, quartz, iron oxide, and sand). The wavelength ranges are generally between 0.2 and 40 μm (and for many compositions, to longer wavelengths).

Other recently published indices included those of amorphous and crystalline NAT at 130 and 175 K, measured by Berland et al[229] at 632 nm. Richwine et al[230] measured NAT indices at 175 K, between 700 and 4000 cm^{-1}, and obtained values similar to those of Toon et al.[228] While Adams and Downing[231] measured room temperature indices of the aqueous ternary system (at 75% H_2SO_4, 10% HNO_3, and 15%H_2O) between 500 and 5000 cm^{-1}, indices of the ternary system for a range of HNO_3 and H_2O weights have not been measured in the laboratory.

New techniques to determine indices, directly from measurements of the infrared spectra of laboratory aerosols, are being developed by R. Miller's group at the University of North Carolina. Using this technique, Clapp et al[232] analyzed infrared spectra of laboratory-generated ice particles for temperatures between 130 and 210 K, between 800 and 4000 cm^{-1}. Miller's group is placing their results on the web site ftp://frenchie.chem.unc.edu/ri as they become available.

Tropospheric aerosols have various compositions. Sutherland and Khanna[233] report the real and imaginary indices of organic nonvolatile aerosols produced by burning vegetation (mixed weeds) from 525 to 5000 cm^{-1}. Transmission spectra for alfalfa, mixed weeds, and lawn are presented, and show similar spectral features.

New studies of tropospheric sulfates and nitrates are reported by Gosse et al[234] and Cziczo et al.[235] Gosse et al[234] tabulate real and imaginary indices of sulfate and nitrate aqueous solutions between 0.7 and 2.6 μm, for temperatures in the -24 to 24 °C range. Cziczo et al[235] report upon deliquescence and the crystallization behavior of ammonium sulfate ($(NH_4)_2SO_4$), ammonium nitrate (NH_4HSO_4), and NaCl particles, as a function of relative humidity.

6. FUTURE PARAMETRIZATION FOR THE DATABASE

6.1. Line mixing

Line mixing is not currently addressed in HITRAN and schemes for including line mixing would require a significant change to the format of the HITRAN files. Several researchers have developed schemes for including line mixing. All of these schemes require multiple parameters in order to handle the temperature and pressure dependence of this effect, and require significant radiative transfer code alterations in order to properly use these parameters.

A recent scheme by Rodrigues et al[236] has been developed which includes line-mixing parameters (as auxiliary files to HITRAN96) as well as the software to properly use these parameters in radiative transfer codes. It currently only includes Q branches of CO_2, but will be expanded to include other molecules in the future. This scheme includes both a two-parameter, first-order calculation and a full relaxation operator approach to line mixing in a way such that the sum-rule is obeyed. The former approach can break down at high pressures for Q branches where the line spacing is extremely small, such as the 597 cm^{-1} Q branch of CO_2. However, this particular Q branch is saturated in the atmosphere. As a result, the first order approach more than adequately accounts for atmospheric opacities. In fact, this scheme has been used to accurately model atmospheric spectra obtained by both solar occultation and thermal emission spectra in the stratosphere and troposphere[236] and has been incorporated into two separate radiative transfer codes with little editing of code.

The parameter files and software for this scheme are available via ftp. The information for obtaining these files is included in Rodrigues et al.[236]

6.2. Collision-induced absorption (CIA) parameters

It is well known that infrared collision-induced absorption (CIA) by O_2 and N_2 are significant in long-path atmospheric spectra. Although several line-by-line atmospheric transmittance and radiance codes have included these absorptions since the early eighties, they are not yet available in HITRAN. In atmospheric spectra at resolutions better than ~ 0.1 cm^{-1}, the quadrupole lines of O_2 and N_2, and the magnetic dipole lines of O_2 are observable, superimposed on the background CIA continuum. These line transitions are modeled quite well, and are included in the HITRAN database.

Some of the more extensive atmospheric spectroscopy studies of the CIA, which also review previous work, are given by Rinsland et al,[237] Rinsland et al,[238] and Roney et al.[239] A number of laboratory measurements of these absorption parameters have been made over the years, the most recent of which are by Menoux et al[240] and by Lafferty et al[241] for the N_2 fundamental near 4.3 μm, by Orlando et al[242] and by Thibault et al[243] for the O_2 fundamental near 6.4 μm. These laboratory studies provide temperature-dependent coefficients for semi-empirical modeling of atmospheric spectra, and also include extensive review of previous studies. The results of these latest laboratory measurements are in good agreement with each other, while the older measurements are less accurate.

The formulation of Lafferty et al[241] and Thibault et al[243] is particularly suitable for modeling atmospheric spectra, including the relative efficiency of N_2–O_2 collisions compared to N_2–N_2. Note, however, that the laboratory spectra used to derive the absorption parameters for O_2 show that the quadrupole line structure is included in the modeling. A similar situation can be assumed for N_2.

Collision-induced absorption bands in the near-infrared and visible are important, and were re-investigated recently in modern, high-resolution atmospheric spectra by Gamache et al,[51] Mlawer et al,[243] and by Solomon et al[245] for O_2, in conjunction with the laboratory study of Greenblatt et al.[246] These papers also provide references to recent discussions on the potential importance of these bands in modeling solar flux absorption.

It is planned to incorporate the available CIA coefficients for modeling O_2 and N_2 in future editions of the HITRAN database.

7. SOFTWARE AND ASSOCIATED FEATURES FOR HITRAN

7.1. Software and auxiliary utilities

The current database release contains a number of HITRAN auxiliary files. They are contained on the CD-ROM in the software subdirectory, and fall into four general categories: executable code to use with the database, FORTRAN and C source code, make files to aid the user in compiling the C code, and data files that contain useful ancillary information about the HITRAN molecules. The more important of these files are briefly discussed in this section.

The most functional of these files is the HAWKS.exe program found in the subdirectory Software/Windows. HAWKS (HITRAN Atmospheric Workstation) is a Microsoft Windows® program that allows the user to: (1) select data from the database; (2) display stick plots of line intensities or energy levels; (3) find journal references for line positions, halfwidths, and intensities; and (4) perform other operations on the database. The software is installed from the CD-ROM by running the setup.exe program. A complete description of the software and operating instructions is given in the HAWKS manual which is described below. The current version of the program, and other updates, can be downloaded from the HITRAN web site which is also discussed below.

A UNIX version of the HAWKS software, for SUN Solaris 2®, and SUN OS 4®, is found in the subdirectory Software/UNIX in a compressed tar format. This software is not as complete as the Windows version, but does allow a user to select and filter data from HITRAN and make plots of line intensities.

At the time HITRAN96 was released, some users either had not converted to Windows or did not have access to a SUN workstation. There is also a small, but significant, group of Macintosh users. For these users, we have provided C code of the major HAWKS routines. The user is, of course, required to compile these programs on their system. A major upgrade of the HAWKS software is planned for release within the next year. The software is being rewritten in the JAVA programming language and will be a complete cross platform application. That is, the same executable code will run on a PC, UNIX workstation, and Macintosh computers. This is a significant improvement because we will only need to maintain a single source and executable code compared to the four versions that are currently maintained. The software will be distributed via the HITRAN web site.

Until the new software is available, non-Windows and other users who cannot run the current HAWKS, have access to a limited version of the data filtering functions called SELECT96. This is a C program derived from the FORTRAN version of SELECT which has been distributed with the database since 1982. The main program is called SELECT96. C and is contained in the Software/Generic subdirectory on the CD-ROM. SELECT96 performs the basic database selection criteria and other similar tasks. Also included are several additional routines with the .C extension which are necessary to compile the program. Two files, MAKEFILE.DOS and MAKEFILE.UNI, are provided to assist the user in compiling the program for DOS and UNIX systems, respectively. Individuals having other operating system should use these files as a guide in compiling the program for their system.

The observant user will notice that several files with the .FOR extension are also provided on the CD-ROM. These routines are the FORTRAN ancestors of the correspondingly named C routines.

They are included for those users who find the FORTRAN programs more easy to read than the C versions, and are also required to compile TIPS.FOR. TIPS computes the total internal partition sum for the HITRAN constituents at temperatures between 70 and 3000 K and is described in greater detail below. Finally, the subroutine BD_VIBS.FOR will be of particular interest to spectroscopists because it provides the relationship between the vibrational or "global" indices in the HITRAN database with the closest ASCII equivalent of quantum vibrational assignments.

There are three other files which may be of interest to HITRAN users: TABLE_96.TXT, BSUMS_96.TXT and MOLPARAM.TXT. The first two are included on the CD-ROM in the Software/Generic subdirectory; while the third, which was inadvertently left off the CD, can be obtained from the HITRAN web site. TABLE_96.TXT is an ASCII file containing the HITRAN journal references for intensities, line positions, half-widths, and the band centers. This table is slightly more current than the one accessed in WINDOWS through hypertext. BSUMS_96.TXT is a table of the band statistics in HITRAN96. This table also can be generated by using the BANDSTAT feature in the WINDOWS version of HAWKS. It contains, band-by-band for each molecule and isotope, the maximum and minimum values of the parameters as well as the sums of the intensities of the lines in a band and the spectral extent of the band.

MOLPARAM.TXT provides a table of the isotopic abundances of the isotopomers present in HITRAN, the total partition function at 296 K for each isotope, the spin-statistical weight, and the molecular weights. Some of this information, which is not contained in the main body of HITRAN parameters is necessary for some applications, such as computing the Einstein-A coefficient from the transition-probability squared parameter on the database.

7.2. Total internal partition sums

The total internal partition sums (TIPS) have been totally recalculated for this edition of the database. Substantial improvements have been made for values at temperatures greater than 750 K. In this edition, only a single analytical form is used to fit the data, regardless of the temperature range,

$$Q(T) = a + bT + cT^2 + dT^3. \tag{3}$$

The coefficients, a, b, c, and d, are obtained by fitting to the calculated partition functions using a Simplex nonlinear minimization algorithm.[247] Coefficients to Eq. (3) have been determined in 3 temperature ranges: a low-temperature range, $70\ \mathrm{K} \leq T \leq 500\ \mathrm{K}$, a mid-temperature range, $500\ \mathrm{K} < T \leq 1500\ \mathrm{K}$, and a high-temperature range, $1500\ \mathrm{K} < T \leq 3005\ \mathrm{K}$. The data for the low temperature range are calculated at every 5 K and those for the mid- and high-temperature ranges are at every 20 K.

Calculations were made for each isotopomer on the database at the required temperatures. Depending on the species and the temperature range, the calculation of the partition sums were made using direct sums and analytical formulas. The fits to the calculated partition sums were made with a criterion of 1% maximum error over the temperature range. For those species for which the error in the partition function obtained from the polynomial representation exceeds the criterion, the a coefficient is set to -1 and the other coefficients are set to zero. These species are listed in Table 11. For several species for which the error was only slightly larger than the criterion, the coefficients were retained. These species are listed in Table 12. The coefficients have been incorporated into the FORTRAN program TIPS.FOR, which rapidly calculates the partition function.

The partition functions of the $^2\Pi$ molecules, NO, OH, and ClO, on this database are incorrect by an integral factor. These partition functions are also used to calculate the transition-moment squared parameter on the database. This error was due to a misinterpretation of the nuclear spin statistical weight factor when including the hyperfine levels in the formulation presented by Gamache et al.[127] Consequently, some of the transition-moment squared parameters listed for these molecules are incorrect.

The total internal partition sum for a molecule can be written

$$Q(T) = \sum_i \exp(-c_2 E_i/T) = \sum_m g_m \exp(-c_2 E_m/T), \tag{4}$$

where i sums over all states of the molecule and m sums only over the degenerate states with g_m being the degeneracy of state m, and c_2 is the second radiation constant (hc/k). The degeneracy factors

Table 11. Molecules for which partition sum coefficients are set to default values

Molecule	Isotopomer (AFGL code)	Temperature range†
CH_4	211	2 and 3
	311	2 and 3
	212	2 and 3
HNO_3	146	1,2, and 3
CH_3Cl	215	2 and 3
	217	2 and 3
C_2H_6	1221	1,2, and 3
COF_2	269	2 and 3
SF_6	29	1,2, and 3
HCOOH	126	2 and 3
$ClONO_2$	5646	1,2, and 3
	7646	1,2, and 3

† The three ranges correspond to: $70 \leq T \leq 500$, $500 < T \leq 1500$, and $1500 < T \leq 3005$ K

Table 12. Molecules for which partition sum coefficients are reported and error $> 1\%$

Molecule	Isotopomer (AFGL code)	|Fit error|% Temperature range (K) $70 \leq T \leq 500$	$500 < T \leq 1500$	$1500 < T \leq 3005$
H_2CO	126		2.2	2.2
	136		2.2	2.2
	128		2.2	2.2
CH_3Cl	215	1.3		
	217	1.3		
PH_3	1111		2.7	2.5
COF_2	269	1.7		
HCOOH	126	1.7		

depend explicitly on the molecule in question and on the detail in which the energy levels are calculated. In general, all rotational levels of a molecule exist and the inclusion of nuclear spin yields different statistical weights. Identical nuclei that are related by symmetry operations give rise to statistical factors that depend on the rotational state. Such factors are state dependent. For nuclei that are not related by symmetry operations, the degeneracy factors are not dependent on the rotational state of the molecule and are called state-independent factors. These factors appear, in various texts,[248,249] as additional factors multiplying Q, but strictly, the texts assume that the Q calculations are done for the rotational states only. An example of state-dependent factors are the 3:1 ratio for odd and even states of H_2O or the $(2J'' + I)$ factors for the rotational state J''. The effects of the nuclear spin states can be accounted for[248] by the additional factor $\Pi(2I_j + 1)$, where the product is over nuclei j that do not couple with the rotational wavefunctions. For molecules with hyperfine levels F, M_F, where $F = I + J$, the summation over all states includes the nuclear spin factors and the factor $\Pi(2I_j + 1)$ should not be included into the partition sum. To correct the HITRAN partition function values, they should be divided by the factor $\Pi(2I + 1)$, that is 3, 2, 3 for $^{14}N^{16}O$, $^{15}N^{16}O$, and $^{14}N^{18}O$, 2, 2, 3 for ^{16}OH, ^{18}OH, and ^{16}OD, and 4, 4 for $^{35}Cl^{16}O$ and $^{37}Cl^{16}O$, respectively.

In most applications, where the line intensity $S(T)$ is calculated from $S(T_{ref})$ by the ratio of partition functions, the state-independent statistical weights cancel out, so that these factors do not lead to errors. However, these are important in relations that require the exact statistical weights,

such as the weighted transition probabilities

$$\Re_{\eta\xi} = (1/d_\eta)\Sigma_{\xi\xi'}|R_{(\eta\xi)(\eta'\xi')}|^2. \quad (5)$$

In particular, the conversion from S to the weighted transition probabilities requires the partition sum calculation to be compatible with the statistical weight used in the conversion. On the 1996 HITRAN database, there may be problems with some of the transition-moment squared parameters. This error is due to the algorithm used to compute this quantity, for which the degeneracy factors from the partition sum calculations were used, regardless of the particular ro-vibrational transition under consideration. This can lead to several problems because for many transitions on the database the complete quantum numbers are not specified. Care must be taken for transitions for which hyperfine, lambda doubling, or the combination of hyperfine and lambda doubling are given relative to transitions for which such quantum numbers are not reported.

As an example consider $^{14}N^{16}O$ (see Goldman et al[70] and Gamache and Rothman[250] for more details). For the transitions for which the hyperfine with individual lambda quantum numbers are given (full quantum information), the weighted transition-moment squared given on HITRAN must be multiplied by $(2F + 1)/(2J + 1)$. Note, this factor is 1 for lines for which $F = J$. Next, transitions for which the hyperfine structure is summed over and individual lambda quantum numbers are given, the weighted transition-moment squared given on HITRAN is too large by $\Pi(2I + 1) = 3$. Last, transitions for which the hyperfine structure and the two lambda components are summed over, the weighted transition-moment squared given on HITRAN must be multiplied by $2(2I + 1) = 6$.

Similar problems are encountered for other species on the database that have hyperfine, lambda doubling structure or the combination of hyperfine and lambda doubling structure. These discrepancies will be considered when creating the next version of the database.

7.3. Documentation

A comprehensive users manual is provided with the HAWKS software. It is designed to assist the user in easily adapting to the manipulation of the HITRAN96 molecular spectroscopic database and associated molecular databases by proper utilization of the HAWKS software package. It includes installation instructions for the Windows and UNIX software, and a detailed description of the capabilities of the HAWKS software.

Two versions of the manual are provided on the CD-ROM in the DOCUMENT directory in a PKZIP executable file format. The first, called HAWKS_WP.EXE, contains the manual in the Corel WordPerfect® format. The second, called HAWKS_PS.EXE, contains the manual in an Adobe Postscript® format. A user can expand these files by copying them into the desired directory on his hard disk and typing the file name. A document file and several linked image files will be generated for the former while a large Postscript file will be produced for the latter. A third version, and perhaps the easiest to use, is available on the HITRAN web page in the Adobe Acrobat® (PDF) format. The document, along with a reader, can be easily downloaded. Those users who wish to make a printed copy of the manual are encouraged to use this version.

7.4. HITRAN Web Site: www.HITRAN.com

Numerous references have been made in the preceding material to the HITRAN World Wide Web site (www.HITRAN.com). This is a new service and will be greatly expanded in the future. Historically, new databases have been released at 4–5 year intervals. The primary purpose of the site is to significantly decrease this time. We will continue periodic archival database releases on a CD-ROM; however new validated data will be released via the web site as they become available.

The following files and programs are currently available on the web site. The file 19_HIT97.par contains all the OCS data for the next HITRAN update. There are many new ro-vibrational bands (fundamentals, hot bands, combination bands). To these parameters have been added the earlier HITRAN pure rotation bands. In addition, there are now five isotopomers. Note, that we have corrected the order of the last two isotopes ($^{16}O^{12}C^{33}S$ − 623 and $^{18}O^{12}C^{32}S$ − 822) to correspond to their decreasing order in terrestrial abundance (the 4th isotope of earlier HITRANs thus becomes number 5 on all subsequent issues). The transition-probability squared parameter is

currently not consistent with the HITRAN definition for the ro-vibrational bands, and will be corrected on a final version. This file is meant to totally replace all OCS data on previous HITRANs.

The file 38_HIT97.par represents the ethylene molecule (C_2H_4). This species is new to HITRAN. The spectral range covered is 701–3242 cm^{-1}, and the file contains 12 978 lines.

The file, MOLPARAM.TXT, is a June 1997 update. It contains information such as the statistical factors and partition sum at 296 K which a small number of users require.

zApp is an optional resource file for the motif version of Hawks.

HAWKS.exe version 1.1 is now available. HAWKS.exe is the latest MS-Windows version of the HAWKS software.

The web site also provides a number of other services. These services include a form to request the HITRAN CD-ROM, the HAWKS software manual in Adobe Acrobat® format, a listing of technical meetings related to HITRAN, and links to other spectroscopic databases. The reader is encouraged to regularly check the site for software upgrades, new data, and added features.

Acknowledgements—The HITRAN molecular database has been a project with strong international cooperation during its development. Laboratories throughout the world have contributed both experimental data and theoretical calcul!ations. We in particular want to thank the major contributions of A. Barbe, D. Chris Benner, C. Chackerian, E. A. Cohen, V. Malathy Devi, H. Dothe, J. Esmond, M. P. Esplin, L. P. Giver, D. Goorvitch, R. L. Hawkins, M. L. Hoke, W. J. Lafferty, K. Minschwaner, D. Nelson, J. Orphal, P. Pracna, M. A. H. Smith, R. A. Toth, Š. Urban, M. Weber, and M. Zahniser. P. Morris and A. Berk were instrumental in discovering correctable errors prior to the release of HITRAN96. We wish to especially thank M. D. King, D. O'C. Starr, G. M. Stokes, and T. S. Cress for their support for this project.

The current effort has been supported by the NASA Earth Observing System (EOS), contract NAS5-96023; the NASA Upper Atmospheric Research Satellite (UARS) program; the Atmospheric Radiation Measurement (ARM) program of the Environmental Sciences Division, Office of Biological and Environmental Research, U.S. Department of Energy; and the U.S. Air Force Office of Scientific Research. The research at the University of Denver was supported in part by NSF and NASA.

REFERENCES

1. L. S. Rothman, R. R. Gamache, R. H. Tipping, C. P. Rinsland, M. A. H. Smith, D. Chris Benner, V. Malathy Devi, J.-M. Flaud, C. Camy-Peyret, A. Perrin, A. Goldman, S.T. Massie, L.R. Brown, and R.A. Toth, "The HITRAN molecular database: editions of 1991 and 1992", *JQSRT* **48,** 469–507 (1992).
2. L. S. Rothman, R. R. Gamache, A. Goldman, L. R. Brown, R. A. Toth, H. M. Pickett, R. L. Poynter, J.-M. Flaud, C. Camy-Peyret, A. Barbe, N. Husson, C.P. Rinsland, and M. A. H. Smith, "The HITRAN database: 1986 edition", *Appl. Opt.* **26,** 4058–4097 (1987).
3. M. D. King, D. D. Herring, and D. J. Diner, "The Earth Observing System (EOS): A space-based program for assessing mankind's impact on the global environment", *Opt. Photon. News* **6,** 34–39 (1995).
4. G. M. Stokes and S. E. Schwartz, "The atmospheric radiation measurement (ARM program): programmatic and design of the cloud and radiation test bed", *Bull. Am. Met. Soc.* **75,** 1201–1221 (1994).
5. L. S. Rothman, R. B. Wattson, R. R. Gamache, D. Goorvitch, R. L. Hawkins, J. E. A. Selby, C. Camy–Peyret, J.-M. Flaud, A. Goldman, and J. Schroeder, "HITEMP, the high-temperature molecular spectroscopic database", *JQSRT* (in preparation).
6. H. M. Pickett, R. L. Poynter, E. A. Cohen, M. L. Delitsky, J. C. Pearson, and H. S. P. Müller, "Submillimeter, millimeter, and microwave spectral line catalogue", *JQSRT* **60** (1998) this issue.
7. C. P. Rinsland, A. Goldman, M. A. H. Smith, and V. Malathy Devi, "Measurements of Lorentz air-broadening coefficients and relative intensities in the $H_2{}^{16}O$ pure rotational and ν_2 bands from long horizontal path atmospheric spectra", *Appl. Opt.* **30,** 1427–1438 (1991).
8. R. A. Toth, "ν_2 band of $H_2{}^{16}O$: line strengths and transition frequencies", *J. Opt. Soc. Am.* **B 8,** 2236–2255 (1991).
9. R. A. Toth, "Transition frequencies and absolute strengths of $H_2{}^{17}O$ and $H_2{}^{18}O$ in the 6.2-μm region", *J. Opt. Soc. Am.* **B 9,** 462–482 (1992).
10. K. Chance, W. A. Traub, D. G. Johnson, K. W. Jucks, P. Ciarpallini, R.A. Stachnik, R. J. Salawitch, and H. Michelsen, "Simultaneous measurements of stratospheric HOx, NOx, and Clx: Comparison with a photochemical model", *J. Geophys. Res.* **101,** 9031–9043 (1996).
11. L. H. Coudert, "Analysis of the line positions and line intensities in the ν_2 band of the water molecule", *J. Mol. Spectrosc.* **181,** 246–273 (1997).
12. M. P. Esplin, R. B. Wattson, M. L. Hoke, and L. S. Rothman, "High-temperature spectrum of H_2O in the 720 to 1400 cm^{-1} Region", *JQSRT* **60** (1998) this issue.
13. R. B. Wattson and L. S. Rothman, "Determination of vibrational energy levels and parallel band intensities of $^{12}C^{16}O_2$ by direct numerical diagonalization", *J. Mol. Spectrosc.* **119,** 83–100 (1986); R. B. Wattson and L. S. Rothman, "Direct numerical diagonalization: wave of the future", *JQSRT* **48,** 763–780 (1992).
14. J. C. Pearson, T. Anderson, E. Herbst, F. C. DeLucia, and P. Helminger, "Millimeter- and submillimeter-wave spectrum of highly excited states of water", *Astrophys. J.* **379,** L41–L43 (1991).

15. G. E. Becker and S. H. Autler, "Water vapor absorption of electromagnetic radiation in the centimeter wave-length range", *Phys.Rev.* **70,** 300–307 (1946); R. B. Sanderson and N. Ginsburg, "Line widths and line strengths in the rotational spectrum of water vapor", *JQSRT* **3,** 435–444 (1963); J. R. Rusk, "Line-breadth study of the 1.64-mm absorption in water vapor", *J. Chem. Phys.* **42,** 493–500 (1965); L. Frenkel and D. Woods, "The microwave absorption by H_2O vapor and its mixtures with other gases between 100 and 300 Gc/s", *Proc. IEEE* **54,** 498–505 (1966); V. Ya. Ryadov and N. I. Furashov, *Opt. Spectrosc.* (*USSR*) **24,** 93–97 (1968); H. J. Liebe and T. A. Dillon, "Accurate foreign-gas-broadening parameters of the 22-GHz H_2O line from refraction spectroscopy", *J. Chem. Phys.* **50,** 727–732 (1969); J. E. Pearson, D. T. Llewellyn-Jones, and R. J . Knight, "Water vapour absorption near a wavelength of 0.79 mm", *Infrared Phys.* **9,** 53–58 (1969); R. Emery, "Atmospheric absorption measurements in the region of 1 mm wavelength", *Infrared Phys.* **12,** 65–79 (1972); V. Ya. Ryadov and N. I. Furashov, "Measurement of the parameters of the absorption line $\lambda_{ij} = 398$ μm in the rotational spectrum of water vapor", *Opt. Spectrosc.* (*USSR*) **35,** 255–257 (1973).
16. S. D. Gasster, C. H. Townes, D. Goorvitch, and F. P. J. Valero, "Foreign-gas collision broadening of the far-infrared spectrum of water vapor", *J. Opt. Soc. Am.* **B 5,** 593–601 (1988); B. E. Grossmann and E. V. Browell, "Spectroscopy of water vapor in the 720-nm wavelength region: Line strengths, self-induced pressure broadenings and shifts, and temperature dependence of linewidths and shifts", *J. Mol. Spectrosc.* **136,** 264–294 (1989); B. E. Grossmann and E. V. Browell, "Water-vapor line broadening and shifting by air, nitrogen, oxygen, and argon in the 720-nm wavelength region", *J. Mol. Spectrosc.* **138,** 562–595 (1989); J. Remedios, "Spectroscopy for remote sensing of the atmosphere", Ph.D. Thesis, Oxford University (1990); C. P. Rinsland, A. Goldman, M. A. H. Smith, and V. M. Devi, "Measurements of Lorentz air-broadening coefficients and relative intensities in the $H_2{}^{16}O$ pure rotation and ν_2 bands from long horizontal path atmospheric spectra", *Appl. Opt.* **30,** 1427–1438 (1991).
17. R. R. Gamache, J.-M. Hartmann, and L. Rosenmann, "Collisional broadening of water vapor lines—I. A survey of experimental results", *JQSRT* **52,** 481–499 (1994).
18. R. R. Gamache and R. W. Davies, "Theoretical calculations of N_2-broadened halfwidths of H_2O using quantum Fourier transform theory", *Appl. Opt.* **22,** 4013–4019 (1983).
19. R. R. Gamache and L. S. Rothman, "Temperature dependence of N_2-broadened halfwidths of water: the pure rotation and ν_2 bands", *J. Mol. Spectrosc.* **128,** 360–369 (1988).
20. R. D. Cess, M. H. Zhang, P. Minnis, L. Corsetti, E. G. Dutton, B. W. Forgan, D. P. Garber, W. L. Gates, J. J. Hack, E. F. Harrison, X. Jing, J. T. Kiehl, C. N. Long, J.-J. Morcrette, G. L. Potter, V. Ramanathan, B. Subasilar, C. H. Whitlock, D. F. Young, and Y. Zhou, "Absorption of solar radiation by clouds: Observations versus models", *Science* **267,** 496–499 (1995); P. Pilewskie and F. P. J. Valero, "Direct observations of excess solar absorption by clouds", *Science* **267,** 1626–1629 (1995).
21. C. Camy-Peyret, J.-M. Flaud, J.-Y. Mandin, J.-P. Chevillard, J. Brault, D. A. Ramsay, M. Vervloet, and J. Chauville, "The high-resolution spectrum of water vapor between 16500 and 25250 cm^{-1}", *J. Mol. Spectrosc.* **113,** 208–228 (1985).
22. J. W. Harder and J. W. Brault, "Atmospheric measurements of water vapor in the 442-nm region", *J. Geophys. Res.* **102,** 6245–6252 (1997).
23. J.-M. Flaud, C. Camy-Peyret, A. Mahmoudi, and G. Guelachvili, "The ν_2 band of $HD^{16}O$", *Internat. J. Infrared and Millimeter Waves* **7,** 1063–1090 (1986); R. A. Toth, "$HD^{16}O$, $HD^{18}O$, and $HD^{17}O$ transition frequencies and strengths in the ν_2 bands", *J. Mol. Spectrosc.* **162,** 20–40 (1993).
24. L. S. Rothman, R. L. Hawkins, R. B. Wattson, and R. R Gamache, "Energy levels, intensities, and linewidths of atmospheric carbon dioxide bands", *JQSRT* **48,** 537–566 (1992).
25. J. B. Pollack, J. B. Dalton, D. Grinspoon, R. B. Wattson, R. Freedman, D. Crisp, D. A. Allen, B. Bezard, C. DeBergh, L. P. Giver, Q. Ma, and R. Tipping, "Near-infrared light from Venus' nightside: a spectroscopic analysis", *Icarus* **103,** 1–42 (1993).
26. L. P. Giver, C. Chackerian, Jr., M. N. Spencer, L. R. Brown, and R. B. Wattson, Sixth International Conference on Laboratory Research for Planetary Atmospheres, Bethesda, MD (October 30, 1994).
27. L. P. Giver, L. R. Brown, R. B. Wattson, M. N. Spencer, and C. Chackerian, Jr., Proceedings of the Fiftieth International Symposium on Molecular Spectroscopy, paper RL04, Ohio State Univ., Columbus, Ohio (June12–16, 1995).
28. R. A. Toth, R. H. Hunt, and E. K. Plyler, "Intensities of CO_2 Σ-Σ bands in the 1.43–1.65 μm region", *J. Mol. Spectrosc.* **38,** 107–117 (1971).
29. L. P. Giver, C. Chackerian, Jr., M. N. Spencer, and R. B. Wattson, Fifth International Conference on Laboratory Research for Planetary Atmospheres, Boulder, CO (October 17, 1993).
30. L. P. Giver, C. Chackerian, Jr., M. N. Spencer, L. R. Brown, and R. B. Wattson, "The rovibrational intensities of the $(40^01) \leftarrow (00^00)$ pentad absorption bands of $^{12}C^{16}O_2$ between 7284 and 7921 cm^{-1}", *J. Mol. Spectrosc.* **175,** 104–111 (1996).
31. F. P. J. Valero and R. W. Boese, "The absorption spectrum of CO_2 around 7740 cm^{-1}", *JQSRT* **18,** 391–398 (1977).
32. F. P. J. Valero, "Absolute intensity measurements of the CO_2 bands $401_{III} \leftarrow 000$ and $411_{III} \leftarrow 010$", *J. Mol. Spectrosc.* **68,** 269–279 (1977).
33. F. P. J. Valero and R. W. Boese, "Comments on the note by Arié et al. on the transition moment of the CO_2 band near 4400 cm^{-1}", *JQSRT* **20,** 427 (1978).

34. V. Malathy Devi, D. C. Benner, C. P. Rinsland, and M. A. H. Smith, "Measurements of pressure broadening and pressure shifting by nitrogen in the 4.3-μm band of $^{12}C^{16}O_2$", *JQSRT* **48,** 581–589 (1992).
35. C. P. Rinsland, J.-M. Flaud, A. Goldman, A. Perrin, C. Camy-Peyret, M. A. H. Smith, V. Malathy Devi, D. Chris Benner, A. Barbe, T. M. Stephen, and F. J. Murcray, "Spectroscopic parameters for ozone and its isotopes: current status, prospects for improvement, and the identification of $^{16}O^{16}O^{17}O$ and $^{16}O^{17}O^{16}O$ lines in infrared ground-based and stratospheric solar absorption spectra", *JQSRT* **60** (1998) this issue.
36. C. P. Rinsland, M. A. H. Smith, V. Malathy Devi, A. Perrin, J.-M. Flaud, and C. Camy-Peyret, "The ν_2 bands of $^{16}O^{17}O^{16}O$ and $^{16}O^{16}O^{17}O$: line positions and intensities", *J. Mol. Spectrosc.* **149,** 474–480 (1991).
37. S. Bouazza, A. Barbe, J. J. Plateaux, J.-M. Flaud, and C. Camy-Peyret, "The $3\nu_1$ and $\nu_1 + 3\nu_3 - \nu_2$ absorption bands of $^{16}O_3$", *J. Mol. Spectrosc.* **160,** 371–377 (1993).
38. J.-M. Flaud, C. Camy-Peyret, A. Perrin, V. Malathy Devi, A. Barbe, S. Bouazza, J. J. Plateaux, C. P. Rinsland, M. A. H. Smith, and A. Goldman, "Line parameters for ozone hot bands in the 3.3-μm spectral region", *J. Mol. Spectrosc.* **160,** 378–386 (1993).
39. K. Chance, K. W. Jucks, D. G. Johnson, and W. A. Traub, "The Smithsonian Astrophysical Observatory database SAO92", *JQSRT* **52,** 447–457 (1994).
40. J. W. C. Johns, Z. Lu, M. Weber, J. M. Sirota, and D. C. Reuter, "Absolute intensities in the ν_2 fundamental of N_2O at 17 μm", *J. Mol. Spectrosc.* **177,** 203–210 (1996).
41. M. Weber, J. M. Sirota, and D. C. Reuter, "l-resonance intensity effects and pressure broadening of N_2O at 17 μm", *J. Mol. Spectrosc.* **177,** 211–220 (1996).
42. T. D. Varberg and K. M. Evenson, "Accurate far-infrared rotational frequencies of carbon monoxide", *Astrophys. J.* **385,** 763–765 (1992).
43. R. Farrenq, G. Guelachvili, A. J. Sauval, N. Grevesse, and C. B. Farmer, "Improved Dunham coefficients for CO from infrared solar lines of high rotational excitation", *J. Mol. Spectrosc.* **149,** 375–390 (1991); N. Authier, N. Bagland, and A. LeFloch, "The 1992 evaluation of mass-independent Dunham parameters for the ground state of CO", *J. Mol. Spectrosc.* **160,** 590–592 (1993).
44. C. Chackerian and R. H. Tipping, "Vibration–rotational and rotational intensities for CO isotopes", *J. Mol. Spectrosc.* **99,** 431–449 (1983).
45. D. Goorvitch, "Infrared CO line list for the $X^1\Sigma^+$ state", *Astrophys. J. Suppl. Ser.* **95,** 535–552 (1994).
46. G. Tarrago, G. Restelli, and F. Cappellani, "Absolute absorption intensities of the triad ν_3, ν_5, ν_6 of $^{12}CH_3D$ at 6–10 μm", *J. Mol. Spectrosc.* **129,** 326–332 (1988).
47. O. Ouardi, J. C. Hilico, M. Loëte, and L. R. Brown, "The hot bands of methane between 5 and 10 μm", *J. Mol. Spectrosc.* **180,** 311–322 (1996).
48. J. C. Hilico, J. P. Champion, S. Toumi, V. G. Tyuterev, and S. A. Tashkun, "New analysis of the pentad system of methane and prediction of the (pentad-pentad) spectrum", *J. Mol. Spectrosc.* **168,** 455–476 (1994).
49. A. Nikitin, J. P. Champion, Vl. G. Tyuterev, and L. R. Brown, "The high resolution spectrum of CH_3D in the region 900–1700 cm^{-1}", *J. Mol. Spectrosc.* **184,** 120–128 (1997).
50. N. Jacquinet-Husson, N. A. Scott, A. Chedin, B. Bonnet, A. Barbe, Vl. G. Tyuterev, J. P. Champion, M. Winnewisser, L. R. Brown, R. Gamache, V. F. Golovko, and A. A. Chursin, "The GEISA system in 1996: towards an operational tool for the second generation vertical sounders radiance simulation", *JQSRT* **59,** 511–527 (1998).
51. R. R. Gamache, A. Goldman, and L. S. Rothman, "Improved spectral parameters for the three most abundant isotopomers of the oxygen molecule", *JQSRT* **59,** 495–509 (1998).
52. L. S. Rothman, R. R. Gamache, A. Barbe, A. Goldman, J. R. Gillis, L. R. Brown, R. A. Toth, J.-M. Flaud, and C. Camy-Peyret, "AFGL atmospheric absorption line parameters compilation: 1982 edition", *Appl. Opt.* **22,** 2247–2256 (1983).
53. G. Rouillé, G. Millot, R. Saint-Loup, and H. Berger, "High resolution simulated Raman spectroscopy of O_2", *J. Mol. Spectrosc.* **154,** 372–382 (1992); M. Mizushima and S. Yamamoto, "Microwave absorption lines of $^{16}O^{18}O$ in its $X^3\Sigma_g^-$, $v = 0$ state", *J. Mol. Spectrosc.* **148,** 447–452 (1991); K. W. Hillig II, C. C. W. Chiu, W. G. Read, and E. A. Cohen, "The pure rotation spectrum of $a^1\Delta_g$ O_2", *J. Mol. Spectrosc.* **109,** 205 (1985); T. Scalabrin, R. J. Saykally, K. M. Evenson, H. E. Radford, and M. Mizushima, "Laser magnetic resonance measurement of rotational transitions in the metastable $a^1\Delta_g$ state of oxygen", *J. Mol. Spectrosc.* **89,** 344–351 (1981); R. N. Zare, A. L. Schmeltekopf, W. J. Harrop, and D. L. Albritton, "A direct approach for the reduction of diatomic spectra to molecular constants for the construction of RKR potentials", *J. Mol. Spectrosc.* **46,** 37–66 (1973).
54. E. A. Cohen and G. Birnbaum, "Influence of the potential function on the determination of multipole moments from pressure-induced far-infrared spectra", *J. Chem. Phys.* **66,** 2443–2447 (1977).
55. W. S. Benedict and L. D. Kaplan, "Calculation of line widths in H_2O–H_2O and H_2O–O_2 collisions", *JQSRT* **4,** 453–459 (1964).
56. R. M. Badger, A. C. Wright, and R. F. Whitlock, "Absolute intensities of the discrete and continuous absorption bands of oxygen gas at 1.26 and 1.065 μm and the radiative lifetime of the $^1\Delta_g$ state of oxygen", *J. Chem. Phys.* **43,** 4345–4350 (1965).
57. L.-B. Lin, Y.-P. Lee, and J. F. Ogilvie, "Linestrengths of the band $a^1\Delta_g(v' = 0)$-$X^3\Sigma_g^-$ $(v'' = 0)$ of $^{16}O_2$", *JQSRT* **39,** 375–380 (1988).

58. Y. T. Hsu, Y. P. Lee, and J. F. Ogilvie, "Intensities of lines in the band $a^1\Delta_g(v' = 0)$-$X^3\Sigma_g^1(v'' = 0)$ of $^{16}O_2$ in absorption", *Spectrochim. Acta* **48A,** 1227–1230 (1992).
59. M. G. Mlynczak and D. J. Nesbitt, "The Einstein coefficient for spontaneous emission of the $O_2(a^1\Delta_g)$ state", *Geophys. Res. Lett.* **22,** 1381–1384 (1995).
60. W. R. Pendelton, Jr., D. J. Baker, R. J. Reese, and R. R. O'Neil, "Decay of $O_2(a^1\Delta_g)$ in the evening twilight airglow: Implications for the radiative lifetime", *Geophys. Res. Lett.* **23,** 1013–1016 (1996).
61. B. J. Sandor, R. T. Clancy, D. W. Rusch, C. E. Randall, R. S. Eckman, D. S. Siskind, and D. O. Muhleman, "Microwave observations and modeling of $O_2(^1\Delta_g)$ and O_3 diurnal variations in the mesosphere", *J. Geophys. Res.* **102,** 9013–9028 (1996).
62. W. J. Lafferty, A. M. Slodov, C. L. Lugez, and G. T. Fraser, "Rotational linestrengths and self-pressure-broadening coefficients for the 1.27 μm $a^1\Delta_g - X^3\Sigma_g^-$, $v = 0$–0 band of O_2'", *J. Mol. Spectrosc.* (1998) in press.
63. D. A. Newnham, J. Ballard, and M. S. Page, "Visible absorption spectroscopy of molecular oxygen", paper A7, Atmospheric Spectroscopy Applications Workshop, Sept. 4–6, Reims, France (1996).
64. P. H. Krupenie, "The spectrum of molecular oxygen", *J. Phys. Chem. Ref. Data* **2,** 423–534 (1972).
65. K. J. Ritter and T. D. Wilkerson, "High-resolution spectroscopy of the oxygen A band", *J. Mol. Spectrosc.* **121,** 1–19 (1987).
66. L. P. Giver, R. W. Boese, and J. H. Miller, "Intensity measurements, self-broadening coefficients, and rotational intensity distribution for lines of the oxygen B band at 6880 Å", *JQSRT* **14,** 793–802 (1974).
67. M. A. Mélières, M. Chenevier, and F. Stoeckel, "Intensity measurements and self-broadening coefficients in the γ band of O_2 at 628 nm using intracavity laser-absorption spectroscopy (ICLAS)", *JQSRT* **33,** 337–345 (1985).
68. V. Dana, J.-Y. Mandin, L. H. Coudert, M. Badaoui, F. Le Roy, G. Guelachvili, and L. S. Rothman, "Λ-splittings and line intensities in the $2 \Leftarrow 1$ hot band of nitric oxide", *J. Mol. Spectrosc.* **165,** 525–540 (1994).
69. J.-Y. Mandin, V. Dana, L. H. Coudert, M. Badaoui, F. Le Roy, M. Morillon-Chapey, R. Farrenq, and G. Guelachvili, "Line positions and intensities in the fundamental $1 \leftarrow 0$ forbidden $^2\Pi_{1/2}$–$^2\Pi_{3/2}$ and $^2\Pi_{3/2}$–$^2\Pi_{1/2}$ subbands of nitric oxide", *J. Mol. Spectrosc.* **167,** 262–271 (1994); L. H. Coudert, V. Dana, J.-Y. Mandin, M. Morillon-Chapey, R. Farrenq, and G. Guelachvili, "The spectrum of nitric oxide between 1700 and 2100 cm^{-1}", *J. Mol. Spectrosc.* **172,** 435–448 (1995).
70. A. Goldman, L. R. Brown, W. G. Schoenfeld, M. N. Spencer, C. Chackerian Jr, L. P. Giver, H. Dothe, C. P. Rinsland, L. H. Coudert, V. Dana, and J.-Y. Mandin, "Nitric oxide line parameters: Review of 1996 HITRAN update and new results", *JQSRT* **60** (1998) this issue.
71. A. Goldman, F. J. Murcray, C. P. Rinsland, R. D. Blatherwick, S. J. David, F. H. Murcray, and D.G. Murcray, "Mt Pinatubo SO_2 column measurements from Mauna Loa", *Geophys. Res. Lett.* **19,** 183–186 (1992).
72. G. J. Bluth, S. D. Doiron, C. C. Schnetzler, A. J. Krueger, and L. S. Walter, "Global tracking of the SO_2 clouds from June 1991 Mount Pinatubo eruptions", *Geophys. Res. Lett.* **19,** 151–154 (1992); J. Hansom, A. Lacis, R. Ruedy, and M. Sata, "Potential climate impact of Mt Pinatubo eruption", *Geophys. Res. Lett.* **19,** 215–218 (1992); C. P. Rinsland, M. R. Gunson, M. K. W. Ko, D. W. Weisenstein, R. Zander, M. C. Abrams, A. Goldman, N. D. Sze, and G. K. Yue, "H_2SO_4 photolysis: a source of sulfur dioxide in the upper stratosphere", *Geophys. Res. Lett.* **22,** 1109–1112 (1995).
73. W. G. Mankin, M. T. Coffey, and A. Goldman, "Airborne observations of SO_2, HCl and O_3 in the stratospheric plume of the Pinatubo volcano in July 1991", *Geophys. Res. Lett.* **19,** 179–182 (1992).
74. A. Perrin, J.-M. Flaud, A. Goldman, C. Camy-Peyret, W. J. Lafferty, Ph. Arcas and C. P. Rinsland, "NO_2 and SO_2 line parameters: 1996 HITRAN update and results", *JQSRT* **60** (1998) this issue.
75. J.-M. Flaud, A. Perrin, L. M. Salah, W. J. Lafferty, and G. Guelachvili, "A reanalysis of the (010) (020) (100) and (001) rotational levels of $^{32}S^{16}O_2$", *J. Mol. Spectrosc.* **160,** 272–278 (1993).
76. P. M. Chu, S. J. Wetzel, W. J. Lafferty, A. Perrin, J.-M. Flaud, Ph. Arcas, and G. Guelachvili, "Line intensities for the 8μm bands of SO_2", *J. Mol. Spectrosc.* **189,** 55–63 (1998).
77. W. J. Lafferty, A. S. Pine, G. Hilpert, R. L. Sams, and J.-M. Flaud, "The $\nu_1 + \nu_3$ and $2\nu_1 + \nu_3$ band systems of SO_2: line positions and intensities", *J. Mol. Spectrosc.* **176,** 280–286 (1996).
78. W. J. Lafferty, A. S. Pine, J.-M. Flaud, and C. Camy-Peyret, "The $2\nu_3$ band of SO_2: line positions and intensities", *J. Mol. Spectrosc.* **157,** 499–511 (1993).
79. B. Bezard, C. deBergh, D. Crisp, and J. P. Maillard, "The deep atmosphere of Venus revealed by high resolution nightside spectra", *Nature* **345,** 508–511 (1990).
80. W. J. Lafferty, G. T. Fraser, A. S. Pine, J.-M. Flaud, C. Camy-Peyret, V. Dana, J.-Y. Mandin, A. Barbe, J. J. Plateaux, and S. Bouazza, "The $3\nu_3$ band of $^{32}S^{16}O_2$: line positions and intensities", *J. Mol. Spectrosc.* **154,** 51–60 (1992).
81. J.-M. Flaud and W. J. Lafferty, "$^{32}S^{16}O_2$: a refined analysis of the $3\nu_3$ band and determination of equilibrium rotational constants", *J. Mol. Spectrosc.* **161,** 396–402 (1993).
82. G. D. Tejwani, "Calculation of pressure broadened linewidths of SO_2 and NO_2", *J. Chem. Phys.* **57,** 4676–4681 (1972).

83. W. H. Yang, J. A. Roberts, and G. D. Tejwani, "Linewidths parameters for $\Delta J = 1$ $0 < J < 43$ rotational transitions of the sulfur dioxide molecule", *J. Chem. Phys.* **58,** 4916–4918 (1973).
84. C. D. Ball, J. M. Dutta, T. M. Goyette, P. Helminger, and F. C. DeLucia, "The pressure broadening of SO_2 by N_2, O_2, He, and H_2 between 90 and 500 K", *JQSRT* **56,** 109–118 (1996).
85. K.. Kuhnemann, Y. Meiner, B. Sumpf, and Ka. Hermann, "Line broadening in the v_3 band of SO_2 studied with diode laser spectroscopy", *J. Mol. Spectrosc.* **152,** 1–12 (1992); B. Sumpf, O. Flieschmann, and H. D. Kronfeldt, "Self-, air- and nitrogen-broadening in the v_1 band of SO_2", *J. Mol. Spectrosc.* **176,** 127–132 (1996); B. Sumpf, M. Schöne, and H. D. Kronfeldt, "Self- and air-broadening in the v_3 band of SO_2", *J. Mol. Spectrosc.* **179,** 137–141 (1996); B. Sumpf, M. Schöne, O. Flieschmann, Y. Meiner, and H. D. Kronfeldt, "Quantum number and temperature dependence of foreign gas-broadening coefficients in the v_1 and v_3 bands of SO_2", *J. Mol. Spectrosc.* **183,** 61–71 (1997).
86. A. Perrin, C. Camy-Peyret, and J.-M. Flaud, "Infrared nitrogen dioxide in the HITRAN database", *JQSRT* **48,** 645–652 (1992).
87. A. Perrin, J.-M. Flaud, C. Camy-Peyret, A. Goldman, F. J. Murcray, R. D. Blatherwick, and C. P. Rinsland, "The v_2 and $2v_2$ bands of $^{14}N^{16}O_2$: electron spin-rotation and hyperfine contact resonances in the (010) vibrational state", *J. Mol. Spectrosc.* **160,** 456–463 (1993).
88. V. Malathy Devi, P. P. Das, A. Bano, K. Narahari Rao, J.-M. Flaud, C. Camy-Peyret, and J. P. Chevillard, "Diode laser measurements of intensities, N_2 broadening and self broadening coefficients of lines of the v_2 band of $^{14}N^{16}O_2$", *J. Mol. Spectrosc.* **88,** 251–258 (1981).
89. A. Perrin, J.-M. Flaud, C. Camy-Peyret, A. M. Vasserot, G. Guelachvili, A. Goldman, F. J. Murcray, and R. D. Blatherwick, "The $\{v_3, 2v_2, v_1\}$ interacting bands of NO_2: line positions and intensities", *J. Mol. Spectrosc.* **154,** 391–406 (1992).
90. R. A. Toth, "High resolution measurements and analysis of NO_2 in the (001)–(000) and (011)–(010) bands", *J. Opt. Soc. Am* **B9,** 433–461 (1992).
91. V. Malathy Devi, B. Fridovitch, G. D. Jones, G. D. Snyder, P. P. Das, J.-M. Flaud, C. Camy-Peyret, and K. Narahari Rao, "Tunable diode laser spectroscopy of NO_2 at 6.2μm", *J. Mol. Spectrosc.* **93,** 179–195 (1982).
92. A. Perrin, J.-M. Flaud, C. Camy-Peyret, D. Hurtmans, M. Herman, and G. Guelachvili, "The $v_2 + v_3$ and the $v_2 + v_3 - v_2$ bands of NO_2: line positions and intensities", *J. Mol. Spectrosc.* **168,** 54–66 (1994).
93. B. J. Kerridge and E. E. Remsberg, "Evidence from the Limb Infrared Monitor of the Stratosphere for non local thermodynamic equilibrium in the v_2 mode of mesospheric water vapour and the v_3 mode of stratospheric nitrogen dioxide", *J. Geophys. Res.* **94,** 16323–16342 (1989).
94. H. Fischer and H. Oelhaf, "Remote sensing of vertical profiles of atmospheric trace gas constituents with MIPAS limb-emission spectrometers", *Appl. Opt.* **35,** 2787–2796 (1996).
95. A. Perrin, J.-M. Flaud, C. Camy-Peyret, D. Hurtmans, and M. Herman, "The $(2v_3, 4v_2, 2v_2 + v_3)$ and $2v_3$-v_3 bands of NO_2; line positions and intensities", *J. Mol. Spectrosc.* **177,** 58–65 (1996).
96. A. Perrin, J.-M. Flaud, and C. Camy-Peyret, "Calculated line positions and intensities for the $v_1 + v_3$ and $v_1 + v_2 + v_3 - v_2$ bands of NO_2", *Infrar. Phys.* **22,** 343–348 (1982).
97. J.-Y.Mandin, V. Dana, A. Perrin, J.-M. Flaud, C. Camy-Peyret, L. Regalia, and A. Barbe, "The $(v_1 + 2v_2, v_1 + v_3)$ bands of NO_2: line positions and intensities, line intensities in the $v_1 + v_2 + v_3 - v_2$ hot bands", *J. Mol. Spectrosc.* **181,** 379–388 (1997).
98. I. Kleiner, G. Tarrago, and L. R. Brown, "Analysis of $3v_2$ and $v_2 + v_4$ of $^{14}NH_3$ near 4 μm", *J. Mol. Spectrosc.* **173,** 120–145 (1995).
99. G. Guelachvili, A. Abdulah, N. Tu, K. Narahari Rao, Š. Urban, and D. Papoušek, "Analysis of High-Resolution Fourier Transform Spectra of $^{14}NH_3$ at 3.0 μm", *J. Mol. Spectrosc.* **133,** 345–364 (1989).
100. Š. Urban, N. Tu, K. Narahari Rao, and G. Guelachvili, "Analysis of High-Resolution Fourier Transform Spectra of $^{14}NH_3$ at 2.3 μm", *J. Mol. Spectrosc.* **133,** 312–330 (1989).
101. L.R. Brown and J.S. Margolis, "Empirical line parameters of NH_3 from 4791–5294 cm^{-1}", *JQSRT* **56,** 283–294 (1996).
102. A. S. Pine and M. Dang-Nhu, "Spectral Intensities in the v_1 band of NH_3", *JQSRT* **50,** 565–570 (1993).
103. J. S. Margolis and Y. Y. Kwan, "The measurement of the absorption strengths of some lines in the $v_1 + v_2$ and $v_2 + v_3$ bands of ammonia", *J. Mol. Spectrosc.* **50,** 266–280 (1974).
104. A. S. Pine, V. N. Markov, G. Buffa, and O. Tarrini, "N_2, O_2, H_2, Ar and He broadening in the v_1 Band of NH_3", *JQSRT* **50,** 337–348 (1993).
105. V. N. Markov, A. S. Pine, G. Buffa, and O. Tarrini, "Self broadening in the v_1 band of NH_3", *JQSRT* **50,** 167–178 (1993).
106. L. R. Brown and D. B. Peterson, "An empirical expression for linewidths of ammonia from far-infrared measurements", *J. Mol. Spectrosc.* **168,** 593–606 (1994).
107. A. Goldman, and C. P. Rinsland, "HNO_3 line parameters: New results and comparisons of simulations with high-resolution laboratory and atmospheric spectra", *JQSRT* **48,** 653–666 (1992).
108. A. Perrin, J.-M. Flaud, C. Camy-Peyret, V. Jaquen, R. Farrenq, G. Guelachvili, Q. Kou, F. Le Roy, M. Morillon-Chapey, J. Orphal, M. Badaoui, J.-Y. Mandin, and V. Dana, "Line intensities in the 11 - and 7.6-μm bands of HNO_3", *J. Mol. Spectrosc.* **160,** 524–539 (1993).
109. A. Perrin, V. Jaouen, A. Valentin, J.-M. Flaud, and C. Camy-Peyret, "The v_5 and $2v_9$ bands of nitric acid", *J. Mol. Spectrosc.* **157,** 112–121 (1993).

110. A. Perrin, J.-M. Flaud, C. Camy-Peyret, B. P. Winnewisser, S. Klee, A. Goldman, F. J. Murcray, R. D. Blatherwick, F. S. Bonomo, and D. G. Murcray, "First analysis of the $3\nu_9 - \nu_9$, $3\nu_9 - \nu_5$, and $3\nu_9 - 2\nu_9$, bands of HNO_3: Torsional splitting in the ν_9 vibrational mode", *J. Mol. Spectrosc.* **166,** 224–243 (1994).
111. A. Perrin, J.-M. Flaud, C. Camy-Peyret, A. Goldman, C. P. Rinsland, and M. R. Gunson, "Identification of the HNO_3 $3\nu_9 - \nu_9$ band Q branch in stratospheric solar occultation spectra", *JQSRT* **52,** 319–322 (1994).
112. J. M. Sirota, M. Weber, D. C. Reuter, and A. Perrin, "HNO_3: Absolute line intensities for the ν_9 fundamental", *J. Mol. Spectrosc.* **184,** 140–144 (1997).
113. L. H. Coudert and A. Perrin, "Accounting for the torsional splitting in the ν_5 and $2\nu_9$ bands of nitric acid", *J. Mol. Spectrosc.* **172,** 352–368 (1995).
114. T. M. Goyette, C. D. Paulse, L. C. Oesterling, F. C. DeLucia, and P. Helminger, "Torsional splitting in the $2\nu_5$ and ν_5 vibrational band of HNO_3", *J. Mol. Spectrosc.* **167,** 365–374 (1994); T. M. Goyette, L. C. Oesterling, D. T. Petkie, R. A. Booker, P. Helminger, and F. C. DeLucia, "Rotational spectrum of HNO_3 in the ν_5 and $2\nu_9$ vibration states", *J.Mol.Spectrosc.* **175,** 395–410 (1996).
115. C. D. Paulse, L. H. Coudert, T. M. Goyette, R. L. Crownover, P. Helminger, and F. C. DeLucia, "Torsional splitting in the ν_9 band of nitric acid", *J. Mol. Spectrosc.* **177,** 9–18 (1996).
116. W. F. Wang, P. P. Ong, T. L. Tan, E. C. Looi, and H. H. Teo, "Infrared analysis of the anharmonic resonance between $\nu_8 + \nu_9$ and the dark state $\nu_6 + \nu_7$ of HNO_3", *J. Mol. Spectrosc.* **183,** 407–413 (1997).
117. A. Goldman, C. P. Rinsland, A. Perrin, and J.-M. Flaud, "HNO_3 line parameters: 1996 HITRAN update and new results", *JQSRT* **60** (1998) this issue.
118. A. Goldman, J. B. Burkholder, C. J. Howard, R. Escribano, and A. G. Maki, "Spectroscopic constants for the ν_9 band of HNO_3", *J. Mol. Spectrosc.* **131,** 195–200 (1988).
119. L. P. Giver, F. P. J. Valero, D. Goorvitch, and F. S. Bonomo, "Nitric-acid band intensities and band-model parameters from 610 to 1760 cm^{-1}", *J. Opt. Soc. Am.* **B1,** 715–722 (1984).
120. A. Perrin, O. Lado-Bordowsky, and A. Valentin, "The ν_3 and ν_4 interacting bands of HNO_3 line positions and line intensities", *Mol. Phys.* **67,** 249–270 (1989).
121. R. D. May and C. R. Webster, "Measurements of line positions, intensities, and collisional air-broadening coefficients in the HNO_3 7.5 μm band using a computer controlled tunable diode laser spectrometer", *J. Mol. Spectrosc.* **138,** 383–397 (1989).
122. C. B. Farmer and R. H. Norton, "High resolution infrared spectroscopy of the sun and the Earth's atmosphere from space", *Mikrochimica Acta* [*Wien*] **3,** 189–214 (1987).
123. Two Special Issues on the ATMOS mission: *Geophys. Res. Lett.* **23,** 2203–2412 (1996) and *Appl. Opt.* **35,** 2732–2947 (1996).
124. L. S. Rothman, A. Goldman, J. R. Gillis, R. R. Gamache, H. M. Pickett, R. L. Poynter, N. Husson, and A. Chedin, "AFGL trace gas compilation: 1982 version", *Appl. Opt.* **22,** 1616–1627 (1983).
125. R. L. Poynter and H. M. Pickett, "Submillimeter, millimeter, and microwave spectral line catalog", *Appl. Opt.* **24,** 2235–2240 (1985).
126. A. Goldman, "Line parameters for the atmospheric band system of OH", *Appl. Opt.* **21,** 2100–2102 (1982).
127. R. R Gamache, R. L. Hawkins, and L. S. Rothman, "Total internal partition sums in the temperature range 70–3000 K: atmospheric linear molecules", *J. Mol. Spectrosc.* **142,** 205–219 (1990).
128. A. Goldman, W. G. Schoenfeld, D. Goorvitch, C. Chackerian, Jr., H. Dothe, F. Mélen, M. C. Abrams, and J. E. A. Selby, "Updated line parameters for OH $X^2\Pi$–$X^2\Pi$ (v'', v') transitions", *JQSRT* **59,** 453–469 (1998).
129. J. A. Coxon and S. C. Foster, "Rotational analysis of hydroxyl vibration–rotation emission bands: molecular constants for OH $X^2\Pi$, , $6 \leq v \leq 10$", *Can. J. Phys.* **60,** 41–48 (1982).
130. M. C. Abrams, S. P. Davis, M. L. P. Rao, R. Engleman Jr., and J. W. Brault, "High-resolution Fourier transform spectroscopy of the Meinel system of OH", *Astrophys. J. Suppl. Ser.* **93,** 351–395 (1994).
131. F. Mélen, A. J. Sauval, N. Grevesse, C. B. Farmer, Ch. Servais, L. Delbouille, and G. Roland, "A new analysis of the OH radical spectrum from solar infrared observations", *J. Mol. Spectrosc.* **174,** 490–509 (1995).
132. D. Goorvitch and D. C. Galant, "Schrodinger's radial equation: solution by extrapolation", *JQSRT* **47,** 391–399 (1992); D. Goorvitch and D. C. Galant, "The solution of coupled Schrodinger equations using an extrapolation method", *JQSRT* **47,** 505–513 (1992); C. Chackerian Jr., D. Goorvitch, A. Benidar, R. Farrenq, G. Guelachvili, P. M. Martin, M. C. Abrams, and S. P. Davis, "Rovibrational intensities and electric dipole moment function of the $X^2\Pi$ hydroxyl radical", *JQSRT* **48,** 667–673 (1992); D. Goorvitch, A. Goldman, H. Dothe, R. H. Tipping, and C. Chackerian, Jr., "Hydroxyl $X^2\Pi$ pure rotational transitions", *J. Geophys. Res.* **97,** 20771–20786 (1992).
133. D. D. Nelson Jr., A. Schiffman, D. J. Nesbitt, J. J. Orlando and J. B. Burkholder, "$H + O_3$ Fourier-transform infrared emission and laser absorption studies of $OH(X^2\Pi)$ radical: an experimental dipole moment function and state-to-state Einstein A coefficients", *J. Chem. Phys.* **93,** 7003–7019 (1990); C. Chackerian, Jr., D. Goorvitch, A. Benidar, R. Farrenq, G. Guelachvili, M. C. Abrams, and S. P. Davis, *J. Chem. Phys.* (to be published).
134. D. Bastard, A. Bretenoux, A. Charru, and F. Picherit, "Determination of mean collision cross-sections of free radical OH with foreign gases", *JQSRT* **21,** 369–372 (1979).

135. K. V. Chance, D. A. Jennings, K. M. Evenson, M. D. Vanek, I. G. Nolt, J. V. Radostitz, and K. Park, "Pressure broadening of the 118.455 cm^{-1} rotational lines of OH by H_2, He, N_2, and O_2", *J. Mol. Spectrosc.* **146,** 375–380 (1991).
136. A. Schiffman and D. J. Nesbitt, "Pressure broadening and collisional narrowing in OH ($v = 1$–0) rovibrational transitions with Ar, He, O_2, and N_2", *J. Chem. Phys.* **100,** 2677–2689 (1994).
137. K. Park, L. R. Zink, K. M. Evenson, K. V. Chance, and I. G. Nolt, "Pressure broadening of the 83.869 cm^{-1} rotational lines of OH by N_2, O_2, H_2 and He", *JQSRT* **55,** 285–287 (1996).
138. G. Buffa, O. Tarrini, and M. Inguscio, "Prediction for collisional broadening of far-infrared OH rotational lines of atmospheric interest", *Appl. Opt.* **26,** 3066–3068 (1987).
139. A. Goldman and J. R. Gillis, "Spectral line parameters for the $A^2\Sigma$–$X^2\Pi(0, 0)$ band of OH for atmospheric and high temperatures", *JQSRT* **25,** 111–135 (1981).
140. R. P. Cageao, Y. L. Ha, Y. Jiang, M. F. Morgan, Y. L. Yung, and S. P. Sander, "Calculated hydroxyl $A^2\Sigma$–$X^2\Pi(0, 0)$ band emission rate factors applicable to atmospheric spectroscopy", *JQSRT* **57,** 703–717 (1997).
141. I. G. Nolt, J. V. Radostitz, B. DiLonardo, K. M. Evenson, D. A. Jennings, K. R. Leopold, M. D. Vanek, L. R. Zink, A. Hinz, and K. V. Chance, "Accurate rotational constants of CO, HCl, and HF: spectral standards for the 0.3- to 6-THz (10- to 200-cm^{-1}) region", *J. Mol. Spectrosc.*, **125,** 274–287 (1987).
142. A. S. Pine and J. P. Looney, "N_2 and air broadening in the fundamental bands of HF and HCl", *J. Mol. Spectrosc.* **122,** 41–55 (1987).
143. C. P. Rinsland, M. A. H. Smith, A. Goldman, V. M. Devi, and D. C. Benner, "The fundamental bands of $H^{35}Cl$ and $H^{37}Cl$: line positions from high-resolution laboratory data", *J. Mol. Spectrosc.* **159,** 274–287 (1993).
144. G. DiLonardo, L. Fusina, P. DeNatale, M. Inguscio, and M. Prevedelli, "The pure rotational spectrum of HBr in the submillimeter wave region", *J. Mol. Spectrosc* **148,** 86–92 (1991).
145. M. T. Coffey, A. Goldman, J. W. Hannigan, W. G. Mankin, W. G. Schoenfeld, C. P. Rinsland, C. Bernado, and D. W. T. Griffith, "Improved vibration–rotation (0–1) HBr line parameters for validating high-resolution infrared atmospheric spectra measurements", *JQSRT* **60** (1998) this issue.
146. K. V. Chance, T. D. Varberg, K. Park, and L. R. Zink, "The far-infrared spectrum of HI", *J. Mol. Spectrosc.* **162,** 120–126 (1993); A. Goldman, K. V. Chance, M. T. Coffey, J. W. Hannigan, W. G. Mankin, and C. P. Rinsland, "Improved line parameters for the $X^1\Sigma^+$ (0–0) and (0–1) bands of HI", *JQSRT* **60** (1998) this issue.
147. A. Goldman, J. R. Gillis, C. P. Rinsland, and J. B. Burkholder, "Improved line parameters for the $X^2\Pi$–$X^2\Pi$ (1–0) bands of ^{35}ClO and ^{37}ClO", *JQSRT* **52,** 357–360 (1994).
148. J. D. Burkholder, P. D. Hammer, C. J. Howard, A. G. Maki, G. Thompson, and C. Chackerian Jr., "Infrared measurements of the ClO radical", *J. Mol. Spectrosc.* **124,** 139–161 (1987).
149. J. D. Burkholder, P. D. Hammer, C. J. Howard, and A. Goldman, "Infrared line intensity measurements in the $v = 0$–1 band of the ClO radical", *J. Geophys. Res.* **94,** 2225–2234 (1989).
150. C. P. Rinsland and A. Goldman, "Search for infrared absorption lines of atmospheric chlorine monoxide (ClO)", *JQSRT* **48,** 685–692 (1992).
151. J. Notholt, A. Meier, and S. Peil, "Total column densities of tropospheric and stratospheric trace gases in the undisturbed Arctic summer atmosphere", *J. Atm. Chem.* **20,** 311–332 (1995).
152. W. Bell, C. Paton-Walsh, T. D. Gardiner, P. T. Woods, N. R. Swann, N. A. Martin, L. Donohoe, and M. P. Chipperfield, "Measurements of stratospheric chlorine monoxide (ClO) from groundbased FTIR observations", *J. Atmos. Chem.* **24,** 285–297 (1996).
153. M. Birk and G. Wagner, "Experimental line strengths of the ClO fundamental", *J. Geophys. Res.* **102,** 19 199–19 206 (1997).
154. M. W. Waters, W. G. Reed, L. Froidevaux, T. A. Lungu, V. S. Peran, R. A. Stachnik, R. F. Jarnot, R. E. Cofield, E. F. Fishbein, D. A. Flower, J. R. Burke, J. C. Hardy, L. L. Nakamura, B. P. Ridenoure, Z. Shippony, R. P. Thurstans, L. M. Avallone, D. W. Toohey, R. L. deZafra, and D. T. Shindell, "Validation of UARS microwave limb sounder ClO measurements", *J. Geophys. Res.* **101,** 10 091–10 127 (1996).
155. J. J. Oh and E. A. Cohen, "Pressure broadening of ClO by N_2 and O_2 near 204 and 649 GHz and new frequency measurements between 632 and 725 GHz", *JQSRT* **52,** 151–156 (1994).
156. D. P. Donovan, H. Fast, Y. Makino, J. C. Bird, A. I. Carlswell, J. Davies, T. J. Duck, J. W. Kaminski, C. T. McElroy, R. J. Mittermeier, S. R. Pal, V. Savastiouk, D. Velkov, and J. A. Whiteway, "Ozone, column ClO, and PSC measurements made at the NDSC Eureka Observatory (80 deg N, 86 deg W, during the Spring of 1997)", *Geophys. Res. Lett.* **24,** 2709–2712 (1997).
157. Selected references for the global analysis: A. Fayt, R. Vandenhaute, and J. G. Lahaye, "Global rovibrational analysis of carbonyl sulfide", *J. Mol. Spectrosc.* **119,** 233–266 (1986); J. G. Lahaye, R. Vandenhaute, and A. Fayt, "CO_2 laser saturation Stark spectra and global Stark analysis of carbonyl sulfide", *J. Mol. Spectrosc.* **119,** 267–279 (1986); L. S. Masukidi, J. G. Lahaye, and A. Fayt, "Intracavity CO laser Stark spectroscopy of the ν_3 band of carbonyl sulfide", *J. Mol. Spectrosc.* **148,** 281–302 (1991); Ch. Hornberger, B. Boor, R. Stuber, W. Demtröeder, S. Naim, and A. Fayt, "Sensitive overtone spectroscopy of carbonyl sulfide between 6130 and 6650 cm^{-1} and at 12 000 cm^{-1}", *J. Mol. Spectrosc.* **179,** 237–245 (1996). References for the intensities: A. Belafhal, A. Fayt, and G. Guelachvili, "Fourier transform spectroscopy of

carbonyl sulfide from 1800 to 3120 cm^{-1}: the normal species", *J. Mol. Spectrosc.* **174,** 1–19 (1995); G. Blanquet, P. Coupe, F. Derie, and J. Walrand, "Spectral intensities in the $2\nu_2^0$ band of carbonyl sulfide", *J. Mol. Spectrosc.* **147,** 543–545 (1991); J.-P. Bouanich, G. Blanquet, J. Walrand, and C. P. Courtoy, "Diode laser measurements of line strengths and collisional half-widths in the ν_1 band of OCS at 298 and 200 K", *JQSRT*, **36,** 295–306 (1986); M. Dang-Nhu and G. Guelachvili, *Mol. Phys.* **58,** 535–540 (1986); R. H. Kagann, "Infrared absorption intensities of OCS", *J. Mol. Spectrosc.* **94,** 192–198 (1982).

158. M. Carlotti, G. DiLonardo, L. Fusina, A. Trombetti, and B. Carli, "The far-infrared spectrum of hypochlorous acid, HOCl", *J. Mol. Spectrosc.* **141,** 29–42 (1990).
159. C. P. Rinsland, A. Goldman, and J.-M. Flaud, "Infrared spectroscopic parameters of COF_2, SF_6, ClO, N_2, and O_2", *JQSRT* **48,** 693–699 (1992).
160. A. Perrin, J.-M. Flaud, C. Camy-Peyret, R. Schermaul, M. Winnewisser, J.-Y. Mandin, V. Dana, M. Badaoui, and J. Koput, "Line intensities in the far-infrared spectrum of H_2O_2", *J. Mol. Spectrosc.* **176,** 287–296 (1996).
161. R. D. May, "Absolute linestrengths in the H_2O_2 ν_6 band", *JQSRT* **45,** 267–272 (1991).
162. A. Perrin, A. Valentin, J.-M. Flaud, C. Camy-Peyret, L. Schriver, A. Schriver, and Ph. Arcas, "The 7.9-μm band of hydrogen peroxide: Line positions and intensities". *J. Mol. Spectrosc.* **171,** 358–373 (1995).
163. K. W. Jucks, D. G. Johnson, K. V. Chance, W. A. Traub, G. C. Toon, B. Sen, J.-F. Blavier, B. B. Osterman, and R. J. Salawitch, "Atmospheric chemistry of H_2O_2; evidence for a missing sink", *J. Geophys. Res.* (1998), in press.
164. J. J. Hillman, D. E. Jennings, G. W. Halsey, S. Nadler, and W. E. Blass, "An infrared study of the bending region of acetylene", *J. Mol. Spectrosc.* **146,** 389–401 (1991).
165. M. Weber, Ph.D. thesis, University of Tennessee (1992).
166. J. Vander Auwera, D. Hurtmans, M. Carleer, and M. Herman, "The ν_3 fundamental of C_2H_2", *J. Mol. Spectrosc.* **157,** 337–357 (1993).
167. V. Malathy Devi, D. C. Benner, C. P. Rinsland, M. A. H. Smith, and B. D. Sidney, "Tunable diode laser measurements of N_2 and air-broadened halfwidths: lines of the $(\nu_4 + \nu_5)^0$ band of $^{12}C_2H_2$ near 7.4 μm", *J. Mol. Spectrosc.* **114,** 49–53 (1985).
168. P. Varanasi, L. P. Giver, and F. P. J. Valero, "Measurements of nitrogen-broadened line widths of acetylene at low temperatures", *JQSRT* **30,** 505–509 (1983).
169. A. Babay, M. Ibrahimi, V. Lemaire, B. Lemoine, F. Rohart, and J. P. Bouanich, "Line frequency shifting in the ν_5 band of C_2H_2", *JQSRT* **59,** 195–202 (1998).
170. L. R. Brown, M. R. Gunson, R. A. Toth, F. W. Irion, C. P. Rinsland, and A. Goldman, "The 1995 atmospheric trace molecule spectroscopy (ATMOS) linelist", *Appl. Opt.* **35,** 2828–2848 (1996).
171. M. Dang-Nhu and A. Goldman, "Line parameters for C_2H_6 in the 3000 cm^{-1} region", *JQSRT* **38,** 159–161 (1987).
172. D. H. Ehhalt, U. Schmidt, R. Zander, P. Demoulin, and C. P. Rinsland, "Seasonal cycle and secular trend of the total and tropospheric column abundance of ethane above the Jungfraujoch", *J. Geophys. Res.* **96,** 4985–4994 (1991); C. P. Rinsland, A. Goldman, F. J. Murcray, S. J. David, R. D. Blatherwick, and D. G. Murcray, "Infrared spectroscopic measurements of the ethane (C_2H_6) total column abundance above Mauna Loa, Hawaii-Seasonal variations", *JQSRT* **52,** 273–279 (1994); C. P. Rinsland, N. B. Jones, and W. A. Matthews, "Infrared spectroscopic measurements of the total column abundance of ethane (C_2H_6) above Lauder, New Zealand", *J. Geophys. Res.* **99,** 25 941–25 945 (1994).
173. A. S. Pine and S. C. Stone, "Torsional tunneling and A_1–A_2 splittings and air broadening of the $^rQ_0$ and $^pQ_3$ subbranches of the ν_7 band of ethane", *J. Mol. Spectrosc.* **175,** 21–30 (1996).
174. A. S. Pine and W. J. Lafferty, "Torsional splittings and assignments of the Doppler-limited spectrum of ethane in the C-H stretching region", *J. Res. Natl. Bur. Stand.* **87,** 237–256 (1982).
175. P. Varanasi, Z. Li, V. Nemtchinov, and A. Cherukuri, "Spectral absorption-coefficient data on HCFC-22 and SF_6 for remote-sensing applications", *JQSRT* **52,** 323–332 (1994).
176. A. D. Bykov, O. V. Naumenko, M. A. Smirnov, L. N. Sinitsa, L. R. Brown, J. Crisp, and D. Crisp, "The infrared spectrum of H_2S from 1 to 5 μm", *Can. J. Phys.*: Herzberg Special Issue **72,** 989–1000 (1994).
177. L. Lechuga-Fossat, J.-M. Flaud, C. Camy-Peyret, and J. W. C. Johns, "The spectrum of natural hydrogen sulfide between 2150 and 2950 cm^{-1}", *Can. J. Phys.* **62,** 1889–1923 (1984).
178. L. R. Brown, J. A. Crisp, D. Crisp, O. V. Naumenko, M. A. Smirnov, L. N. Sinitsa, and A. Perrin, "The absorption spectrum of H_2S between 2150 and 4260 cm^{-1}: Analysis of the positions and intensities in the first ($2\nu_2$, ν_1, and ν_3) and second ($3\nu_2$, $\nu_1 + \nu_2$, and $\nu_2 + \nu_3$) triad regions", *J. Mol. Spectrosc.* **187,** 148–171 (1998).
179. A. Goldman and J. R. Gillis, "Line parameters and line calculation for molecules of stratospheric interest", Progress Report, Dept. of Physics, University of Denver, April 1984.
180. A. Goldman, F. H. Murcray, D. G. Murcray, and C. P. Rinsland, "A search for formic acid in the upper troposphere: a tentative identification of the 1105 cm^{-1} ν_6 band Q branch in high-resolution balloon-borne solar absorption spectra", *Geophys. Res. Lett.* **11,** 307–310 (1984).
181. C. P. Rinsland and A. Goldman, "Infrared spectroscopic measurements of tropospheric trace gases", *Appl. Opt.* **31,** 6969–6971 (1992).

182. R. J. Yokelson, D. W. T. Griffith, and D. E. Ward, "Open-path Fourier transform infrared studies of large-scale laboratory biomass fires", *J. Geophys. Res.* **101,** 21 067–21 080 (1996); R. J. Yokelson, R. Susott, D. E. Ward, J. Reardon, and D. W. T. Griffith, "Emissions from smoldering combustion of biomass measured by open-path Fourier transform infrared spectroscopy", *J. Geophys. Res.* **102,** 18 865–18 877 (1997).
183. R. E. Bumgarner, Jong-In Choe, and S. G. Kukolich, "High-resolution spectroscopy of the ν_6 and ν_8 bands of formic acid", *J. Mol. Spectrosc.* **132,** 261–276 (1988).
184. J. Vander Auwera, "High-resolution investigation of the far-infrared spectrum of formic acid". *J. Mol. Spectrosc.* **155,** 136–142 (1992).
185. K. V. Chance, K. Park, K. M. Evenson, L. R. Zink, F. Stroh, E. H. Fink, and D. A. Ramsay, "Improved molecular constants for the ground state of HO_2", *J. Mol. Spectrosc.* **183,** 418 (1997).
186. S. Saito and C. Matsumura, "Dipole moment of the HO_2 radical from its microwave spectrum", *J. Mol. Spectrosc.* **80,** 34–40 (1980).
187. K. Chance, P. De Natale, M. Bellini, M. Inguscio, G. Di Lonardo, and L. Fusina, "Pressure broadening of the 2.4978 THz rotational lines of HO_2 by N_2 and O_2", *J. Mol. Spectrosc.* **163,** 67–70 (1994).
188. D. D. Nelson, Jr. and M. S. Zahniser, "Diode laser spectroscopy of the ν_3 vibration of the HO_2 radical", *J. Mol. Spectrosc.* **150,** 527–534 (1991).
189. C. Yamada, Y. Endo, and E. Hirota, "Diode laser spectroscopy of the HO_2 ν_2 band", *J. Mol. Spectrosc.* **89,** 520–527 (1981).
190. C. Yamada, Y. Endo, and E. Hirota, "Difference frequency laser spectroscopy of the ν_1 band of the HO_2 radical", *J. Chem. Phys.* **78,** 4379–4384 (1983).
191. M. S. Zahniser, K. E. McCurdy, and A. C. Stanton, "Quantitative spectroscopic studies of the HO_2 radical: band strength measurements for the ν_1 and ν_2 vibrational bands", *J. Chem. Phys.* **93,** 1065–1070 (1989).
192. D. D. Nelson and M. S. Zahniser, "Air-broadening measurements in the ν_2 vibrational band of the hydroperoxyl radical", *J. Mol. Spectrosc.* **166,** 273–279 (1994).
193. L. R. Zink, K. M. Evenson, F. Matsushima, T. Nelis, and R. L. Robinson, "Atomic oxygen fine-structure splittings with tunable far-infrared spectroscopy", *Astrophys. J.* **371,** L85 (1991).
194. W. Bell, G. Duxbury, and D. D. Stuart, "High-resolution spectra of the ν_4 band of chlorine nitrate", *J. Mol. Spectrosc.* **152,** 283–297 (1992).
195. A. Goldman, C. P. Rinsland, F. J. Murcray, R. D. Blatherwick, and D. G. Murcray, "High resolution studies of heavy NO_y molecules in atmospheric spectra", *JQSRT* **52,** 367–377 (1994).
196. A. Goldman, C. P. Rinsland, J.-M. Flaud, and J. Orphal, "$ClONO_2$: spectroscopic line parameters and cross-sections in 1996 HITRAN", *JQSRT* **60** (1998) this issue.
197. A. S. Jursa (ed.), *Handbook of Geophysics and the Space Environment*, Air Force Geophysics Laboratory, 1985.
198. F. P. Billingsley, "Calculation of the absolute infrared intensities for the 0–1, 0–2, and 1–2 vibrational–rotational transitions in the ground state of NO^+", *Chem. Phys. Lett.* **23,** 160–166 (1973).
199. K. P. Huber and G. Herzberg, *Molecular Spectra and Molecular Structure IV. Constants of Diatomic Molecules.* Van Nostrand Reinhold, New York, 1979.
200. D. R. Smith, E. R. Huppi, and R. M. Nadile, "Improved rotational constants for the ground electronic state of NO^+ from atmospheric emission spectra", *JQSRT* (1998) to be submitted.
201. H.-J. Werner and P. Rosmus, "Ab initio calculations of radiative transition probabilities in the $X^1\Sigma^+$ ground state of the NO^+ ion", *J. Mol. Spectrosc.* **96,** 362–367 (1982).
202. E. A. Cohen, G. A. McRae, T. L. Tan, R. R. Friedl, J. W. C. Johns, and N. Noël, "The ν_1 band of HOBr", *J. Mol. Spectrosc.* **173,** 55–61 (1995).
203. Y. Koga, H. Takeo, S. Kondo, M. Sugie, C. Matsumura, G. A. Rae, and E. A. Cohen, "The rotational spectra, molecular structure, dipole moment, and hyperfine constants of HOBr and DOBr", *J. Mol. Spectrosc.* **138,** 467–481 (1989).
204. S. T. Massie and A. Goldman, "Absorption parameters of very dense molecular spectra of the HITRAN compilation", *JQSRT* **48,** 713–719 (1992).
205. A. H. McDaniel, C. A. Cantrell, J. A. Davidson, R. E. Shetter, and J. G. Calvert, *J. Atmos. Chem.* **12,** 211 (1991); S. T. Massie, A. Goldman, A. H. McDaniel, C. A. Cantrell, J. A. Davidson, R. E. Shetter, and J. G. Calvert, "Temperature dependent infrared cross sections for CFC-11, CFC-12, CFC-13, CFC-14, CFC-22, CFC-13, CFC-114, and CFC-115", NCAR Technical Note/TN-358 + STR (1991); C. A. Cantrell, J. A. Davidson, A. H. McDaniel, R. E. Shetter, and J. G. Calvert, *Chem. Phys. Lett.* **148,** 358–363 (1988); Erratum *Chem. Phys. Lett.* **152,** 274 (1988); J. Ballard, W. B. Johnston, M. R. Gunson, and P. T. Wassel, "Absolute absorption coefficients of $ClONO_2$ infrared bands at stratospheric temperatures", *J. Geophys. Res.* **93,** 1659–1665 (1988).
206. P. Varanasi, "Absorption coefficients of CFC-11 and CFC-12 needed for atmospheric remote sensing and global warming studies", *JQSRT* **48,** 205–219 (1992); P. Varanasi, "Absorption spectra of HCFC-22 around 829 cm^{-1} at atmospheric conditions", *JQSRT* **47,** 251–255 (1992); P. Varanasi, A. Gopalan, and J.F. Brannon Jr., "Infrared absorption coefficient data on SF_6 applicable to atmospheric remote sensing", *JQSRT* **48,** 141–145 (1992).

207. P. Varanasi and V. Nemtchinov, "Thermal infrared absorption coefficients of CFC-12 at atmospheric conditions", *JQSRT* **51,** 679–687 (1994); Z. Li and P. Varanasi, "Measurement of the absorption cross-sections of CFC-11 at conditions representing various model atmospheres", *JQSRT* **52,** 137–144 (1994).
208. J. Orphal, M. Morillon-Chapey, and G. Guelachvili, "High-resolution absorption cross sections of chlorine nitrate in the v_2 band regional around 1292 cm^{-1} at stratospheric temperatures", *J. Geophys. Res.* **99,** 14 549–14 555 (1994).
209. J. J. Orlando, G. S. Tyndall, A. Huang, and J. G. Calvert, "Temperature dependence of the infrared absorption cross sections of carbon tetrachloride", *Geophys. Res. Lett.* **19,** 1005–1008 (1992).
210. K. Smith, D. Newnham, M. Page, J. Ballard, and G. Duxbury, "Infrared absorption cross-sections and integrated absorption intensities of HFC-134 and HFC-143a vapour", *JQSRT* **59,** 437–451 (1998).
211. B. R. Lewis, L. Berzins, and J. H. Carver, "Oscillator strengths for the Schumann–Runge bands of O_2", *JQSRT* **36,** 209–232 (1986).
212. K. Yoshino, D. E. Freeman, J. R. Esmond, and W. H. Parkinson, "High resolution absorption cross section measurements and band oscillator strengths of the (1, 0)–(12, 0) Schumann–Runge bands of O_2", *Planet. Space Sci.* **31,** 339–353 (1983); K. Yoshino, J. R. Esmond, A. S.-C. Cheung, D. E. Freeman, and W. H. Parkinson, "High resolution absorption cross-sections in the transmission window region of the Schumann–Runge bands and Herzberg continuum of O_2", *Planet. Space Sci.* **40,** 185–192 (1992).
213. K. Minschwaner, G. P. Anderson, L. A. Hall, and K. Yoshino, "Polynomial coefficients for calculating O_2 Schumann–Runge cross sections at 0.5 cm^{-1} resolution", *J. Geophys. Res.* **97,** 10 103–10 108 (1992).
214. B. R. Lewis, L. Berzins, C. J. Dedman, T. T. Scholz, and J. H. Carver, "Pressure broadening in the Schumann–Runge system of molecular oxygen", *JQSRT* **39,** 271–282 (1988).
215. K. Yoshino, D. E. Freeman, and W. H. Parkinson, "High resolution absorption cross section measurements of N_2O at 295–299 K in the wavelength region 170–222 nm", *Planet. Space. Sci.* **32,** 1219–1222 (1984).
216. D. E. Freeman, K. Yoshino, J. R. Esmond, and W. H. Parkinson, "High resolution absorption cross section measurements of SO_2 at 213 K in the wavelength region 172–240 nm", *Planet. Space Sci.* **32,** 1125–1134 (1984).
217. K.-N. Liou, *An Introduction to Atmospheric Radiation.* Academic Press, New York, 1980.
218. P. W. Barber and S. C. Hill, *Light Scattering by Particles, Computational Methods.* World Scientific, New Jersey, 1990.
219. B. T. Draine and P. J. Flatau, "Discrete-dipole approximation for scattering calculations", *J. Opt. Soc. Am.* **A11,** 1491–1499 (1994).
220. S. T. Massie, "Indices of refraction for the HITRAN compilation", *JQSRT* **52,** 501–513 (1994).
221. S. G. Warren, "Optical constants of ice from the ultraviolet to the microwave", *Appl. Opt.* **23,** 1206–1225 (1984).
222. L. Kou, D. Labrie, and P. Chylek, "Refractive indices of water and ice in the 0.65- to 2.5-μm spectral range", *Appl. Opt.* **32,** 3531–3540 (1993).
223. H. D. Downing and D. Williams, "Optical constants of water in the infrared", *J. Geophys. Res.* **80,** 1656–1661 (1975).
224. K. F. Palmer and D. Williams, "Optical constants of sulfuric acid; application to the clouds of Venus?", *Appl. Opt.* **14,** 208–219 (1975).
225. E. E. Remsberg, "Stratospheric aerosol properties and their effects on infrared radiation", *J. Geophys. Res.* **78,** 1401–1408 (1973); E. E. Remsberg, D. Lavery, and B. Crawford, Jr., "Optical constants for sulfuric acid and nitric acids", *J. Chem. Engng Data* **19,** 263–265 (1974).
226. A. Tabazadeh, R. P. Turco, and M. Z. Jacobson, "A model for studying the composition and chemical effects of stratospheric aerosols", *J. Geophys. Res.* **99,** 12 897–12 914 (1994).
227. M. R. Querry and I. L. Tyler, "Reflectance and complex refractive indices in the infrared for aqueous solutions of nitric acid", *J. Chem. Phys.* **72,** 2495–2499 (1980).
228. O. B. Toon, M. A. Tolbert, B. G. Koehler, A. M. Middlebrook, and J. Jordan, "Infrared optical constants of H_2O ice, amorphous nitric acid solutions, and nitric acid hydrates", *J. Geophys. Res.* **99,** 25 631–25 654 (1994).
229. B. S. Berland, D. R. Haynes, K. L. Foster, S. M. George, and O. B. Toon, "Refractive indices of amorphous and crystalline HNO_3/H_2O films representative of polar stratospheric clouds", *J. Phys. Chem.* **98,** 4358–4364 (1994).
230. L. J. Richwine, M. L. Clapp, R. E. Miller, and D. R. Worsnop, "Complex refractive indices in the infrared of nitric acid trihydrate aerosols", *Geophys. Res. Lett.* **22,** 2625–2628 (1995).
231. R. W. Adams and H. D. Downing, "Infrared optical constants of a ternary system of 75% H_2SO_4, 10% HNO_3, and 15% H_2O", *J. Opt. Soc. Am.* **A3,** 22–28 (1986).
232. M. L. Clapp, R. E. Miller, and D. R. Worsnop, "Frequency-dependent optical constants of water ice obtained directly from aerosol extinction spectra", *J. Phys. Chem.* **99,** 6317–6326 (1995).
233. R. A. Sutherland and R. K. Khanna, "Optical properties of organic-based aerosols produced by burning vegetation", *Aer. Sci. and Tech.* **14,** 331–342 (1991).
234. S. F. Gosse, M. Wang, D. Labrie, and P. Chylek, "Imaginary part of the refractive index of sulfates and nitrates in the 0.7–2.6-μm spectral region", *Appl. Opt.* **36,** 3622–3634 (1997).

235. D. J. Cziczo, J. B. Nowak, J. H. Hu, and J. P. D. Abbatt, "Infrared spectroscopy of model tropospheric aerosols as a function of relative humidity: observations of deliquescence and crystallization", *J. Geophys. Res.* (accepted for publication).
236. R. Rodrigues, K. W. Jucks, N. Lacome, Gh. Blanquet, J. Walrand, W. A. Traub, B. Khalil, R. LeDoucen, A. Valentin, C. Camy-Peyret, L. Bonamy, and J.-M. Hartmann, "Model, software, and database for computation of line-mixing effects in infrared Q-branches of atmospheric CO_2. I. Symmetric isotopomers", *JQSRT* (accepted for publication).
237. C. P. Rinsland, M. A. H. Smith, R. K. Seals, Jr., A. Goldman, F. J. Murcray, D. G. Murcray, J. C. Larsen and P. L. Rarig, "Stratospheric measurements of collision-induced absorption by molecular oxygen", *J. Geophys. Res.* **87,** 3119–3122 (1982).
238. C. P. Rinsland, R. Zander, J. S. Namkung, C. B. Farmer, and R. H. Norton, "Stratospheric infrared continuum absorption observed by the ATMOS instrument", *J. Geophy. Res.* **94,** 16 303–16 322 (1989).
239. P. L., Roney, F. Reid, and J.-M. Theriault, "Transmission window near 2400 cm^{-1}: an experimental and modeling study", *Appl. Opt.* **30,** 1995–2004 (1991).
240. V. Menoux, R. Le Doucen, C. Boulet, A. Robin, and A. M. Bouchardy, "Collision-induced absorption in the fundamental band of N_2: temperature dependence of the absorption for N_2–N_2 and N_2–O_2 pairs", *Appl. Opt.* **32,** 263–268 (1993).
241. W. J. Lafferty, A. M. Solodov, A. Weber, W. B. Olson, and J.-M. Hartmann, "Infrared collision-induced absorption by N_2 near 4.3 μm for atmospheric applications: measurements and empirical modeling", *Appl. Opt.* **35,** 5911–5917 (1996).
242. J. J. Orlando, G. S. Tyndall, K. E. Nickerson, and J. G. Calvert, "The temperature dependence of collision-induced absorption by oxygen near 6 μm", *J. Geophys. Res.* **96,** 20 755–20 760 (1991).
243. F. Thibault, V. Menoux, R. Le Doucen, J.-M. Hartmann, and C. Boulet, "Infrared collision-induced absorption by O_2 near 6.4 μm for atmospheric applications: measurements and empirical modeling", *Appl. Opt.* **36,** 563–567 (1997).
244. E. J. Mlawer, S. A. Clough, P. D. Brown, T. M. Stephen, J. C. Landry, A. Goldman, and F. J. Murcray, "Observed atmospheric collision-induced absorption in near-infrared oxygen bands", *J. Geophys. Res.* **103,** 3859–3863 (1998).
245. S. Solomon, R. W. Portmann, R. W. Sanders, and J. S. Daniel, "Absorption of solar radiation by water vapor, oxygen, and related collision pairs in the Earth's atmosphere", *J. Geophys. Res.* **103,** 3847–3858 (1998).
246. G. D. Greenblatt, J. J. Orlando, J. B. Burkholder, and A. R. Ravishankara, "Absorption measurements of oxygen between 330 and 1140 nm", *J. Geophys. Res.* **95,** 18 577–18 582 (1990).
247. J. A. Nelder and R. Mead, "A simplex method for function minimization", *Comput. J.* **7,** 308–313 (1965).
248. G. Herzberg, Molecular Spectra and Molecular Structure Vol. II, *Infrared and Raman Spectra of Polyatomic Molecules*. D. Van Nostrand, New York, 1962, pp. 507–509.
249. C. H. Townes and A. L. Schawlow, *Microwave Spectroscopy*. Dover, New York, 1975, pp. 102–105.
250. R. R. Gamache and L. S. Rothman, "Extension of the HITRAN database to non-LTE applications", *JQSRT* **48,** 519–525 (1992).
251. S. S. Penner, *Quantitative Molecular Spectroscopy and Gas Emissivities*. Addison-Wesley, Reading, MA, 1959.
252. L. S. Rothman and L. D. G. Young, "Infrared energy levels and intensities of carbon dioxide—II", *JQSRT* **25,** 505–524 (1981).
253. R. M. Goody and Y. L. Yung, *Atmospheric Radiation*. Oxford University Press, New York, 1989.
254. D. P. Edwards, M. Lopez-Puertas, and M.A. Lopez-Valverde, "Non-local thermodynamic equilibrium studies of the 15-μm bands of CO_2 for atmospheric remote sensing", *J. Geophys. Res.* **98,** 14 955–14 977 (1993).

APPENDIX A—HITRAN PARAMETERS: DEFINITIONS AND USAGE

A.1. Definitions and units

The purpose of this appendix is to describe the definition, units, and basic usage of the HITRAN spectral line parameters. Some of the parameters are shown schematically in Fig. 1. In the following discussion h [ergs s], c [cm/s], and k [ergs/K] are the Planck constant, speed of light, and Boltzmann constant, respectively.

Mol — The molecular species identification (ID) number. HITRAN96 uses Mol = 1 (for H_2O) through 37 (for HOBr). The gas IDs and corresponding molecules are listed in Table 2.

Iso — The isotope ID number. Iso = 1 for the most abundant isotope of gas Mol, Iso = 2 for the next most abundant, etc. An isotope description shorthand is often used such that, for example, $^{16}O^{13}C^{16}O$ is referred to as CO_2 636 (Mol = 2, Iso = 2). A list of the gases and isotopes is given in the file MOLPARAM.TXT (see Section 7.1)

$\nu_{\eta\eta'}$ — The spectral line transition frequency [cm^{-1}]. The transition between lower and upper states η and η' is accompanied by the emission or absorption of a photon of energy $E = \nu_{\eta\eta'}$ [cm^{-1}]. (Other designations use $''$ and $'$ for lower and upper states, respectively.)

$S_{\eta\eta'}$ — The spectral line intensity [cm^{-1}/(molecule cm^{-2})] at $T_{ref} = 296$ K. The intensity is defined here for a single molecule. Radiative transfer theory[251] for the two states of a vibrational-rotational system defines the spectral line intensity as

$$S_{\eta\eta'} = \frac{h\nu_{\eta\eta'}}{c}\frac{n_\eta}{N}\left(1 - \frac{g_\eta\, n_{\eta'}}{g_{\eta'}\, n_\eta}\right) B_{\eta\eta'}, \tag{A1}$$

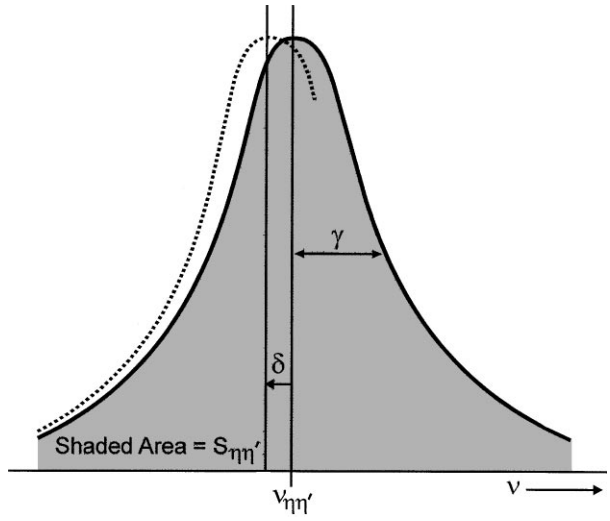

Fig. 1. Schematic of fundamental spectroscopic parameters of a line transition in HITRAN. The dotted line refers to a perturbed transition (with a negative δ).

where $B_{\eta\eta'}$ [$cm^3/(ergs\,s^2)$] is the Einstein coefficient for induced absorption, n_η and $n_{\eta'}$ are the populations of the lower 1and upper states, respectively, g_η and $g_{\eta'}$ are the state statistical weights, and N is the molecular number density. The weight includes electronic, vibrational, rotational, and nuclear statistics, and caution must be exercised when calculating weights for degenerate states (see Section 7.2). The quantity in parentheses represents the effect of stimulated emission. The Einstein coefficient $B_{\eta\eta'}$ is related to the weighted transition-moment squared $\mathfrak{R}$ [$Debye^2 = 10^{-36}$ ergs cm^3], discussed below, by

$$\mathfrak{R}_{\eta\eta'} = \frac{3h^2}{8\pi^3} B_{\eta\eta'} \times 10^{36}. \tag{A2}$$

Assuming local thermodynamic equilibrium (LTE), the population partition between states is governed by Boltzmann statistics at the ambient temperature T [K]. This allows us to write

$$\frac{g_\eta\, n_{\eta'}}{g_{\eta'}\, n_\eta} = \exp(-c_2\, \nu_{\eta\eta'}/T) \quad \text{and} \quad \frac{n_\eta}{N} = \frac{g_\eta \exp(-c_2\, E_\eta/T)}{Q(T)}, \tag{A3}$$

where E_η is the lower state energy [cm^{-1}], and c_2 the second radiation constant $= hc/k = 1.4388$ cm K. The total internal partition sum $Q(T)$ [see Eq. (4) in Section 7.2] is given by

$$Q(T) = \sum_\eta g_\eta \exp(-c_2\, E_\eta/T). \tag{A4}$$

Substituting Eq. (A2) and Eq. (A3) in Eq. (A1) at T_{ref}, and introducing I_a, the natural terrestrial isotopic abundance, gives

$$S_{\eta\eta'}(T_{\text{ref}}) = \frac{8\pi^3}{3hc}\, \nu_{\eta\eta'}\, \frac{I_a\, g_\eta \exp(-c_2\, E_\eta/T_{\text{ref}})}{Q(T_{\text{ref}})} [1 - \exp(-c_2\, \nu_{\eta\eta'}/T_{\text{ref}})]\, \mathfrak{R}_{\eta\eta'} \times 10^{-36}. \tag{A5}$$

This is the definition that appears in HITRAN. It should be understood that $S_{\eta\eta'}$ is weighted according to the natural terrestrial isotopic abundances given in the file MOLPARAM.TXT. For applications that do not assume this isotope mixture, studies of other planetary atmospheres for example, this weighting should be renormalized.

$\mathscr{R}_{\eta\eta'}$ The weighted transition-moment squared [$Debye^2 = 10^{-36}$ ergs cm^3]. This quantity is defined by

$$\mathfrak{R}_{\eta\eta'} = \frac{1}{g_\eta} \sum_{\zeta,\zeta'} |R_{(\eta\zeta)(\eta'\zeta')}|^2, \tag{A6}$$

where $R_{(\eta\zeta)(\eta'\zeta')}$ is the transition moment [Debye]. The Einstein coefficients for induced absorption $B_{\eta\eta'}$, induced emission $B_{\eta'\eta}$ [$cm^3/(ergs\,s^2)$], and spontaneous emission $A_{\eta'\eta}$ [s^{-1}] are related to this quantity by

$$B_{\eta\eta'} = \frac{8\pi^3}{3h^2}\, \mathfrak{R}_{\eta\eta'} \times 10^{-36}, \tag{A7}$$

$$B_{\eta'\eta} = \frac{8\pi^3}{3h^2}\, \frac{g_\eta}{g_{\eta'}}\, \mathfrak{R}_{\eta\eta'} \times 10^{-36}, \tag{A8}$$

$$A_{\eta'\eta} = \frac{64\pi^4}{3h}\, \nu_{\eta'\eta}^3\, \frac{g_\eta}{g_{\eta'}}\, \mathfrak{R}_{\eta'\eta} \times 10^{-36}. \tag{A9}$$

$\mathfrak{R}_{\eta\eta'}$ is independent of both temperature and isotopic abundance. A detailed discussion of $S_{\eta\eta'}$ and $\mathfrak{R}_{\eta\eta'}$ is given by Gamache and Rothman.[250]

γ_{air} The air-broadened halfwidth at half maximum (HWHM) [cm^{-1}/atm] at $T_{ref} = 296$ K and reference pressure $p_{ref} = 1$ atm. This parameter is transition dependent.

γ_{self} The self-broadened halfwidth (HWHM) [cm^{-1}/atm] at $T_{ref} = 296$ K and $p_{ref} = 1$ atm. This parameter is transition dependent.

E_η The lower state energy of the transition [cm^{-1}]. This quantity has been scaled such that the minimum possible level is set to zero. However, the HITRAN database uses a "flag" value of minus one (-1) for some unidentified transitions whose lower state energy is unknown, but where confidence in the intensity at 296 K is achieved.

n The coefficient of temperature dependence of the air-broadened halfwidth as appearing in the relation

$$\gamma_{air}(p_{ref}, T) = \gamma_{air}(p_{ref}, T_{ref})(T_{ref}/T)^n; \tag{A10}$$

it is assumed to be transition dependent.

δ The air-broadened pressure shift [cm^{-1}/atm] at $T_{ref} = 296$ K, $p_{ref} = 1$ atm, of the line transition frequency $\nu_{\eta\eta'}$. This parameter is transition dependent.

$iv_{\eta'}$, iv_η Upper state global quanta index, lower state global quanta index. The state quantum numbers v corresponding to each index are given by the CD-ROM program BD_VIBS.FOR (see Sec. 7.1). These states are usually expressed by the quantum numbers v of each of the fundamental modes of vibration v_1, v_2, v_3, etc. A notable exception is CO_2, which uses the 5 integer notation (v_1, v_2, l, v_3, r) described in Rothman and Young[252] where l is the angular momentum associated with the v_2 bending mode, and r is a ranking index for members of a Fermi resonance.

$q_{\eta'}$, q_η Upper state local quanta, lower state local quanta. These quantum identifications are defined in Table 4.

A.2. Applications

A.2.1. *Temperature correction of line intensity.* With reference to Eq. (A5), the following expression is used to calculate the line intensity $S_{\eta\eta'}(T)$ from the HITRAN quantity $S_{\eta\eta'}(T_{ref})$,

$$S_{\eta\eta'}(T) = S_{\eta\eta'}(T_{ref})\frac{Q(T_{ref})}{Q(T)}\frac{\exp(-c_2 E_\eta/T)}{\exp(-c_2 E_\eta/T_{ref})}\frac{[1-\exp(-c_2 \nu_{\eta\eta'}/T)}{[1-\exp(-c_2 \nu_{\eta\eta'}/T_{ref})]}. \tag{A11}$$

The ratio of total internal partition functions is calculated using the parameterization of Gamache et al.[127] This approach is an improvement over the usual classical approximation for the independent temperature variation of the rotational and vibrational components of the partition function. The third term on the right in Eq. (A11) accounts for the ratio of Boltzmann populations, and the fourth term for the effect of stimulated emission.

A.2.2. Temperature and pressure correction of line halfwidth. The pressure broadened line halfwidth $\gamma(p,T)$ for a gas at pressure p [atm], temperature T [K], and partial pressure p_s [atm], is calculated as

$$\gamma(p, T) = \left(\frac{T_{ref}}{T}\right)^n (\gamma_{air}(p_{ref}, T_{ref})(p - p_s) + \gamma_{self}(p_{ref}, T_{ref})\, p_s). \tag{A12}$$

In the absence of other data, the coefficient of temperature dependence of the self-broadened halfwidth has been assumed to be equal to that of the air-broadened halfwidth. Alternatively, the classical value[253] of 0.5 could be used by default.

A.2.3. Pressure-shift correction of line position. The pressure shift of the transition frequency leads to a shifted frequency $\nu^*_{\eta\eta'}$ given by

$$\nu^*_{\eta\eta'} = \nu_{\eta\eta'} + \delta(p_{ref})\, p. \tag{A13}$$

A.2.4. Absorption coefficient. In the atmosphere, a spectral line is broadened about the transition wave number $\nu_{\eta\eta'}$, the spread being represented by the normalized line shape function $f(\nu, \nu_{\eta\eta'}, T, p)$ [$1/cm^{-1}$].[253] In the lower atmosphere, pressure broadening of spectral lines dominates and if a Lorentz profile is assumed,

$$f(\nu, \nu_{\eta\eta'}, T, p) = \frac{1}{\pi}\frac{\gamma(p, T)}{\gamma(p, T)^2 + [\nu - (\nu_{\eta\eta'} + \delta(p_{ref})\, p)]^2}. \tag{A14}$$

The monochromatic absorption coefficient $k_{\eta\eta'}(\nu,T,p)$ [1/(molecule cm^{-2})] at wave number ν [cm^{-1}] due to this transition is then given by

$$k_{\eta\eta'}(\nu,T,p) = S_{\eta\eta'}(T) f(\nu,\nu_{\eta\eta'},T,p). \tag{A15}$$

The dimensionless optical depth $\tau_{\eta\eta'}(\nu,T,p)$ is formed by multiplying the absorption coefficient by the number density of absorbing molecules per unit path length u [molecules cm^{-2}], such that

$$\tau_{\eta\eta'}(\nu, T, p) = u\, k_{\eta\eta'}(\nu, T, p). \tag{A16}$$

A.2.5. Non-LTE applications. Under conditions of non-LTE, the partition of population between states is not dictated by Boltzmann statistics and Eq. (A3) is not valid. The line intensity under these conditions may be obtained directly from the weighted transition-moment squared $\mathfrak{R}_{\eta\eta'}$ as described in Ref. 250, or by correcting the HITRAN intensity $S_{\eta\eta'}(T_{ref})$ as described in Ref. 254.